Novel routes of hydroperoxide detoxification in *Mycobacterium tuberculosis*

Von der Gemeinsamen Naturwissenschaftlichen Fakultät

der Technischen Universität Carolo-Wilhelmina

zu Braunschweig

zur Erlangung des Grades eines

Doktors der Naturwissenschaften

(Dr. rer. nat.)

genehmigte

D i s s e r t a t i o n

von

Timo Jäger

aus Gießen

1. Referent: Prof. Dr. Dr. h.c. Leopold Flohé

2. Referent: Prof. Dr. Mahavir Singh

eingereicht am: 30.06.2003

mündliche Prüfung am: 03.09.2003

Druckjahr: 2003

Vorveröffentlichungen der Dissertation

Teilergebnisse aus dieser Arbeit wurden mit Genehmigung der Gemeinsamen Naturwissenschaftlichen Fakultät, vertreten durch den Mentor der Arbeit, in folgenden Beiträgen vorab veröffentlicht:

Tagungsbeiträge

Jaeger,T., Ottenhoff,T.H.M., Flohé,L., and Singh,M. Interaction of *Mycobacterium tuberculosis* thioredoxin A and B with thioredoxin reductase. Fifth International Conference on the Pathogenesis of Mycobacterial Infections. 27.06. – 30.06.2002, Stockholm, Sweden.

nach Einreichung der Dissertation:

Jaeger,T., Radi,R., Trujillo,M., and Flohé,L. Peroxidase systems of *Mycobacterium tuberculosis*. The Second International Symposium on Redox Life Science. 20.08. – 22.08.2003, Hokkaido, Japan.

Table of contents

1 Introduction

Mycobacterium tuberculosis is a leading pathogen worldwide, infecting an estimated 8 million and killing 2 – 3 million people each year (Dye *et al.*, 1999). In addition, it is estimated that ~ 2 billion people have been exposed to *M. tuberculosis*, and thus are at risk of developing the active disease. Although most of the infected individuals reside in less industrialized countries, the rates of infection are also increasing at an alarming rate in areas undergoing rapid social change, such as the countries of the former Soviet Union (Keshavjee and Becerra, 2000). In part because of the symbiotic relationship between human immunodeficiency virus (HIV) and tuberculosis, and because of the increasingly rapid displacement of populations, the incidence of multi-drug-resistant (MDR) tuberculosis is an important worldwide concern. Thus, in a survey of 35 countries, 12.6 % of *M. tuberculosis* isolates were found to be resistant to at least one drug, and 2.2 % were resistant to both isoniazid and rifampicin, the two primary drugs used to treat tuberculosis (Pablos-Mendez *et al.*, 1998). This resurgence of tuberculosis has led to renewed efforts to find new drugs for the treatment of this dreaded disease, particularly agents that exhibit activity against drug-resistant strains, completely sterilize the infection, or shorten the duration of drug therapy and thus promote drug compliance.

1.1 Epidemiology

Tuberculosis (TB) is a worldwide public health problem and is usually transmitted by droplet infection. As noted previously, approximately one third of the earth's population is infected with *M. tuberculosis*. Although less than ten per cent become sick, in 1995 more humans died of tuberculosis than ever before. An increasing drug resistance problem coupled with the HIV-

induced acquired immunodeficiency syndrome is leading to further epidemic spread among population. The common infectious agent is *M. tuberculosis*, more rarely *Mycobacterium bovis*, *Mycobacterium africanum*, *Mycobacterium microti*, and the newly discovered *Mycobacterium canettii* (Pfyffer *et al.*, 1998; Am. Thorac. Soc., 2003). In about 85 % of all clinical cases the lung is involved. However, with the increase of the HIV infections, the proportion of extra-pulmonary types is on the increase. In 1997, 8 million new TB cases were assessed, adding to 16 million cases already registered. Of the latter, approximately 2 million could have died since then (Dye *et al*., 1999). Some 80 % of all patients were registered in 22 countries. More than half of them were from five nations belonging to the southeast region of Africa (Fig. 1.1). Not surprisingly, 9 out of 10 of the highest incidences are located in that continent (Dye *et al*., 1999). This situation is likely to deteriorate in the future. The World Health Organization (WHO) expects an increase of the annual disease rates from 8 million in 1997 to 10.2 million per year in 2005 (WHO, 2001). This alarming sign of the spreading of an endemic disease and the fact that drug resistant strains have emerged on a massive scale underscore the importance of studying mycobacterial defense mechanisms. Although scientific breakthroughs in the field have been rare, the release of the complete genome sequence of *M. tuberculosis* (Cole *et al.*, 1998) has initiated a hunt for genes of interest for vaccine development, either as targets for gene knockout or as candidates for protective antigens.

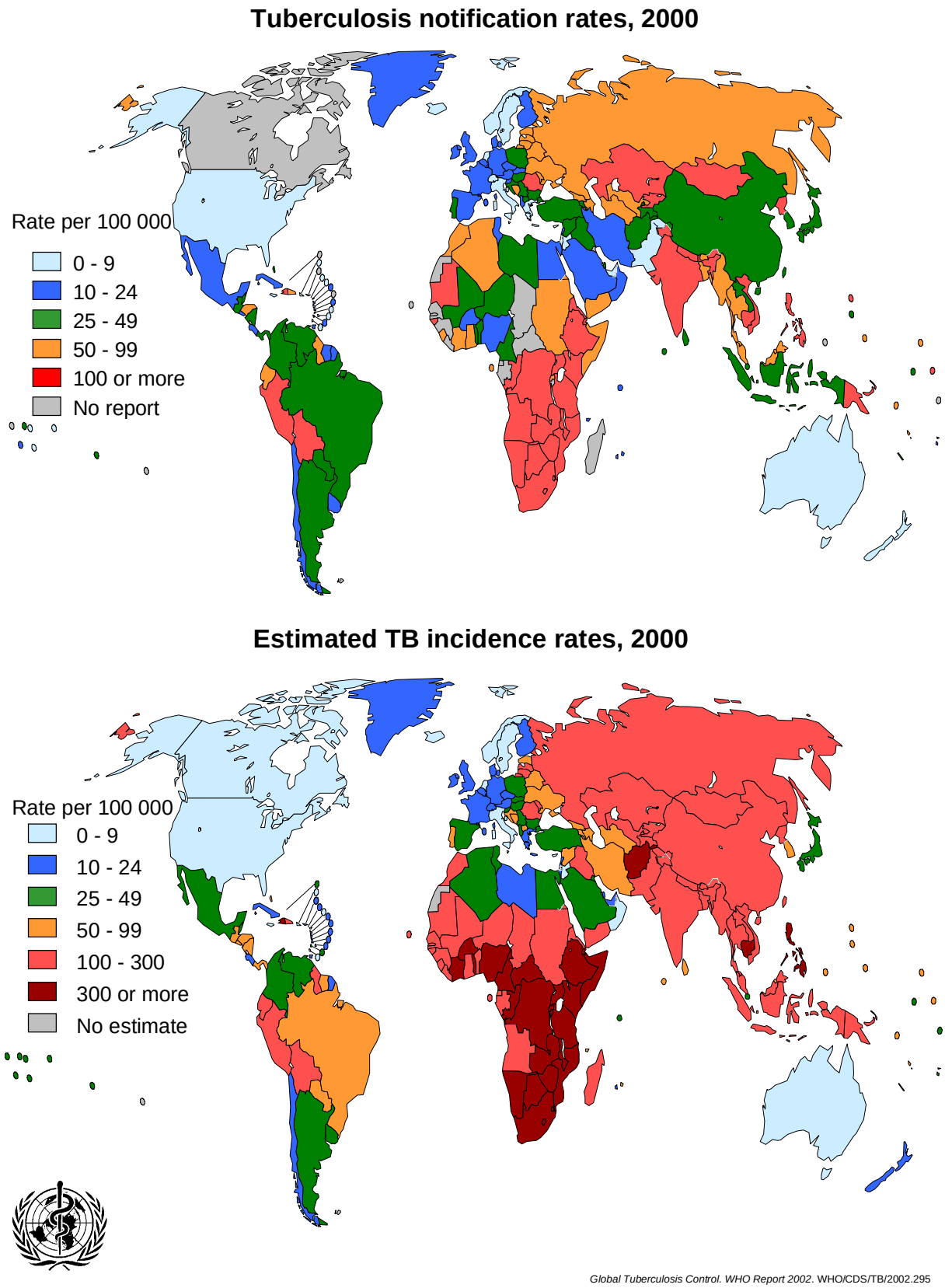

Fig. 1.1: **Tuberculosis (TB) notification rates and estimated TB incidence rates in 2000.** The 202 countries reporting to WHO notified a total of 3,671,973 cases (61 per 100,000 population). This represents only one quarter (27 %) of the estimated total (WHO, 2002).

1.2 Infection and disease

Tuberculosis is caused by the acid-fast, rod shaped bacillus, *Mycobacterium tuberculosis*. The microorganism is shielded by a unique wax-rich cell wall that is composed of long-chain fatty acids, glycolipids and other components. Accordingly, approximately 250 genes within the *M. tuberculosis* genome are involved in the fatty-acid metabolism. The robust shell contributes to the capacity of *M. tuberculosis* to survive in host phagocytes. *M. tuberculosis* is a slow-growing organism, with a replication time of approximately 20 hours. This slow growth forms the basis for the chronic nature of infection and disease, complicates microbiological diagnosis and necessitates long-term drug treatment.

In clinical terms tuberculosis is divided into primary (I) and reactivated forms (II).

(I) The typical source of a primary infection is a person with pulmonary tuberculosis producing up to 3,000 aerosol droplets per cough attack (Fig. 1.2). A primary infection need not be fatal and can be treated with appropriate chemotherapy. However, on occasions (AIDS etc.) the illness will not stay localized but can progress and the person will suffer from secondary complications. Generally, incorporated mycobacteria can survive after phagocytosis by macrophages. To do so, they must be able to resist many cellular defense strategies in the human body: reactive oxygen species and nitrogen compounds as well as enzyme acitivities such as myeloperoxidases, phosphatases, hydrolases, proteases, lysozyme, and lipases. In particular, the lipid-rich cell wall plays an important role as protective layer against aggressive lysosomal factors and as a diffusion barrier against drugs.

(II) Reactivated tuberculosis is a recurrence of the pulmonary form after sensitization to *M. tuberculosis* during the primary infection: after an interval of

latency, a cellular immune response leads to the formation of tissue tumors (granuloma) (Fig. 1.2). These highly characteristic pathological lesions are also known as tubercles. Tissue destruction (fibrosis) presents focal areas with dead cells (necrosis), forming a friable and amorphous granular mass, cheese-like in appearance (caeseous detritus). Often these foci show spontaneous remission; otherwise they become calcified. However, on occasion such material is liberated into the bronchioles of the respiratory tract and is expectorated. Subsequently, the aspiration can cause inflammation of the lungs, known as tuberculous pneumonia. Alternatively, the material persists in cavities as encapsulated tuberculosis (Rubin and Farber, 1999).

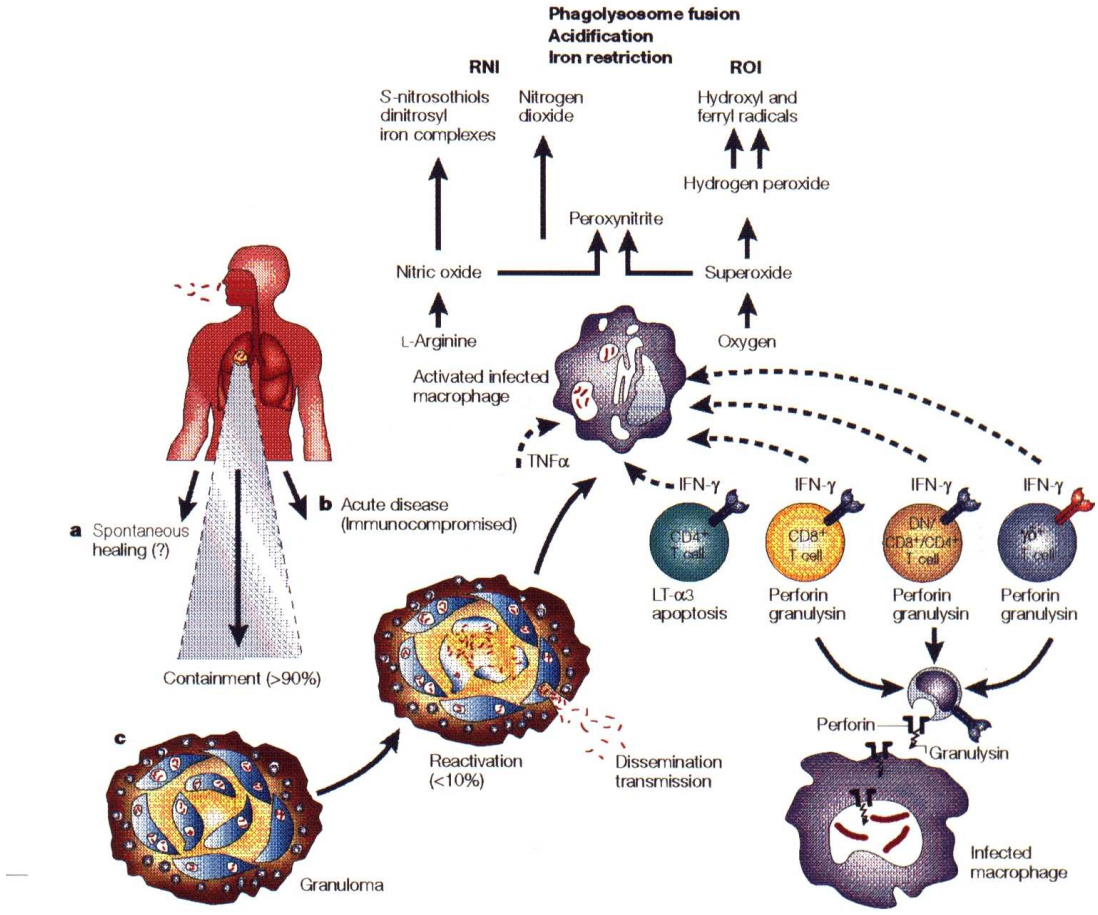

Fig. 1.2: Main features of tuberculosis: from infection to host defense. There are three potential outcomes of infection of the human host in *M. tuberculosis*. a) The frequency of abortive infection resulting in spontaneous healing is unknown, but is assumed to be minute. b) In the immunocompromised host, disease can develop directly after infection. c) In most cases, mycobacteria are initially contained and disease develops later as a result of reactivation. The granuloma is the site of infection, persistence, pathology and protection. Effector T cells (including conventional $CD4^+$ and $CD8^+$ T cells, and unconventional T cells, such as γδ T cells, and double-negative or CD4/CD8 single-positive T cells that recognize antigen in the context of CD1) and macrophages participate in the control of tuberculosis. Interferon-γ (IFN-γ) and tumour-necrosis factor-α (TNF-α), produced by T cells, are important macrophage activators. Macrophage activation permits phagosomal maturation and the production of antimicrobial molecules such as reactive nitrogen intermediates (RNI) and reactive oxygen intermediates (ROI). LT-α3, lymphotoxin-α3 (Kaufmann, 2001).

1.3 The intracellular lifestyle of *M. tuberculosis*

M. tuberculosis uses macrophages as its preferred habitat, which has two important implications for its survival (Schaible *et al*., 1999). First, macrophages, as professional phagocytes, are endowed with several surface receptors that facilitate antigen uptake, thereby rendering specific host-invasion strategies dispensable (Ernst, 1998; Ehlers and Daffe, 1998). Cholesterol has been shown to act as a docking site for the pathogen, promoting receptor-ligand interactions (Gatfield and Pieters, 2000). The initial interaction with surface receptors influences the subsequent fate of *M. tuberculosis* within the macrophage. Interactions with the constant regions of immunglobulin receptors and Toll-like receptors stimulate host-defense mechanisms, whereas those with complement receptors promote mycobacterial survival (Armstrong and Hart, 1975; Schorey *et al*., 1997; Brightbill *et al.*, 1999; Thoma-Uszynski *et al.*, 2001). The second consequence, which warrants more sophisticated coping mechanisms, is the survival of *M. tuberculosis* within the phagosome, as this constitutes a harsh environment that is detrimental to many microbes (Schaible *et al*., 1999). *M. tuberculosis* overcomes this obstacle by arresting the phagosome at an early stage of maturation, and by preventing fusion of the phagosome with lysosomes (Armstrong and Hart, 1975; Russell *et al*., 1996; Harth and Horwitz, 1999; Ferrari *et al.*, 1999).

The arrest of phagosomal maturation is not an all-or-nothing event. Some mycobacterial phagosomes can proceed to develop to the more mature stages of the phagolysosome. Phagosomal maturation is promoted by activation with interferon-γ (IFN-γ), which stimulates anti-mycobacterial mechanisms in macrophages (Fig. 1.2), notably the formation of reactive oxygen intermediates (ROI) and reactive nitrogen intermediates (RNI) (Schaible *et al.*, 1998; Schaible *et al*., 1999). However, even IFN-γ-activated macrophages fail to fully eradicate their resident *M. tuberculosis* (Kaufmann,

1999). Persistent microbes might proceed to a stage of dormancy with a reduced metabolic activity that facilitates their survival under conditions of nutrient and oxygen deprivation. These bacteria can persist without producing disease and therefore create a state of latency. Nevertheless, the risk of disease outbreak at a later time remains. *In vitro* experiments indicate that mycobacteria switch to lipid catabolism and nitrate respiration to ensure their survival (McKinney *et al.*, 2000; Weber *et al.*, 2000). Lipids are abundant in the caeseous detritus of granulomas, providing a rich source of nutrients during persistence.

1.4 Drug-resistant tuberculosis

Most forms of drug resistance are iatrogenic by their nature, i.e. acquired during pharmacotherapy. The most common causes leading to the selection of drug-resistant strains among microorganisms are: (i) administration of a single drug (instead of a combination), (ii) sub-therapeutic dosage below the pharmacologically required minimum inhibiting concentration (MIC), (iii) treatment applied for too short a time period, (iv) non-compliance of patients, (v) socio-economical problems, circumstances under which poor people strive to obtain medical assistance, (vi) insufficient regional drug availability, and (vii) lack of dispensation facilities and professional pharmaceutical care (Crofton *et al.*, 1997).

A typical clinical case of drug resistant tuberculosis would be one of the pulmonary types, in which the patient spreads resistant bacilli. Resistance implies lack of any anti-infectious effects at least for the front line drugs (in decreasing or increasing order of efficiency or toxicity, respectively): isoniazid (isonicotinic acid hydrazide, INH), rifampicin (rifampin, RMP), pyrazinamide, ethambutol, and streptomycin. Second-line drugs are protionamide, ethionamide, thiacetazone, thiocarlide, cycloserine, capreomycine, and paraaminosalicylic acid. Those are all bacteriostatic in action whereas the

primary-line drugs are bactericidal. Overall, some form part of the recommended treatment for tuberculosis issued by the WHO. Due to the required administration of antituberculous agents for prolonged durations (several months to years), resistance has rapidly developed in 5 – 10 % of the strains (1 – 3 % multidrug resistant disease). To avoid selection of even more primarily resistant bacteria the WHO recommends a treatment scheme within their DOTS (Directly Observed Treatment Short-Course) program. That consists of a two-months treatment with a combination of 4 antibiotics including isoniazid, rifampicin, and pyrazinamide, complemented with either streptomycin or ethambutol. It is followed by a 6-months treatment with isoniazid, combined with either ethionamide or ethambutol, or a 4-months treatment with isoniazid and rifampicin (WHO, 1998; WHO, 1999).

Shortly after the introduction of isoniazid chemotherapy in 1952, mycobacteria resistant to that antituberculous agent were described (Middlebrook, 1952). Nevertheless, isoniazid has remained as the basic medication. The mode of action of isoniazid is not fully understood, but there is evidence that certain isoniazid-resistant strains of mycobacteria have reduced catalase/peroxidase (KatG) enzyme activity. It suggests that the antibiotic is acted upon by that enzyme and, therefore, isoniazid is a prodrug (Zhang *et al.*, 1992; Johnsson and Schultz, 1994; Johnsson *et al*., 1995). Expression of KatG is a requirement for bacterial sensitivity to isoniazid (Zhang *et al*., 1992; Zhang *et al*., 1993). In its active form, isoniazid generates a range of reactive oxygen species and reactive organic radicals, which then attack multiple targets (DNA, carbohydrates, lipids) in the tubercle bacillus (Winder, 1982). The most well known target is the cell wall mycolic acid synthesis pathway (Winder and Collins, 1970; Banerjee *et al.*, 1994; Mdluli *et al.*, 1998). Mutations in *katG*, *inhA* (acyl carrier protein-enoyl reductase), and *ndh* (NADH dehydrogenase, resulting in an increased NADH/NAD^+ ratio), cause isoniazid resistance (Zhang *et al*., 1992; Banerjee *et al*., 1994; Lee *et al*., 2001). Point mutations or deletions in *katG* are the most common

mechanism of isoniazid resistance in *M. tuberculosis* clinical isolates (Heym *et al.*, 1994; Musser, 1995; Musser *et al.*, 1996; Rouse *et al.*, 1996; Heym and Cole, 1997). Isolates most resistant to isoniazid tend to carry mutations that severely reduce or eliminate KatG-peroxidase activity, whereas *M. tuberculosis* mutants that retain some percent of peroxidase activity remain moderately resistant to isoniazid. In addition, introduction of *M. tuberculosis katG* into isoniazid-resistant mutants restores innate susceptibility to this drug (Zhang *et al*., 1992; Zhang and Young, 1993; Heym *et al.*, 1995; Rouse and Morris, 1995).

1.5 Oxidative stress response in *M. tuberculosis*

In addition to its role in the activation of isoniazid, KatG is thought to play another key role in the infection with the tubercle bacillus. As intracellular pathogens capable of surviving and multiplying within host macrophages, mycobacteria have to survive exposure to macrophage killing mechanisms, including the oxidative stress response (see 1.3). The catalase/peroxidase KatG is a component of the bacterial OxyR response, which is induced by oxidative stress and protects the bacteria against oxidative killing (Storz *et al*., 1990; Farr and Kogoma, 1991; Aslund *et al.*, 1999; Zahrt and Deretic, 2002). Thus, the loss of a functional KatG in isoniazid-resistant strains of *M. tuberculosis* would be expected to lead to a reduced ability of the pathogen to survive within the intracellular environment; indeed it was reported many years ago that isoniazid resistance was associated with loss of virulence in the guinea pig (Middlebrook and Cohn, 1953).

It was found that the gene encoding the OxyR transcription factor of *M. tuberculosis* is defective as a result of a number of mutations, and with the exception of KatG, *M. tuberculosis* does not have a peroxide-inducible response (Sherman *et al.*, 1995; Deretic *et al.*, 1995). However, some isoniazid-resistant *katG* mutants compensate their loss of catalase/peroxidase ac-

tivity by overexpression of the alkyl hydroperoxide reductase AhpC (alkyl hydroperoxide reductase subunit C). Thus, it has been claimed that during infection with isoniazid-resistant, KatG-deficient *M. tuberculosis*, there is a selection for compensatory *ahpC* promoter mutations, enabling the organisms to grow intracellularly (Sherman *et al.*, 1996; Sherman *et al.*, 1999).

The mycobacterial *ahpC* gene encodes an orthologue of bacterial alkyl hydroperoxidases (Christman *et al.*, 1985; Jacobson *et al.*, 1989; Sherman *et al*., 1996; Dhandayuthapani *et al.*, 1996; Sreevatsan *et al.*, 1997; Heym *et al.*, 1997; Wilson *et al.*, 1998; Pagan-Ramos *et al.*, 1998; Chen *et al*., 1998; Cooper *et al.*, 2000; Springer *et al.*, 2001). In most mycobacteria, the *ahpC* gene is linked to *oxyR* and is activated by its gene product, an orthologue of the global regulator OxyR, controlling the peroxide stress. As mentioned previously, in *M. tuberculosis* as a species, and in all members of the *M. tuberculosis* complex, the *oxyR* gene is inactivated and represents a pseudogene. Recently it was shown that there exists a second level of *ahpC* regulation independent of *oxyR*. The *ahpC* gene is silenced in aerobic cultures of virulent *M. tuberculosis*, but is activated in statically grown organisms (Springer *et al*., 2001; Master *et al.*, 2002). AhpC has been indirectly implicated in nitric oxide metabolism using expression in heterologous systems like *Salmonella* (Chen *et al*., 1998). Purified AhpC has been shown to reduce hydroperoxides (Hillas *et al.*, 2000; Chauhan and Mande, 2001) and has also been suggested to have peroxynitrite reductase activity (Bryk *et al*., 2000).

1.6 The peroxiredoxin family

The mycobacterial AhpC belongs to a family of bacterial and eukaryotic antioxidant proteins with alkyl hydroperoxidase (Ahp) and thioredoxin-dependent peroxidase (TPx) activities. The two are peroxiredoxin-type peroxidases. Peroxiredoxins (Prxs) are a new and expanding family of thiol-

specific antioxidant proteins, also termed the thioredoxin peroxidases and alkyl hydroperoxide reductase proteins (Chae *et al.*, 1994a; Chae *et al*., 1994b; Schroeder and Ponting, 1998). Prxs exert their protective antioxidant role in cells through their peroxidase activity ($ROOH + 2e^- \rightarrow ROH + H_2O$), whereby hydrogen peroxide, peroxynitrite and a wide range of organic hydroperoxides (ROOH) are reduced and detoxified (Jacobson *et al*., 1989; Poole and Ellis, 1996; Bryk *et al*., 2000; Peshenko and Shichi, 2001; Hofmann *et al*., 2002; Wood *et al.*, 2003a). Peroxiredoxins are proteins without any prosthetic group. The only redox-active residues are cysteines. Their sequences classify them as a distinct protein family that is unrelated to any of the other peroxidase families. As a rule, the catalytic cycle of peroxiredoxins makes use of redox shuttling of one or two cysteine residues. These enzymes are truly ubiquitous having been identified in yeast, plant and animal cells, including both protozoan and helminth parasites, and most, if not all, eubacteria and archaea. Prxs are produced at high levels in cells (Moore *et al.*, 1991; Link *et al*., 1997; Chae *et al.*, 1999), and many organisms produce more than one isoform of Prx, including at least six Prxs identified in mammalian cells (Wood *et al*., 2003a).The high abundance of Prxs in a wide range of species and a recent finding that AhpC and not catalase is responsible for reduction of endogenously generated H_2O_2 in *Escherichia coli* (Seaver and Imlay, 2001) provide a persuasive argument that Prxs are important players in peroxide detoxification in cells. In addition, Baker and Poole reported very recently, that *E. coli* thiol peroxidase (TPx), also a member of the Prx family, is part of an oxidative defense system that uses reducing equivalents from thioredoxin and thioredoxin reductase to reduce alkyl hydroperoxides (Baker and Poole, 2003), and *tpx* mutation studies in *Helicobacter pylori* showed that TPx plays a significant role in peroxide and superoxide resistance of *H. pylori* (Comtois *et al*., 2003).

In enterobacteria AhpC, together with the flavine-containing disulfide reductase AhpF (alkyl hydroperoxide reductase subunit F), forms a two-

component system achieving hydroperoxide reduction by NAD(P)H without the aid of auxiliary enzymes or low molecular weight redox mediators (Fig. 1.3; Jacobson *et al*., 1989; Storz *et al.*, 1989). In *E. coli* and *Salmonella typhimurium* AhpF and AhpC are jointly regulated by the *oxyR* regulon that responds to oxidative stress and determines hydroperoxide resistance (Zahrt and Deretic, 2002). While AhpC appears to be ubiquitous in bacteria (Hofmann *et al*., 2002), AhpF is not. *H. pylori* lacks AhpF. Instead, *H. pylori* uses a thioredoxin (Trx) as the reductant of AhpC (Fig. 1.3) (Baker *et al.*, 2001). In contrast to enterobacteria, *M. tuberculosis* does not respond to oxidative stress with overexpression of AhpC (Dhandayuthapani *et al*., 1996), but AhpC is constitutively overexpressed in isoniazid-resistant clinical isolates. The resistance to isoniazid is due to a deficiency of catalase, which is required to activate the drug (see 1.4 and 1.5). Also mycobacteria do not contain a functional AhpF. That indicates that *M. tuberculosis* normally relies on catalase for H_2O_2 detoxification but depends on AhpC if catalase is missing.

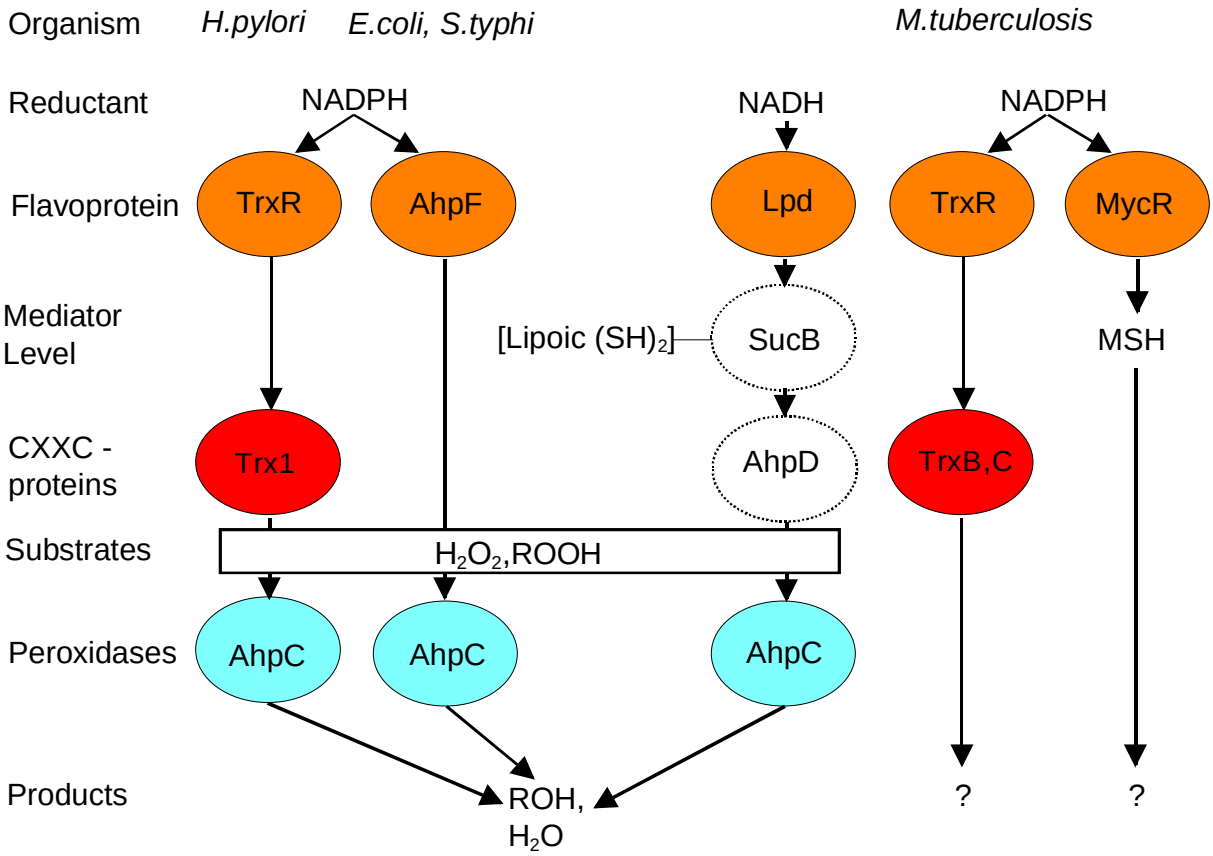

Fig. 1.3: Examples of bacterial antioxidant defense systems. Homologous proteins are shown in identically coloured circles. *H. pylori* makes use of the Trx-system for reduction of Prx-type AhpC like mammals and many other organisms. In enterobacteria AhpC is directly reduced by a flavin-dependent disulfide reductase. In mycobacteria AhpC reduction appears to be linked to energy metabolism. They also contain a thioredoxin system, further glutaredoxin-like proteins and mycothiol as low molecular weight redox mediator. The role of these redox systems in antioxidant defense is still unclear (Budde and Flohé, 2002). AhpC, alkyl hydroperoxe reductase subunit C; AhpD, alkyl hydroperoxide reductase subunit D; AhpF, alkyl hydroperoxide reductase subunit F; Lpd, dihydrolipoamide dehydrogenase; MycR, mycothiol reductase; MSH, mycothiol; SucB, dihydrolipoamide succinyltransferase; Trx, thioredoxin; TrxR, thioredoxin reductase

1.7 Objectives of the study

At the beginning of this thesis it was unclear how AhpC is reduced in mycobacteria. Attempts to substitute the missing AhpF by homologous mycothiol reductase and mycothiol or a thioredoxin/thioredoxin reductase system have failed so far (Hillas *et al*., 2000; Vergauwen *et al.*, 2001). More recently, a quite unique link of AhpC to mycobacterial energy metabolism was proposed (Bryk *et al.*, 2002): The reduction equivalents are transferred by two components of the α-keto acid dehydrogenase complex [dihydrolipoamide dehydrogenase (Lpd) and dihydrolipoamide succinyltransferase (SucB)] to AhpD (alkyl hydroperoxide reductase subunit D) that, like thioredoxins, contains a CXXC motif and thus substitutes for a real thioredoxin in AhpC reduction. The low molecular weight thiol that often mediates the flux from the flavoproteins to CXXC proteins is replaced here by SucB-bound lipoic acid (Fig. 1.3).

The objectives of this study were to:

- search for more likely metabolic partner of the mycobacterial AhpC,
- screen the genome of *M. tuberculosis* (Cole *et al*., 1998) for homologues of AhpF, thioredoxin-related proteins and peroxiredoxins,
- express the genes heterologously, and
- attempt to reconstitute peroxidase systems from the isolated gene products *in vitro* and examine their efficiencies by kinetic analysis.

2 Materials and Methods

2.1 Chemicals and reagents

Most of the chemicals purchased were of the highest purity grade available and were from:

- J. T. Baker B. V., Deventer, Netherlands
- Merck, Darmstadt, Germany
- Serva Electrophoresis, Heidelberg, Germany
- Sigma-Aldrich, Taufenkirchen, Germany
- Roche, Mannheim, Germany

2.2 Bacterial strains, plasmids and culture procedures

2.2.1 Strains

2.2.1.1 *E. coli* strains

The *E. coli* strains used in this study and their characteristics are listed in Table 2.1. All strains were grown in LB medium or on LB agar (see Table 2.3).

Table 2.1: *E. coli* strains and their characteristics

strain	genotype and relevant phenotype	origin / reference
E. coli DH5α	*sup*E44 Δ*lac*U169(Φ80 *lacZ* ΔM15) *hsd*R17 *rec*A1 *end*A1 *gyr*A96 *thi*-1 *rel*A1	(Hanahan, 1983)
E. coli BL21 (DE3)	F^- *omp*T *hsd*S_B (r_B^- m_B^-) *gal dcm* (DE3)	Novagen (Madison, USA)
E. coli Tuner (DE3)	F^- *omp*T *hsd*S_B (r_B^- m_B^-) *gal dcm lac*Y1 (DE3)	Novagen (Madison, USA)

2.2.1.2 *Mycobacterium* strains

All *mycobacterium* strains used in this study are listed in Table 2.2. The *M. bovis* BCG and *M. marinum* strains were purchased from the Statens Serum Institut (Copenhagen, Denmark) and the German Collection of Microorganisms and Cell Cultures (DSMZ; Braunschweig, Germany), respectively. Cell lysates from *M. tuberculosis* were kindly provided by Clara Espitia (Instituto de Investigaciones Biomedicas, UNAM, Mexico City, Mexico).

Table 2.2: *Mycobacterium* strains and their origin

strain	code / ATCC no.	origin
M. bovis BCG Chicago; DSMZ 43990	ATCC 27289	DSMZ, Braunschweig, Germany
M. bovis BCG Copenhagen	Danish strain 1331	Statens Serum Institut, Copenhagen, Denmark
M. marinum; DSMZ 44344	ATCC 927	DSMZ, Braunschweig, Germany
M. marinum; DSMZ 44345	ATCC 11567	DSMZ, Braunschweig, Germany
M. tuberculosis H37Rv	ATCC 25618	C. Espitia, Mexico City, Mexico

2.2.1.3 Plasmids

For cloning and heterologous expression the *E. coli* expression vector pET22b(+) (Novagen, Madison, USA) was used. This 5.5 kb vector carries an N-terminal *pelB* signal sequence for potential periplasmic localization, T7 promoter and terminator, lac operator, pBR322 ori, ampicillin resistance plus optional C-terminal His-tag and is IPTG inducible. The vector pTrcHis A (Invitrogen, Karlsruhe, Germany) containing the mycobacterial thioredoxin reductase open reading frame (ORF) fused to an N-terminal 6xHis-tag was kindly provided by T. H. M. Ottenhoff (Leiden University Medical Centre, Leiden, Netherlands).

For cloning and expression in mycobacteria the plasmid pMV261 was kindly provided by Clara Espitia (Instituto de Investigaciones Biomedicas, UNAM, Mexico City, Mexico). This shuttle plasmid is a 4.5 kb extrachromosomal plasmid designed to express foreign polypeptides as fusion proteins with mycobacterial HSP60. A multicloning site is present after the sixth codon of the HSP60 gene, and expression is under the control of the HSP60 promoter. The *aph* gene from Tn903 confers kanamycin resistance. Origins of replication from *E. coli* pUC19 and mycobacterial pAL5000 are also present (Stover *et al.*, 1991).

2.2.2 Cultivation of *E. coli*

The *E. coli* strain DH5α was used for plasmid transformation and replication. The strains BL21 (DE3) and Tuner (DE3) were used for heterologous expression of recombinant proteins. Cultural conditions were 30 ° C – 37 ° C in LB (Luria-Bertani) medium (Table 2.3) with moderate shaking. For recombinant *E. coli* strains selection was performed by addition of 200 µg/ml ampicillin to the medium. Bacterial stocks were prepared from a single colony and stored at -80 ° C in LB broth containing 50 % (v/v) glycerol.

Table 2.3: Composition of Luria-Bertani (LB) medium

Bacto-Tryptone (Becton Dickinson (BD), Heidelberg, Germany)	10 g/1000 ml
Bacto-Yeast extract (BD, Heidelberg, Germany)	5 g/1000 ml
sodium chloride p.a.	10 g/1000 ml

The pH was adjusted to pH 7.4 with 1 M NaOH. For the preparation of LB agar plates 1.5 % (w/v) Bacto-Agar (BD, Heidelberg, Germany) was added.

2.2.3 Cultivation of mycobacteria

Culture conditions for *M. bovis* BCG and *M. smegmatis* were 37 °C in Middlebrook 7H9 liquid medium or on Middlebrook 7H10 agar (Table 2.4) with moderate shaking of the liquid medium. For recombinant *M. smegmatis* selection was performed by addition of 50 µg/ml kanamycin to the medium. Bacterial stocks were prepared from a single colony and stored at -80 °C in Middlebrook 7H9 broth containing 50 % (v/v) glycerol.

The cultures were frequently tested for contamination by acid fast staining using the ACCUSTAIN Kit (Sigma-Aldrich, Taufenkirchen, Germany).

Table 2.4: Composition of Middlebrook 7H9 medium and 7H10 agar

Middlebrook 7H9 medium:	
Bacto-Middlebrook 7H9 Broth (BD, Heidelberg, Germany)	4.7 g/1000 ml
glycerol (87 % (w/v))	2 ml/1000 ml
Tween 80	5 ml/1000 ml
Bacto-Middlebrook ADC Enrichment (BD, Heidelberg, Germany)	100 ml/1000 ml
Middlebrook 7H10 agar:	
Bacto-Middlebrook 7H10 Agar Base (BD, Heidelberg, Germany)	19 g/1000 ml
glycerol (87 % (w/v))	5 ml/1000 ml
Bacto-Middlebrook OADC Enrichment (BD, Heidelberg, Germany)	100 ml/1000 ml

2.3 General methods of molecular biology

Standard molecular biology methods were used, essentially according to Sambrook *et al*. (2001).

2.3.1 Electrotransformation in *E. coli*

Electroporation was performed according to Dower *et al*. (1988).

Electrocompetent cells were prepared as follows: A single clone of *E. coli* was incubated in 20 ml LB medium overnight at 37 °C with moderate shaking. A volume of 500 ml LB medium was inoculated with 5 ml of this overnight culture and cultivated at 37 °C for 2 – 5 hours until an OD_{600} of 0.6 – 0.8 was reached. The cells were incubated on ice for 30 min and harvested (4 °C, 5000 x g, 15 min). The cells were washed in sequence with 500 ml and 250 ml cold sterile de-ionized water and followed once with sterile 10 % (v/v) glycerol. The pelleted cells were resuspended in 2 ml sterile 10 % (v/v) glycerol, dispensed in 50 µl aliquots and frozen in liquid nitrogen immediately. The competent cells were stored at -80 °C for several months.

For electroporation the cells were thawed on ice. 0.1 - 1 µg desalted DNA to be transformed was added to 50 µl competent cells, mixed well and transferred to a precooled electroporation cuvette (*E. coli* Pulser cuvette, 0.2 cm gap; BioRad, Munich, Germany). Electroporation was carried out at 2.5 kV, 200 Ω and 25 µF with an *E. coli* Pulser (BioRad, Munich, Germany). 1 ml of LB medium was added, the cells were incubated at 37 °C for 1 hour with moderate shaking and then plated on LB plates containing 200 µg/ml ampicillin.

2.3.2 Electrotransformation in *M. smegmatis*

Competent *M. smegmatis* cells were prepared as desribed for *E. coli*. The bacteria were transfected by electroporation (Stover *et al*., 1991) and selection was carried out on 7H10 plates containing 50 µg/ml kanamycin (see 2.3.1).

2.3.3 Preparation of plasmid DNA

Plasmid preparations were performed with the QIAprep Spin Miniprep Kit or the HiSpeed Plasmid Midi Kit (Qiagen, Hilden, Germany) according to the manufacturers advice.

2.3.4 Purification of genomic DNA from mycobacteria

Mycobacterial cells were disrupted in a Mikro-Dismembranator S (Braun, Melsungen, Germany) with 100 µl glass beads (150 – 212 microns; Sigma-Aldrich, Taufenkirchen, Germany). The glass beads were removed and the cell suspension homogenized with a QIAshredder (Qiagen, Hilden, Germany). Isolation of genomic DNA was done with the Dneasy Tissue Kit (Qiagen, Hilden, Germany) according to the manual.

2.3.5 Enzymatic DNA restriction

Restriction endo-nucleases were purchased from MBI Fermentas (St. Leon-Rot, Germany). In each restriction reaction an amount of 3 units enzyme per 1 µg DNA was used. Manufacturer recommended buffer, incubation temperature and time were used.

2.3.6 Ligation

For ligation the molar ratio of insert to plasmid was approximately 3:1. The reaction was carried out in a total volume of 20 µl T4 DNA ligase buffer containing 1 unit T4 DNA ligase (Roche, Mannheim, Germany) per 1 µg DNA. The reaction mixture was incubated at 16 ° C overnight.

2.3.7 Agarose gel electrophoresis of DNA

The separation of DNA by analytical or preparative means was performed at 80 – 100 V in a Wide Mini-Sub Cell or DNA Sub Cell (BioRad, Munich, Germany). 1x TBE buffer (Table 2.5) was used as the gel and running buffer. The GeneRuler 1 kb DNA ladder (MBI Fermentas, St. Leon-Rot, Germany) served as the molecular size marker and 6x Loading Dye Solution (MBI Fermentas, St. Leon-Rot, Germany) as loading buffer. The agarose gels were stained with SYBR Gold solution (1:10000 in TBE; Molecular Probes, Leiden, Netherlands) for 30 min and analyzed with an UV Transilluminator (E.A.S.Y. RH-3 System; Herolab, Wiesloch, Germany).

Table 2.5: Composition of 1x TBE buffer

89 mM	Tris-base
89 mM	boric acid
2 mM	EDTA

2.3.8 DNA extraction from agarose gels

After separation on agarose gels (see 2.3.7) DNA fragments, obtained from PCR, were cut out of the gel and extracted with the QIAquick Gel Extraction Kit (Qiagen, Hilden, Germany) according to the manufacturers advice.

2.3.9 Ethanol precipitation of DNA

1/10 vol 3 M sodium acetate at pH 4.8 and 2 vol ethanol (p.a.) were added to the DNA solution. The mixture was incubated on ice for 10 min and afterwards DNA was precipitated by centrifugation (20000 x g). The DNA pellet was washed twice with 70 % (v/v) ethanol, dried and resuspended in buffer or de-ionized H_2O.

2.3.10 Quantification of DNA

2.3.10.1 Absorbance measurement

The concentration dependent absorbance of nucleotides at 260 nm can be used to determine the concentration and purity of DNA solutions. Absorbance of the DNA solution was measured at 260 nm and 280 nm. An OD_{260} of 1 corresponds to a double stranded DNA concentration of 50 µg/ml. A well purified DNA solution should have an OD_{260}/OD_{280} ratio of 1.5 – 2.

2.3.10.2 Quantification of nucleic acids in agarose gels

Alternatively to the method described in 2.3.10.1, the concentration of nucleic acids can be determined in agarose gels (see 2.3.7). Thus, a defined amount of DNA Mass Ladder (Gibco, Karlsruhe, Germany) was used as a concentration standard.

2.3.11 Oligonucleotides

Desalted and lyophilized oligonucleotides were custom synthesized by Metabion (Martinsried, Germany). The primers used in this study are listed in Table 2.6.

Table 2.6: Primers used in this study

synonym	sequence 5' → 3' (bold letters indicate the restriction site)	restriction site
*Mt*MycRFor	NNN NNN **CTG CAG** ATG GAA ACG TAC GAC ATC GCG ATC	*Pst*I
*Mt*MycRH6Rv	NNN NNN **AAG CTT** TCA GTG ATG GTG ATG GTG ATG ACG CAG GCC AAG CAG CGC GTT	*Hind*III
*Mt*Rv2466cFor	CCC CCC **CAT ATG** CTC GAG AAG GCC CCC CAG	*Nde*I
*Mt*Rv2466cH6Rv	CCC CCC **GAA TTC** CTA GTG GTG GTG GTG GTG GTG GTC GAA CTG AGG CGG CTC GGT	*Eco*RI
*Mt*AhpCFor	G GCG CGC **CAT ATG** CCA CTG CTA ACC ATT GGC GA	*Nde*I
*Mt*AhpCH6Rv	CCG GCG **GGA TCC** TTA GTG GTG GTG GTG GTG GTG GGC CGA AGC CTT GAG GAG TT	*Bam*HI
*Mt*TrxAFor	CCC CCC **CAT ATG** TGT ACC ACT CGA GAC CTC ACG	*Nde*I
*Mt*TrxAH6Rv	CCC CCC **GAA TTC** TCA GTG ATG GTG ATG GTG ATG GGA TGA AGT CTT TGT TCC AGG GCC	*Eco*RI
*Mt*TrxBFor	CCC CCC **CAT ATG** GTG ACT ACC CGA GAC CTC ACT GCC	*Nde*I
*Mt*TrxBH6Rv	CCC CCC **GAA TTC** TCA GTG ATG GTG ATG GTG ATG GGC TTG TTG GGC TCG CCC GTT	*Eco*RI
*Mt*H6TrxCFor	CC CCC CCC **CAT ATG** CAT CAC CAT CAC CAT CAC ACC GAT TCC GAG AAG TCC GCC	*Nde*I
*Mt*TrxCRv	CC CCC CCC **AAG CTT** CTA GTT GAG GTT GGG AAC CAC GTC	*Hind*III
*Mt*AhpDFor	CC CCC CCC **CAT ATG** AGT ATA GAA AAG CTC AAG GCC GCG	*Nde*I
*Mt*AhpDRv	CC CCC CCC **AAG CTT** TTA GCT TGG GCT TAG TGC CTC GAT	*Hind*III
*Mt*H6TPxFor	CCC CCC **CAT ATG** CAT CAC CAT CAC CAT CAC GCA CAG ATA ACC CTG CGA GGA	*Nde*I
*Mt*TPxRv	CCC CCC **AAG CTT** CTA GGC GCC CAG CGC GGC	*Hind*III

2.3.12 Polymerase chain reaction (PCR)

The PCR was performed in a total volume of 50 µl with the PCR Master Mix (ABgene, Hamburg, Germany). The composition of the PCR reaction is listed in Table 2.7.

Table 2.7: PCR reaction compositon

chromosomal DNA / plasmid DNA	0.5 – 1 µg / 10 – 500 ng
5'-primer, 3'-primer	0.5 µM of each
Thermoprime Plus DNA Polymerase	1.25 units
Tris-HCl (pH 8.8)	75 mM
$(NH_4)_2SO_4$	20 mM
Tween 20	0.01 % (v/v)
dATP, dCTP, dGTP, dTTP	200 µM of each
$MgCl_2$	1.5 mM
sterile de-ionized water	to 50 µl total volume

The PCR reaction was carried out in a T3 Thermocycler (Biometra, Göttingen, Germany) as follows:

denaturing:	2 min 96 ° C	1 cycle
denaturing:	1 min 96 ° C	
annealing:	1 min T_A	
elongation:	3 min 72 ° C	30 cycles
elongation:	10 min 72 ° C	1 cycle

2.3.13 DNA sequencing

Automated non-radioactive sequencing of DNA was carried out according to the di-deoxy-method of Sanger (Sanger *et al*., 1977). The ABI PRISM Dye Terminator Cycle Sequencing Ready Reaction Kit (Applied Biosystems, Darmstadt, Germany) was used on a 373A Applied Biosystems DNA Sequencing System (Applied Biosystems, Darmstadt, Germany) according to the manufacturers advice.

2.4 Biochemical methods

2.4.1 SDS polyacrylamide gel electrophoresis (SDS-PAGE)

SDS polyacrylamide gels were used for determining the molecular weight of the denatured proteins and to check the efficiency of recombinant protein expression and purification. SDS-PAGE was performed with the Minigel System (dimension of the gel: 11 cm x 7 cm x 0.1 cm; Biometra, Göttingen, Germany) as described by Laemmli (1970). All samples were diluted 1:2 with 2-fold loading buffer (Table 2.8) and denatured at 95 °C for 10 min. Electrophoresis was performed at 60 V for the stacking gel and at 140 V for the running gel.

Table 2.8: Solutions used for SDS-PAGE

2x SDS loading buffer	**SDS electrophoresis buffer**
100 mM Tris-HCl pH 6.8 200 mM DTT 4 % (w/v) SDS 0.2 % (w/v) bromophenolblue	25 mM Tris-base 250 mM glycin 0.1 % (w/v) SDS
4x Upper Tris	**4 x Lower Tris**
0.5 M Tris-HCl pH 6.8 0.4 % (w/v) SDS	1.5 M Tris-HCl pH 8.8 0.4 % (w/v) SDS
stacking gel (4 %)	**running gel (15 %)**
0.7 ml Rotiphorese Gel 30 (Roth, Karlsruhe, Germany) 1.25 ml Upper Tris 3 ml de-ionized H_2O 12 µl TEMED 6 µl 40 % (w/v) APS	7.5 ml Rotiphorese Gel 30 (Roth, Karlsruhe, Germany) 3.8 ml Lower Tris 3.6 ml de-ionized H_2O 18 µl TEMED 12 µl 40 % (w/v) APS

2.4.2 Coomassie staining

SDS-PAGE gels were fixed for 30 min in a fixing solution (40 % (v/v) ethanol, 10 % (v/v) acetic acid and 50 % (v/v) de-ionized H_2O). The Coomassie staining solution (2 tablets PhastGel Blue R (Amersham Biosciences, Freiburg, Germany) in 1 liter fixing solution) was prewarmed to 55 °C – 60 °C, and the gels were stained for 30 min. After staining the gels were de-stained with a mixture of 25 % (v/v) ethanol, 8 % (v/v) acetic acid and 67 % (v/v) de-ionized H_2O, using a de-stainer model 556 (BioRad, Munich, Germany).

2.4.3 Determination of protein concentration

Protein concentrations were determined by the method of Bradford (1976) using the BioRad Protein Assay (BioRad, Munich, Germany) and BSA (Bovine Serum Albumin) as a standard, according to the manufacturers advice.

2.4.4 Ultra-filtration

Ultra-filtration is a convective process that uses anisotropic semi-permeable membranes to separate macromolecular species and solvents primarily on the basis of their size. It is particularly appropriate for the concentration of macromolecules and has also been used for solvent exchange. For ultra-filtration the Vivaspin centrifugal concentrators (Sartorius, Göttingen, Germany) were used. The molecular weight cut off was chosen to correspond to the molecular weight of the protein.

2.4.5 N-terminal amino acid sequencing

The protein of interest was separated by SDS-PAGE (see 2.4.1), blotted onto PVDF membrane (Immobilon P; Millipore, Schwalbach, Germany) for 30 min at 15 V using a Trans-Blot Semi-Dry Transfer Cell (BioRad, Munich, Germany). The membrane was stained with Coomassie solution (see 2.4.2) until the bands could be seen. The band of interest was cut out of the membrane, washed in de-ionized H_2O and used for sequencing. The N-terminal amino acid sequencing was kindly performed on a protein sequencer 473A (Applied Biosystems, Darmstadt, Germany) by Rita Getzlaff (GBF, Braunschweig, Germany).

2.4.6 Matrix-assisted laser desorption and ionization time-of-flight (MALDI-TOF) mass spectrometry

The molecular masses of the purified recombinant proteins were analyzed by MALDI-TOF mass spectrometry at the GBF (Braunschweig, Germany) using a Bruker Reflex MALDI-TOF (Bruker, Bremen, Germany).

2.4.7 Isolation of mycothiol

Mycothiol (MSH) was isolated from *Mycobacterium smegmatis*. *M. smegmatis* cells were disrupted by boiling them for 10 min at 95 °C in 10 mM Tris-HCl at pH 8. MSH was isolated from the crude *M. smegmatis* soluble extract essentially as described by Unson *et al.* (1998).

2.5 Expression and purification of recombinant proteins

2.5.1 Creation of a Master Seed Bank

To standardize organism cultures and expression conditions a Master Seed Bank (MSB) was set up for each expression strain. Bacterial stocks were prepared from a single colony of each expression strain and stored at -80 ° C in LB (*E. coli*) or 7H9 (*M. smegmatis*) broth containing 50 % (v/v) glycerol.

2.5.2 Induced expression of recombinant proteins in *E. coli*

The open reading frames (ORF) of the genes of interest were cloned into the pET22b(+) expression vector (Novagen, Madison, USA) under the control of an IPTG inducible bacteriophage T7 RNA polymerase promoter. 100 ml preculture (LB + 200 µg/ml ampicillin + 1 % (w/v) glucose) was inoculated with 1 vial from the MSB and incubated overnight at 37 ° C with moderate shaking. The main culture was inoculated with an OD_{600} of 0.1 and grown at 37 ° C until an OD_{600} of 0.6 to 0.8 was reached. At that point expression was induced with 0.5 mM IPTG and the incubation temperature was changed to 30 ° C. The LB medium was supplemented with glucose to maintain low basal expression levels (Grossman *et al.*, 1998). After up to overnight expression, cells were harvested by centrifugation (5000 x g, 15 min, 4 ° C) and cell pellets were stored at -20 ° C until they were used for purification. Cell cultivation and expression was either performed in Erlenmeyer flasks or in a 5-liter Biostat B Fermentor (B. Braun, Melsungen, Germany). All recombinants overexpressed proteins, the corresponding *E. coli* strain and induction times are listed in Table 2.9.

Table 2.9: Overexpressed, recombinant proteins

rec. protein	6xHis-tag	plasmid	strain	induction time
*Mt*Rv2466c	C-terminal	pET22b(+)	*E. coli* Tuner (DE3)	4 h
*Mt*AhpC	C-terminal	pET22b(+)	*E. coli* BL21 (DE3)	overnight
*Mt*AhpD	non	pET22b(+)	*E. coli* Tuner (DE3)	4 h
*Mt*TrxA	C-terminal	pET22b(+)	*E. coli* Tuner (DE3)	5 h
*Mt*TrxB	C-terminal	pET22b(+)	*E. coli* Tuner (DE3)	5 h
*Mt*TrxC	N-terminal	pET22b(+)	*E. coli* Tuner (DE3)	5 h
*Mt*TR	N-terminal	pTrcHis A	*E. coli* Tuner (DE3)	5 h
*Mt*TPx	N-terminal	pET22b(+)	*E. coli* Tuner (DE3)	5 h

2.5.3 Induced expression of *Mt*MycR in *M. smegmatis*

The MycR ORF was cloned with a C-terminal His-tag into the pMV261 vector under the control of the mycobacterial HSP60 promoter. 150 ml preculture (7H9 + 50 µg/ml kanamycin) of the recombinant *M. smegmatis* was inoculated with 1 vial from the MSB and incubated for 48 h at 37 °C with moderate shaking. The main culture was inoculated with an OD_{600} of 0.4 and grown at 30 °C until an OD_{600} of 1.0 was reached. At that point expression was induced by heat shock at 45 °C. At an OD_{600} of 2 the cells were harvested by centrifugation (7000 x g, 30 min, 4 °C) and cell pellets were stored at -20 °C until they were used for purification. Cultivation and expression of the recombinant mycobacterial strain was performed in a 5-liter Biostat B Fermentor (B. Braun, Melsungen, Germany).

2.5.4 Cell disruption by sonication

The pelleted cells were re-supended in 1/10 of the suitable buffer for purification or other means. The cell suspension was cooled on ice and sonicated for 1 min with a Sonoplus Ultrasonic Homogenizer HD 2200 (Bandelin, Berlin, Germany). For volumes more than 10 ml the sonication step was repeated 3 times. After the cell disruption the crude extracts were centrifuged at 25000 x g, 4 °C for 30 min. The supernatant, containing the soluble proteins, was used for purification or for other purposes.

2.5.5 Chromatographic methods

The BioLogic Workstation or the BioLogic DuoFlow System (BioRad, Munich, Germany) was used for all chromatographic applications.

2.5.5.1 Nickel chelate chromatography

For the purification of 6xHis-tagged recombinant proteins the Ni-NTA Superflow resin (Qiagen, Hilden, Germany) was used. This resin allows one-step purification of 6xHis-tagged proteins using high flow rates and pressures for efficient FPLC applications. The capacity for 6xHis-tagged proteins is 5 – 10 mg/ml. Purification buffers and methods were carried out essentially according to the QIAexpressionist Handbook (5^{th} edition; Qiagen, Hilden, Germany). Cells were sonicated in 50 mM NaH_2PO_4, 300 mM NaCl, 10 mM imidazole at pH 8 (binding buffer) and the soluble extract was applied to the column. The column was washed with 5-bed volumes of binding buffer and finally eluted with a linear gradient from 0 % to 100 % elution buffer (binding buffer with 500 mM imidazole). The imidazole concentrations at which the different heterologously expressed proteins eluted, are listed in Table 2.10.

Table 2.10: Imidazole concentration for elution of the recombinant proteins

recombinant protein	imidazole concentration for elution
*Mt*Rv2466c	120 mM
*Mt*MycR	100 mM
*Mt*AhpC	190 mM
*Mt*TrxA	150mM
*Mt*TrxB	125 mM
*Mt*TrxC	100 mM
*Mt*TR	110 mM
*Mt*TPx	180 mM

2.5.5.2 Anion exchange chromatography

An UNOsphere Q column (BioRad, Munich, Germany) was used for anion exchange chromatography according to the manufacturers instruction manual. UNOsphere Q is an high-capacity, high-throughput anion exchange capture support, based on acrylamide and vinylic monomers, designed for process chromatography. The column was equilibrated with 10 bed volumes 20 mM Tris-HCl at pH 7.4. The sample was loaded onto the column, which was then washed with 5 bed volumes of the equilibration buffer. The proteins were eluted by a linear gradient of 0 % to 100 % 20 mM Tris-HCl, 1 M NaCl at pH 7.4.

2.5.5.3 Hydrophobic interaction chromatography (HIC)

For hydrophobic interaction chromatography, a HiLoad 16/10 Phenyl Sepharose High Performance column (Amersham Biosciences, Freiburg, Ger-

many) was used according to the manufacturers advice. HIC separates proteins and peptides on the basis of their varying strength of interaction with hydrophobic groups attached to an uncharged gel matrix. The column was equilibrated with 20 mM Tris-HCl, 1 M $(NH_4)_2SO_4$ at pH 7.4. The protein solution was diluted with 20 mM Tris-HCl, 2 M $(NH_4)_2SO_4$ at pH 7.4 till the final concentration of $(NH_4)_2SO_4$ reached 1 M. The sample was loaded onto the column, which was then washed with 5 bed volumes of the equilibration buffer. The elution was performed by linearly decreasing the concentration of $(NH_4)_2SO_4$. The recombinant expressed mycobacterial AhpD eluted at 400 mM $(NH_4)_2SO_4$.

2.5.5.4 Gel permeation

Sephadex G-25 (Amersham Biosciences, Freiburg, Germany) was used for desalting and for the buffer exchange of larger volumes of protein solutions. Sephadex is a bead-formed gel. Gel filtration separates molecules according to their relative sizes. Large molecules are totally excluded while smaller sized molecules enter the beads to varying extents according to their sizes. Large molecules thus leave the column first followed by smaller molecules in the order of their decreasing size.

2.5.6 Estimation of the molecular size of native proteins

Reduced *Mt*AhpC was chromatographed on a Superdex 200 HR 10/30 column (Pharmacia, Freiburg, Germany) using a mixture of 10 mM sodium phosphate buffer and 20 mM DTT at pH 7.6 as the eluent. High molecular weight standards (Pharmacia, Freiburg, Germany) were used for column calibration. Eluted peroxidase was identified by activity measurements and SDS-PAGE. For size determination of oxidized *Mt*AhpC, the enzyme was incubated with 300 µM *t*-bOOH at room temperature for 30 min in 10 mM

sodium phosphate buffer at pH 7.6. The molecular weight was then estimated by gel permeation chromatography as described above. Gel permeation analyses of reduced and oxidized *Mt*AhpD and *Mt*TPx were performed essentially as described for *Mt*AhpC, using a Superdex 75 HR 10/30 column (Pharmacia, Freiburg, Germany) and low molecular weight standards (Pharmacia, Freiburg, Germany) for column calibration.

2.6 Electron microscopy studies

The electron microscopy studies were kindly facilitated by Heinrich Lünsdorf and Elke Barth (GBF, Braunschweig, Germany). After gel permeation the reduced or oxidized *Mt*AhpC (60 µg/ml final concentration) was adsorbed to an ultrathin carbon foil for 30 s at ambient temperature and was negatively stained immediately in 4 % (w/v) uranyl acetate at pH 4.5, according to Valentine *et al*. (1968). The carbon foil was picked up with perforated collodion microgrids, prepared according to Lünsdorf and Spiess (1986), blotted with filter paper and air-dried. Samples were analyzed with an energy-filtered transmission electron microscope (EFTEM) CEM 902 (Zeiss, Oberkochen, Germany) in the elastic bright-field imaging mode (spectrometer slit: 30 eV; objective aperture: 30 µm; condenser aperture: 300 µm) at 85,000 primary magnification close to the Scherzer focus. Images were directly registered with a cooled 1024 x 1024 CCD-camera (Proscan, Scheuring, Germany) and digitally optimized for sharpness and contrast with Corel Photopaint computer software (Corel Corporation, Ottawa, Canada).

2.7 Enzymatic assays

2.7.1 Insulin reduction assay

Interaction of thioredoxin-like proteins with thioredoxin reductase (TR) was tested through the insulin reduction assay as described by Luthman and Holmgren (1982). In the insulin reduction assay, the rate of conversion of NADPH to $NADP^+$ is measured by the decrease in A_{340}. In this process, reduction equivalents are transferred from NADPH to thioredoxin (Trx) via TR. The reduced form of Trx in turn reduces insulin, thereby separating the A and B chains. The test system contained 13.5 µM *Mt*TR, variable concentrations of Trx-like proteins (*Mt*TrxA, *Mt*TrxB, *Mt*TrxC, *Mt*AhpD or Rv2466c; 0.7 µM to 10 µM), 200 µM bovine insulin (Sigma, Taufenkirchen, Germany), 400 µM NADPH in 50 mM HEPES, 2 mM EDTA at pH 7.4 in a total volume of 500 µl. The decrease in A_{340} was monitored over time, and the amount of NADPH oxidized was calculated with a molar extinction coefficient of 6296 $M^{-1}cm^{-1}$.

2.7.2 MycR assay

The activity of *Mt*AhpC with MSH and *Mt*MycR was tested at 25 °C in a system that contained 450 µM NADH or NADPH, 0.2 µM – 20 µM *Mt*MycR, 0.2 µM – 20 µM MSH, 0.2 µM – 20 µM *Mt*AhpC, 73 µM *t*-bOOH in 50 mM HEPES, 1 mM EDTA at pH 7.4 in a final volume of 500 µl. The decrease in A_{340} was monitored over time.

2.7.3 AhpD assay

The specific activity of *Mt*AhpC with *Mt*AhpD was quantified by measuring the initial velocities through monitoring the NADH oxidation at 340 nm at 25

° C. The test system contained 450 µM NADH, 200 nM *Mt*AhpD, 0.4 U bovine lipoamide dehydrogenase (Sigma, Taufenkirchen, Germany), 50 µM lipoamide, 0.5 µM – 10 µM *Mt*AhpC, 73 µM *t*-bOOH in 50 mM HEPES, 1 mM EDTA at pH 7.4 in a final volume of 500 µl. The reaction was preincubated for 15 min at 25 ° C and started by the addition of peroxide. For the AhpD-dependent kinetic studies of *Mt*AhpC, the conditions were nearly the same as for the measurement of the acitivity using 5 µM *Mt*AhpC and fixed *Mt*AhpD concentrations. A range between 5 µM – 65 µM *t*-bOOH was used for the calculation of the kinetic pattern.

2.7.4 AhpC and TPx assay

The specific activities of *Mt*AhpC with *Mt*TrxC and *Mt*TPx with *Mt*TrxB or *Mt*TrxC were obtained by measuring initial velocities monitoring the NADPH oxidation at 340 nm at 25 ° C. The test system contained 450 µM NADPH, 10 µM *Mt*TR, 10 µM *Mt*TrxB or *Mt*TrxC, 0.5 µM – 15 µM *Mt*AhpC or 0.2 µM – 5 µM *Mt*TPx, 100 nM bovine catalase (Roche, Mannheim, Germany), 73 µM *t*-bOOH in 50 mM HEPES, 1 mM EDTA at pH 7.4 in a final volume of 500 µl. The reaction was preincubated for 15 min at 25 ° C and started by the addtion of peroxide. For the kinetic studies of *Mt*AhpC and *Mt*TPx the conditions were nearly the same as for the measurement of the activities using 5 µM of the peroxidase and fixed thioredoxin concentrations. A range between 5 µM – 65 µM *t*-bOOH was used for the calculation of the kinetic pattern. Specificity for H_2O_2, cumene hydroperoxide, linoleic acid hydroperoxide and phosphatidylcholin hydroperoxide were investigated accordingly. The last two were prepared from soybean lipoxygenase-catalyzed oxidation of the corresponding lipids and were kindly provided by R. Brigelius-Flohé (German Institute of Human Nutrition, Potsdam, Germany).

2.7.5 Steady-state kinetics

Substrate turnover by peroxidases was monitored continuously by NAD(P)H consumption in a coupled test system. The data was analyzed according to Dalziel (1957). Results are presented in terms of the general Dalziel-equation for two substrate reactions:

$$\frac{[E_0]}{v} = \Phi_0 + \frac{\Phi_1}{[A]} + \frac{\Phi_2}{[B]} + \frac{\Phi_{1,2}}{[A]\,[B]} \qquad (1)$$

Where, $[E_0]$ is the total enzyme concentration, v is the initial velocity at pertinent substrate concentrations, and ϕ_0, ϕ_1, ϕ_2, and $\phi_{1,2}$ are kinetic coefficients characterizing a particular enzyme. With enzyme mechanisms not involving ternary complexes between the enzyme and both substrates, the term $\phi_{1,2}$/[A] [B] is zero. In such “ping-pong” or enzyme substitution mechanisms the rate equation simplified to

$$\frac{[E_0]}{v} = \Phi_0 + \frac{\Phi_1}{[A]} + \frac{\Phi_2}{[B]} \qquad (2)$$

Accordingly, re-plotting of the ordinate intercepts, i.e., the reciprocal enzyme-normalized apparent maximum velocities for infinite concentrations of *t*-bOOH (= [A]) against the reciprocal concentrations of the corresponding reductant (= [B]) yields ϕ_0 as ordinate intercepts and ϕ_2 being the slope. ϕ_0 is defined as the reciprocal value of the velocity at infinite concentration of both substrates, that means of k_{cat}. The reciprocal net forward rate constant k'_1, which describes the oxidation of reduced enzyme by ROOH, by definition, equals ϕ_1. ϕ_2 describes a reductant-dependent step, thus must be the reciprocal k'_2.

2.7.6 Stopped-flow kinetics

The stopped-flow analyses were kindly performed by Rafael Radi and Madia Trujillo (Departamento de Bioquímica, Facultad de Medicina, Universidad de la República, Montevideo, Uruguay).

2.7.6.1 Direct measurement of peroxynitrite reduction by *Mt*TPx by stopped-flow technique

*Mt*TPx was reduced by overnight treatment with 10 mM DTT at 4 ° C. Excess reductant was removed immediately before use by gel filtration on Hitrap columns (Amersham Biosciences) using degased 100 mM sodium phosphate buffer, 0.1 mM DPTA (diethylene-triamine-pentaacetic acid) at pH 7 as the eluent, followed by extensive bubbling with argon. Peroxynitrite was synthesized in a quenched flow reactor as described previously (Radi *et al*., 1991; Beckman *et al*., 1994), and excess hydrogen peroxide was removed by treatment with MnO_2. Peroxynitrite concentration was determined spectrophotometrically by the measurement of its absorption at 302 nm in 1 M NaOH (ε_{302} = 1670 $M^{-1}cm^{-1}$). The kinetics of peroxynitrite reaction with reduced *Mt*TPx was studied at 302 nm in a stopped-flow spectrophotometer (SX-17MV, Applied Photophysics) with a mixing time of less than 2 ms, following peroxynitrite decomposition in the presence and absence of the enzyme. To ensure the accuracy of the rate constant determinations, 200 absorbance measurement points were acquired during the initial part of the reaction (first 50 ms) and 200 additional points were acquired until more than 90 % of the peroxynitrite had decomposed (0.5 ms – 20 ms). Computer assisted simulations were performed using Gepasi software (Mendes, 1997). With this experimental approach peroxynitrite can either react with the reduced enzyme to yield the oxidized enzyme and nitrite or it can de-

compose to nitrate after a proton-catalyzed isomerization (k = 0.26 s^{-1} at pH 7.4 and 25 ° C;Koppenol *et al.*, 1992).

$$ONOOH \rightarrow NO_3^- + H^+ \quad (3)$$

$$ONOOH + MtTPx_{red} \rightarrow NO_2^- + MtTPx_{ox} \quad (4)$$

The apparent second order rate constant for the reaction of the enzyme and peroxynitrite at pH 7.4 and 37 ° C was varied in order to get the best fit to experimental data.

2.7.6.2 Rate constant determination of peroxynitrite reduction by competition experiments

Mn^{3+} porphyrins are rapidly oxidized by peroxynitrite (k = 10^5 – 10^7 $M^{-1}s^{-1}$ at pH 7.4 and 37 ° C) to $O{=}Mn^{4+}$ which can be conveniently monitored at the Soret band (Ferrer-Sueta *et al.*, 2003). The inhibitory effect of *Mt*TPx on the oxidation of Mn^{3+}-meso-tetrakis[(N-ethyl)pyridinium-2-yl]porphyrin (Mn^{3+}-TE-2-PyP) by peroxynitrite was determined by stopped-flow techniques, since Mn^{4+} is an unstable species that is readily reduced back to Mn^{3+}, presumably by nitrite (Ferrer-Sueta *et al.*, 1999). Mn^{3+}-TE-2-PyP oxidation by peroxynitrite was monitored at different *Mt*TPx concentrations. Experiments were performed at 25 ° C and the pH was meæsured at the outlet.

Percentage inhibition of peroxynitrite-dependent Mn^{3+}-TE-2-PyP oxidation by *Mt*TPx can be fitted to a hyperbolic function of the type $y = ax/(b+x)$, where "*a*" corresponds to the percentage of initial Mn^{3+}-porphyrin oxidation by peroxynitrite (in the absence of competing enzyme) and "*b*" corresponds to the concentration of enzyme that half-inhibits peroxynitrite-dependent Mn^{3+}-porphyrin oxidation. From this plot a "*b*" value of 5.7 µM was obtained. At that point k_{MtTPx}[*Mt*TPx] equals k_{Mn3+}[Mn^{3+}], which allows the calculation of k_1 for the reaction of the peroxidase with peroxynitrite (k_{MtTPx}).

2.8 Molecular modeling

The molecular modeling was kindly done by Birgit Hofmann (GBF, Braunschweig, Germany). Structure models of *Mt*TPx were generated using Bragi (Schomburg and Reichelt, 1988) and sequence alignments of Clustalx (Thompson *et al.*, 1997). The model of the *Mt*TPx was based on the structure of *Crithidia fasciculata* tryparedoxin peroxidase (TXNPx) (Hofmann *et al.*, 2001) and other peroxiredoxins (Hirotsu *et al.*, 1999; Schroeder *et al.*, 2000). The model of the TPx/Trx intermediate was generated from the model of oxidized *C. fasciculata* TXNPx (Hofmann *et al*., 2001) and the structure of *E. coli* Trx using O (Jones *et al.*, 1991). Initially, the model of oxidized *Mt*TPx alone was refined (Amber6, University of California at San Francisco, www.amber.ucsf.edu/amber/indexs.html) by energy minimization to release strain introduced by sequence exchange. The protein complex was constructed from those refined *Mt*TPx coordinates. Those of *Mt*TrxC were restrained by the introduction of a disulfide bond between C34 of *Mt*TrxC and C93 of *Mt*TPx, and refined by energy minimization, a 50 ps molecular dynamics simulation and a final energy minimization. Calculations were carried out using an 8 Å water shell around the protein molecules.

2.9 Computer analyses

For DNA sequence analysis, alignments, primer design and primer analysis the Vector NTI 6.0 program (InforMax Inc., Oxford, UK) was used. Micrografx Designer 4.1 (Corel Corporation, Ottawa, Canada) was used for creation of figures and schemes. Kinetics data were analyzed by Sigma Plot 8.0 (SPSS Inc., Chicago, USA). Database searches were performed using the NCBI (http://www.ncbi.nlm.nih.gov) and TubercuList (http://genolist.pasteur.fr/TubercuList) databases.

3 Results

3.1 Preparation of system components

The *M. tuberculosis* genome (Cole *et al*., 1998) was screened for homologues of AhpF, thioredoxin-related proteins and peroxiredoxins. For the reconstitution of different peroxidase systems the components were prepared as follows:

The *Mt*MycR ORF (Rv2855) was amplified from *M. tuberculosis* genomic DNA by PCR with the primers *Mt*MycRFor and *Mt*MycRH6Rv. The PCR product was cloned into the mycobacterial expression vector pMV261, digested with corresponding set of restriction enzymes. Protein expression was induced in *M. smegmatis* by heat shock (45 ° C) and the soluble protein was purified by nickel chelate chromatography.

The AhpD ORF (Rv2429) was amplified by PCR using the primers *Mt*AhpDFor and *Mt*AhpDRv and cloned into the procaryotic expression vector pET22b(+) digested with corresponding set of enzymes. Expression was induced in *E. coli* Tuner (DE3) with 0.5 mM IPTG at 30 ° C. The heterologously expressed protein was primarily found in the soluble extract. *Mt*AhpD was purified to homogeneity by anion exchange chromatography and hydrophobic interaction chromatography.

The AhpC (Rv2428), TrxA (Rv1470), TrxB (Rv1471), TrxC (Rv3914), Rv2466c and TPx (Rv1932) ORFs were amplified by PCR using the corresponding primers listed in Table 2.6. The PCR products were cloned into pET22b(+) and expression was induced in *E. coli* Tuner (DE3) or BL21 (DE3) with 0.5 mM IPTG at 30 ° C (induction times are listed in Table 2.9). All proteins were primarily found in the soluble extract. Purification to homo-

geneity of the His-tagged proteins (TrxA, TrxB, TrxC, AhpC, Rv2466c and TPx) was achieved by nickel chelate chromatography (for example see Fig. 3.1).

The correctness of the sequence was verified by DNA sequencing and the identities of the proteins were confirmed by MALDI-TOF analysis and N-terminal Edman degradation.

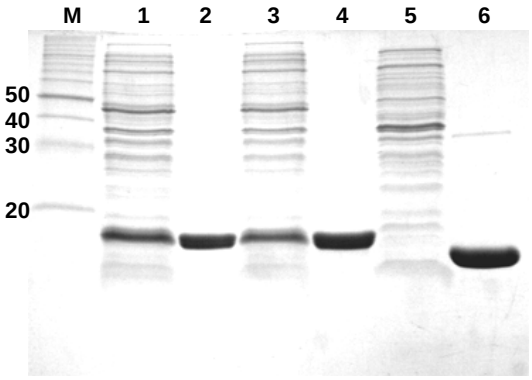

Fig. 3.1: Purification of *Mt*TrxA, B and C using nickel chelate chromatography. SDS-PAGE followed by Coomassie blue staining. Lane 1, crude extract of recombinant *E. coli* Tuner (DE3) [pET22b(+)/*Mt*TrxA] 4 hours after induction; lane 2, purified *Mt*TrxA; lane 3, crude extract of recombinant *E. coli* Tuner (DE3) [pET22b(+)/*Mt*TrxB] 4 hours after induction; lane 4, purified *Mt*TrxB; lane 5, crude extract of recombinant *E. coli* Tuner (DE3) [pET22b(+)/*Mt*TrxC] before induction (control); lane 6, purified *Mt*TrxC; M, protein molecular weight markers. Molecular masses (in kilodaltons) are indicated to the left of the gel.

3.2 Peroxide detoxification pathways

3.2.1 Attempt to reconstitute a mycothiol reductase system

Although attempts to substitute the missing AhpF by homologous mycothiol reductase (*Mt*MycR) and mycothiol (MSH) for alkyl hydroperoxide reductase (*Mt*AhpC) reduction have failed so far (Vergauwen *et al*., 2001), a reconstitution of that system was tried for verification. It was confirmed that *Mt*MycR

does not reduce *Mt*AhpC. Neither did MSH even if kept in its thiol form by NAD(P)H and *Mt*MycR efficiently reduce *Mt*AhpC (see 2.7.2). The potential function of *Mt*MycR and MSH, a small molecular weight thiol proposed to substitute the missing glutathione in mycobacteria, remains elusive. The unsuccessful attempt to reduce *Mt*AhpC rules out its function as *Mt*AhpC reductant.

3.2.2 Reconstitution of the AhpD-dependent AhpC system

It was also confirmed that *Mt*AhpD is reduced by lipoamide and can in turn reduce *Mt*AhpC, as described by Bryk *et al*. (2002). Lipoamide, kept reduced by NADH and, for convenience, by bovine lipoamide reductase, together with *Mt*AhpD and *Mt*AhpC constitute a peroxidase system.

3.2.3 A novel thioredoxin-dependent AhpC system

Intrigued by the recent observation that *Helicobacter pylori*, which like *M. tuberculosis* lacks AhpF, uses thioredoxin for AhpC reduction (Baker *et al*., 2001), attempt was made to reconstitute mycobacterial peroxidase systems by combining AhpC with thioredoxin reductase (*Mt*TR) and various CXXC-containing proteins (Fig. 3.2).

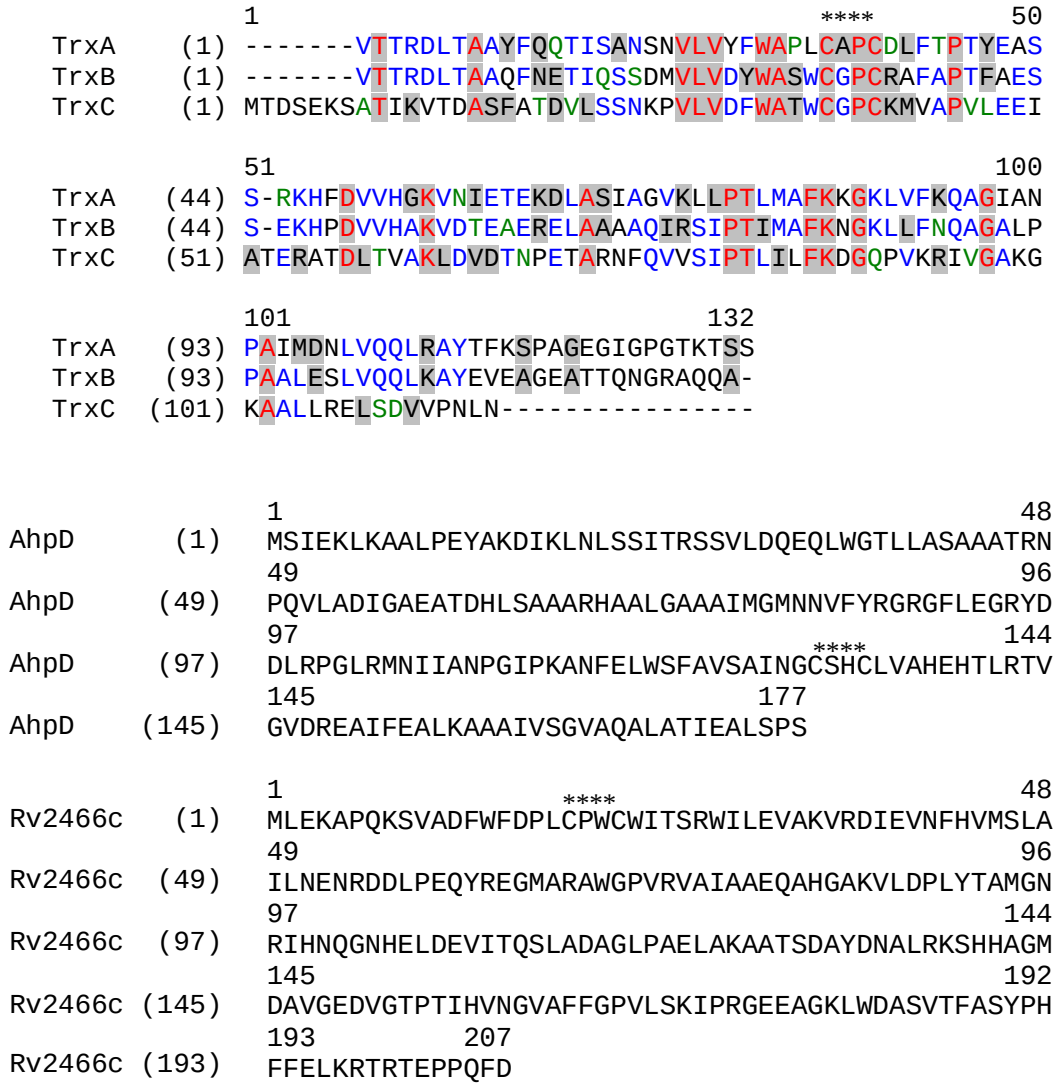

Fig. 3.2: Alignment of thioredoxin A, B and C and amino acid sequences of AhpD and Rv2466c from *M. tuberculosis*. Conserved residues are shown in red, **** indicate the CXXC motifs.

*Mt*TR, which also is homologous to AhpF, did not reduce *Mt*AhpD. *Mt*TR did neither reduce *Mt*TrxA nor the glutaredoxin-related Rv2466c protein but only the *Mt*TrxB and C, as was shown in the insulin reduction assay described by Holmgren and Luthman (1982). TrxB and C were shown to have similar activities, although the redox activity of TrxC was somewhat higher than TrxB (Fig. 3.3). Thus, *M. tuberculosis* has at least two functionally active thiore-

doxins that may protect the pathogen against oxidants derived from the macrophage.

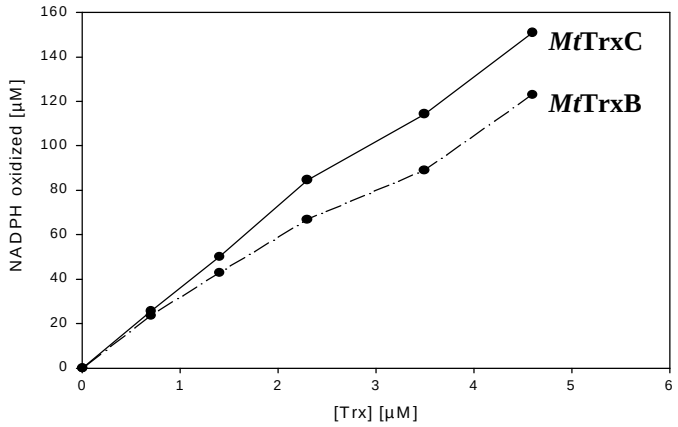

Fig. 3.3: Results of the insulin reduction assay (see 2.7.1). *Mt*TR was used in a concentration of 13.5 µM in combination with variable concentrations of *Mt*TrxB or *Mt*TrxC (0.7 to 4.6 µM) in a total volume of 500 µl. The decrease in A_{340} was monitored over time, and the amount of oxidized NADPH was calculated with a molar extinction coefficient of 6296 $M^{-1}cm^{-1}$.

Surprisingly, *Mt*TrxC efficiently reduced *Mt*AhpC, while *Mt*TrxB did not. Hillas *et al*. (2000) reported that thioredoxin and thioredoxin reductase are not the native partners for *Mt*AhpC and *Mt*AhpD. An explanation for the deviation from the results reported here could be that they did not use TrxC or they could not measure activity due to spontaneous NADPH consumption. When that peroxidase system was reconstituted, the system components led to an unspecific NADPH consumption without the addition of peroxide. H_2O_2 production by autoxidation of reduced *Mt*TR was considered to cause that complication. Indeed there was no NADPH consumption observed after addition of catalase. In further experiments, based on the TR/Trx system, catalase was added to the test systems and the activity was measured with an organic hydroperoxide which is not a substrate of catalase.

3.2.4 Another novel thiol peroxidase system

*Mt*TrxC also reduced another mycobacterial peroxiredoxin (Rv1932) that, by sequence homology, had been classified as a “thiol peroxidase” (TPx) but had never been investigated in regards to its activity and specificity. While studying proteome information on *M. tuberculosis* (Mollenkopf *et al*., 1999) we noticed that Rv1932 (TPx) was present as a dominant spot in 2-D gels. Homologues of TPx are distributed throughout most or all eubacterial species, both Gram-negative and Gram-positive, and are found in pathogenic strains such as *Helicobacter pylori* (Wan *et al.*, 1997), but biochemical and genetic analyses have been limited primarily to *E. coli* TPx (*Ec*TPx). In response to oxidative stress, *E. coli* up-regulates TPx expression (Cha *et al*., 1995; Kim *et al.*, 1996; Kim *et al.*, 1999), and *tpx* deletion mutants, while still viable, were more susceptible to oxidative stress and displayed diminished colony sizes and numbers after exposure to peroxide (Cha *et al*., 1996). *Ec*TPx forms a Trx-linked peroxidase system capable of reducing H_2O_2 and ROOH and protecting against glutamine synthetase inactivation by a mixed function oxidation system (Cha *et al*., 1995; Baker and Poole, 2003).

*Mt*TPx not only accepted *Mt*TrxC, but also *Mt*TrxB although with a slightly lower affinity and reactivity (Table 3.1). *Mt*TPx belongs to a subfamily of 2-Cys-peroxiredoxins which, in contrast to AhpC and other 2-Cys-peroxiredoxins, are considered to be functionally monomeric. Their mechanism of action is believed to involve oxidation of an N-proximal cysteine residue, here Cys-60, to a sulfenic acid derivative by the hydroperoxide substrate. That is followed by formation of an intramolecular disulfide bridge with a distal cysteine, here Cys-94 (see Fig. 4.1). In comparison, in the oligomeric 2-Cys-peroxiredoxins the corresponding reaction center is built up between two subunits (Hofmann *et al*., 2002; Wood *et al*., 2003a; Baker and Poole, 2003).

3.3 Kinetics and particularities

For the characterization and classification of the peroxidase systems discovered in this study, the different systems were analyzed by steady-state kinetics. The kinetic behaviour of the analyzed peroxiredoxins (*Mt*AhpC and *Mt*TPx) was only investigated with the most convenient substrate, *t*-butyl hydroperoxide. As an additional measure of precaution, sufficiently high enzyme concentration was chosen to allow completion of the reaction within less than 10 min. Initial velocities were read from the substrate consumption curves that correspond for up to 13 residual substrate concentrations giving equidistant abscissa points in the double reciprocal plot (primary plot). Thereby, a balanced and unbiased statistical weight of the individual velocities over the substrate range between 95 % and 3 % of the starting concentration was guaranteed. Three data sets were thus generated. The slopes of the regression lines and the ordinate intercepts of three to five independent experiments were averaged and used for the generation of secondary plots to obtain kinetic coefficients and constants (see 2.7.5).

3.3.1 The AhpD-dependent AhpC system

For comparison of the different enzyme systems discovered in this thesis, the *Mt*AhpD/*Mt*AhpC system was analyzed at steady-state kinetics, elucidated here for the first time. The time progression curves were unusual, starting with a lag phase when the fully reduced system was started with *t*-butyl hydroperoxide (*t*-bOOH) as *Mt*AhpC substrate (Fig. 3.4, trace A; arrow). Reversible inhibition by the initially high hydroperoxide concentration does not account for the phenomenon, since it is observed identically from 20 µM up to 73 µM initial [*t*-bOOH]. Surprisingly, the reaction started at maximum rate if *Mt*AhpC and *Mt*AhpD were preincubated with *t*-bOOH for 2 min (Fig. 3.4, trace B) indicating a facilitated interaction of the reactant pairs.

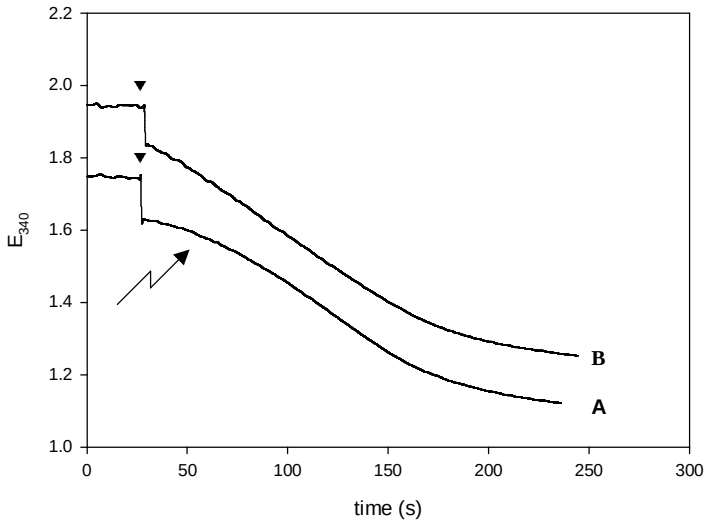

Fig. 3.4: Oxidative activation of the *Mt*AhpC/*Mt*AhpD system by *t*-bOOH. *Mt*AhpC activity with *Mt*AhpD as cosubstrate was tested in a coupled test system where *Mt*AhpD oxidation is continuously monitored by lipoamide/lipoamide dehydrogenase-mediated NADH consumption. Trace A: The reaction mixture was preincubated for 15 min at 25 ° C under reductive conditions and started by the addition of *t*-bOOH (▼). Trace B: The reaction mixture except *Mt*AhpC, *Mt*AhpD and *t*-bOOH was preincubated for 15 min at 25 ° C. *Mt*AhpC, *Mt*AhpD and the hydroperoxide were preincubated together for 2 min at 25 ° C and the reaction was started by the addition of this mixture (▼). Notice the delayed onset of NADH consumption in trace A (arrow).

Redox-dependent conformational changes might improve the accessibility of the reaction centers or transfer the participating proteins into an activated form. Therefore the oligomerization states of *Mt*AhpD and *Mt*AhpC were analyzed.

The X-ray structure of AhpD shows that the protein builds up a trimer in a symmetrical cloverleaf arrangement. Each subunit exhibits a new all-helical protein fold in which the two catalytic sulfhydryl groups, Cys-130 and Cys-133, are located near a central cavity in the trimer (Nunn *et al.*, 2002; Bryk *et al*., 2002). AhpC of *S. typhimurium* tends to form decamers depending on its redox status (Wood *et al.*, 2002). For investigating the impact of the redox state on the oligomerization, the unmodified *Mt*AhpC was reduced by DTT or

oxidized by *t*-bOOH and subjected to gel permeation on a calibrated Superdex 200 column. The effluents were investigated for their: (a) activity by the conventional assay, (b) identity by SDS-PAGE, and (c) shape by electron microscopy (Fig. 3.5 and Fig. 3.6). Reoxidation of the reduced *Mt*AhpC was prevented by equilibrating the column with 20 mM DTT. The reduced protein eluted as a seemingly homogeneous peak with E_{280} paralleling its activity. The eluting material was indistinguishable from authentic *Mt*AhpC in reduced SDS gels displaying a major band complying with the subunit size. Electron micrographs, however, showed a very heterogeneous mixture of ring-shaped, pearl-chain-like, and pearl-like structures (Fig. 3.5 B). The peak fraction eluted with an apparent molecular weight of 224 kDa, which is consistent with the decameric size. The ring structures are considered to represent the pentamers of dimers that were also reported for the AhpC of *S. typhimurium* (Wood *et al*., 2002), and the homologous tryparedoxin peroxidases (TXNPx) of *Leishmania infantum* (Castro *et al.*, 2002) and *Trypanosoma brucei* (Budde *et al.*, 2003). The “pearls” and open chain structures likely represent the dissociating decamers due to reoxidation after gel filtration.

The oxidized enzyme (Fig. 3.6) eluted with a main peak that was similar to the molecular weight of a dimeric protein. Electron microscopy revealed that the main peak consisted of homogeneous dimeric proteins.

For *Mt*AhpD, gel permeation analyses pointed to a trimeric form independent of the redox state (data not shown). Therefore, redox-dependent conformational changes might determine the accessibility of the reaction centers.

For convenience, steady-state analysis was performed without preincubation of *Mt*AhpC and *Mt*AhpD (see 2.7.5). Lipoamide was not oxidized by *t*-bOOH alone: the reaction required the addition of both *Mt*AhpD and *Mt*AhpC. None of the components led to a non-specific NADH consumption. In consequence of the previously mentioned oxidative activation the primary Dalziel plot that

shows the reciprocal hydroperoxide concentration at different fixed *Mt*TrxC concentrations (Fig. 3.7 A) does neither yield constant slopes nor are the slopes measured at different cosubstrate concentrations running in parallel. The apparently 'activated' parts of the turnover curves for *Mt*AhpC yielded a net forward rate constant k'_1, of 1 x 10^4 $M^{-1}s^{-1}$ for the reaction with *t*-bOOH, which marks the lower edge of corresponding peroxiredoxin constants (Hofmann *et al*., 2002; Wood *et al*., 2003a) In that context, a k'_2 for the reduction by *Mt*AhpD of 2.7 x 10^6 $M^{-1}s^{-1}$ which, like the $K_{M\ MtAhpD}$ of 0.23 µM, argues in favour of specific reactivity (Fig. 3.7; Table 3.1).

A

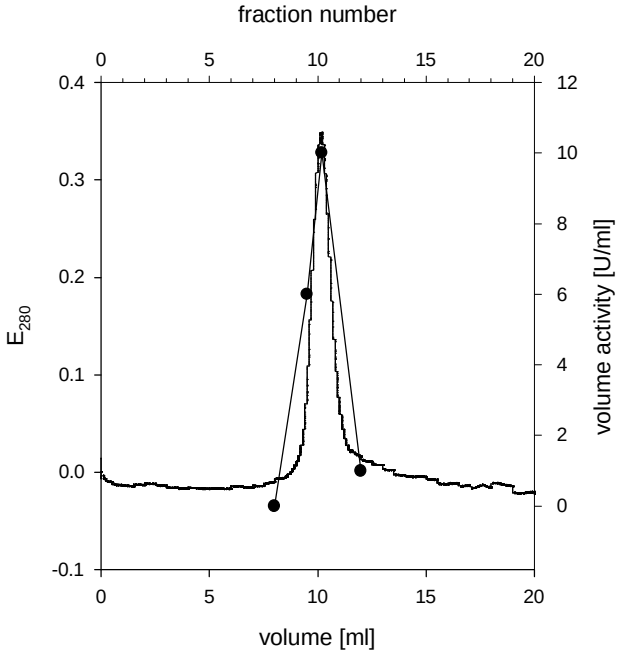

B

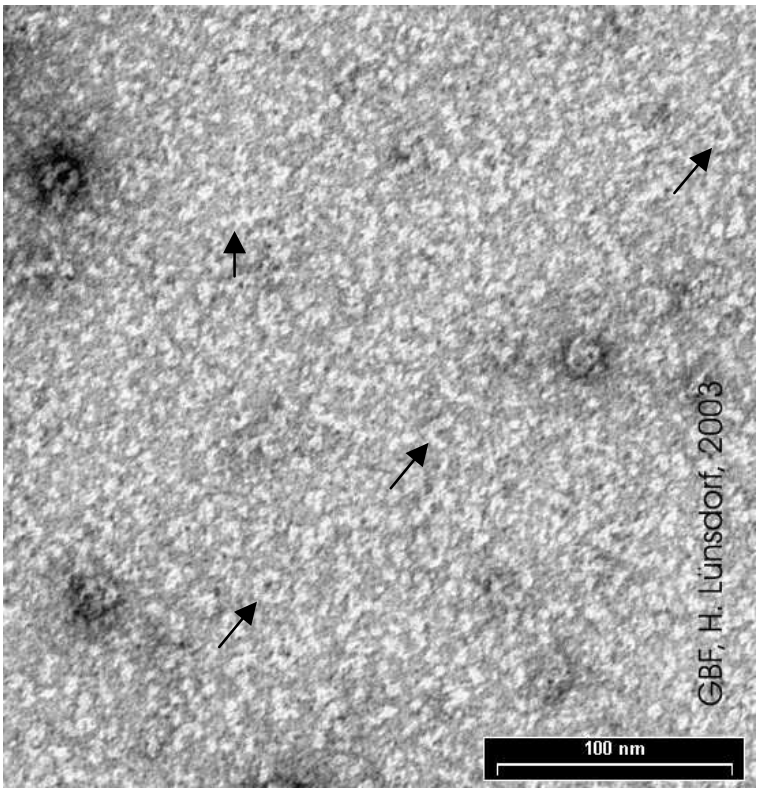

Fig. 3.5: Oligomerization status of reduced *Mt*AhpC. (**A**) Elution profile of DTT-reduced *Mt*AhpC in terms of protein content (E_{280}, solid line) and activity (U/ml, –•–). (**B**) Appearance of the peak fraction in electron microscopy (uranylacetate-stained). Arrows indicate ring-shaped and pearl-chain like structures.

A

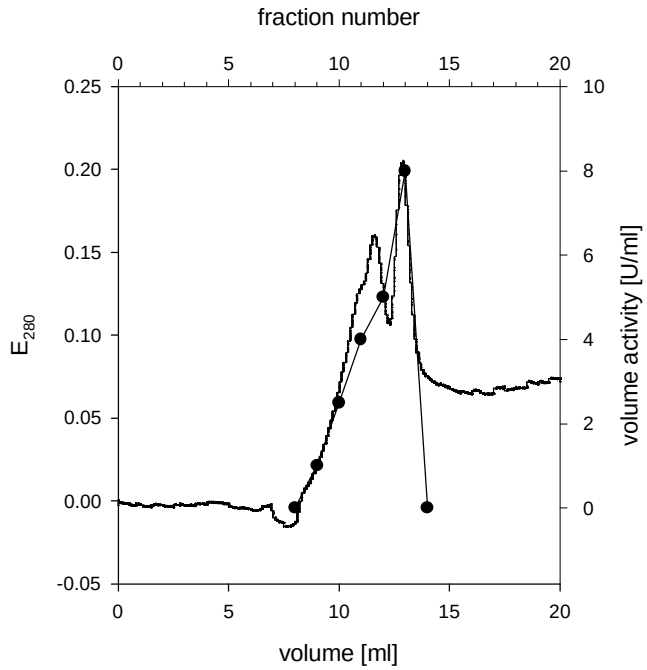

B

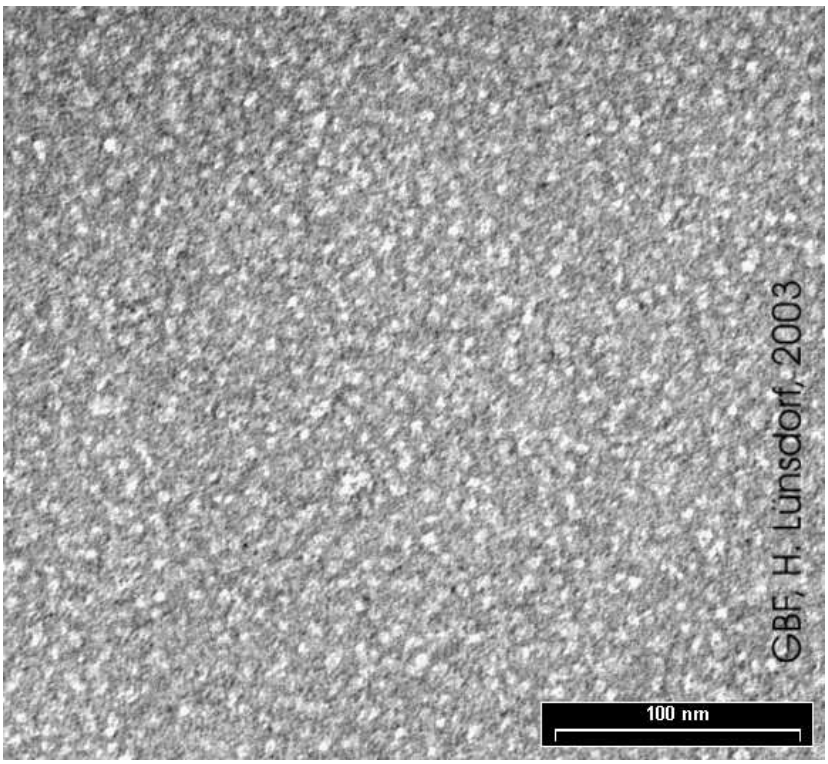

Fig. 3.6: **Oligomerization status of oxidized *Mt*AhpC.** (**A**) Elution profile of *t*-bOOH-oxidized *Mt*AhpC in terms of protein content (E_{280}, solid line) and activity (U/ml, –•–). (**B**) Appearance of the peak fraction in electron microscopy (uranylacetate-stained).

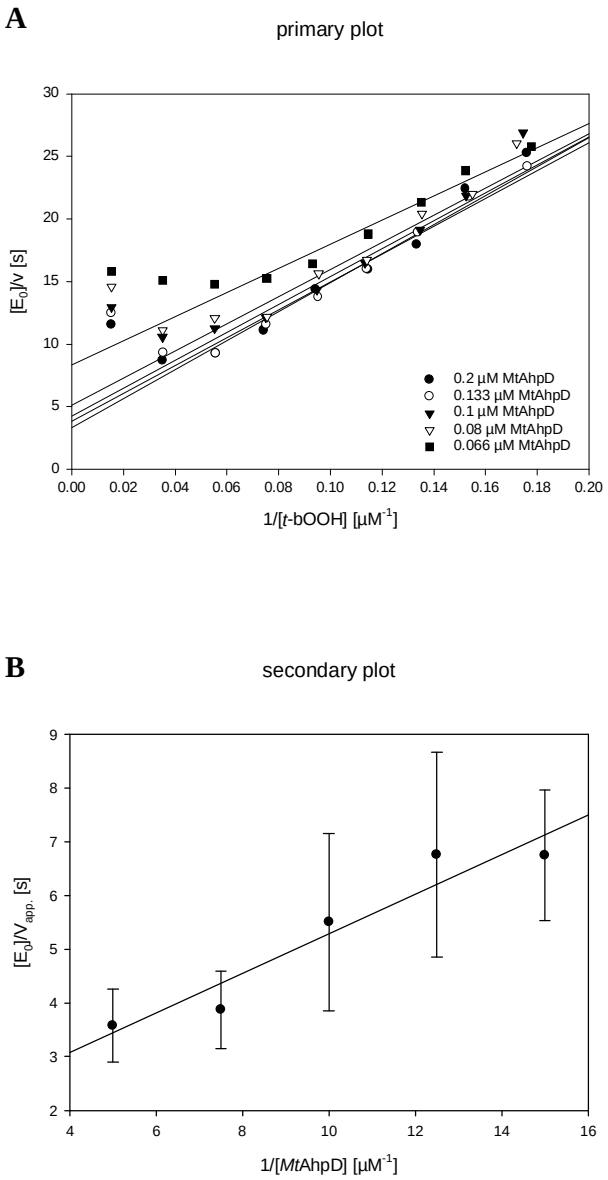

Fig. 3.7: Steady-state-kinetic analysis of *Mt*AhpC with *Mt*AhpD as cosubstrate. Substrate turnover by *Mt*AhpC was monitored continuously by NADH consumption in a coupled test system at 25 °C and pH 7.4 with *t*-butyl hydroperoxide (*t*-bOOH) as substrate and *Mt*AhpD as cosubstrate. Three sets of data were analyzed according to Dalziel (1957). Results are presented in terms of the general Dalziel-equation for a two-substrate reaction ($[E_0]/v = \phi_0 + \phi_1/[ROOH] + \phi_2/[reductant]$; see Table 3.1). **(A)** Example of primary Dalziel plot showing enzyme-normalized inverse initial velocities ($[E_o]/v$) dependent on the reciprocal hydroperoxide concentration at different *Mt*AhpD concentrations, kept constant by continuous regeneration. The slopes correspond to ϕ_1. **(B)** Secondary Dalziel plot: The ordinate intercepts of (A), i. e. the apparent maximum velocities at [A] = ∞, are plotted against 1/[*Mt*AhpD] for evaluation of Dalziel coefficient ϕ_2 (slope), limiting $K_{M\ MtAhpD}$ (abscissa intercept is $1/K_{M\ MtAhpD}$) and real maximum velocities (ordinate intercept is $\phi_0 = [E_0]/V_{max}$). Primary data of three independent analyses, as shown in (A), were used to obtain means and standard deviations.

3.3.2 The thioredoxin-dependent AhpC system

The kinetic analysis of *Mt*AhpC in the system reconstituted by homologous TR and TrxC surprised with irregularities similar to those that had previously been observed with a TXNPx of *L. infantum* (Castro *et al*., 2002) and *T. brucei* (Budde *et al*., 2003), and with the *Mt*TPx in this study. Instead of a typical ping-pong pattern that could be expected from the type of catalysis (Hofmann *et al*., 2002) the primary Dalziel plot does neither yield constant slopes nor appear the slopes measured at different cosubstrate concentrations strictly parallel. In the cases of TXNPx of *L. infantum* and *T. brucei* this kinetic anomaly was interpreted as being indicative of negative cooperativity between subunits. The gel permeation analyses and electron micrographs of reduced *Mt*AhpC (see 3.2.2) yielded an average size of 224 kDa that underscores its decameric nature. The kinetic anomalies of *Mt*AhpC could thus be due to allosteric phenomena as are inferred for other oligomeric peroxiredoxins.

The apparently flatter parts of the turnover curves yielded a k'_1 of 2.3 x 10^4 $M^{-1}s^{-1}$ that is nearly identical to that obtained in the AhpD system, as was expected from the ping-pong-type kinetics of AhpC (Fig. 3.8). Both the k'_2 and the K_M characterizing the reactivity and/or affinity to TrxC compare unfavourately with the constants for AhpD by a factor 10 and 20, respectively, as does the k_{cat} (Table 3.1). Yet the relative cellular abundancies of the potential AhpC reductants (see 4.4) qualify *Mt*TrxC as relevant one.

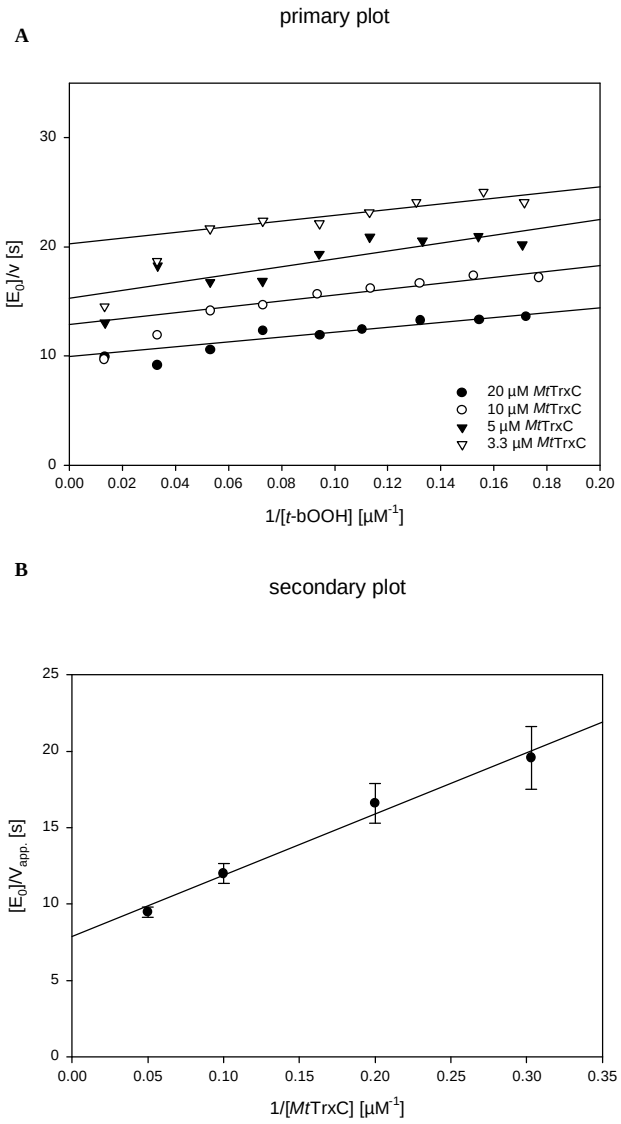

Fig. 3.8: Steady-state-kinetic analysis of *Mt*AhpC with *Mt*TrxC as cosubstrate. Substrate turnover by *Mt*AhpC was monitored continuously by NADPH consumption in a coupled test system at 25 °C and pH 7.4 with *t*-bOOH as substrate and *Mt*TrxC as co-substrate. Three sets of data were analyzed according to Dalziel (1957). Results are presented in terms of the general Dalziel-equation for a two-substrate reaction ($[E_o]/v = \phi_0 + \phi_1/[ROOH] + \phi_2/[reductant]$; see Table 3.1). **(A)** Example of primary Dalziel plot showing enzyme-normalized inverse initial velocities ($[E_0]/v$) dependent on the reciprocal hydroperoxide concentration at different *Mt*TrxC concentrations, kept constant by continuous regeneration. The slopes correspond to ϕ_1. Note the biphasic slopes; only the flatter parts were used for data processing. **(B)** Secondary Dalziel plot: The ordinate intercepts of (A), i. e. the apparent maximum velocities at [A] = ∞, are plotted against 1/[*Mt*TrxC] for evaluation of Dalziel coefficient ϕ_2 (slope), limiting $K_{M\ MtTrxC}$ (abscissa intercept is $1/K_{M\ MtTrxC}$) and real maximum velocities (ordinate intercept is $\phi_0 = [E_0]/V_{max}$). Primary data of three independent analyses, as shown in (A), were used to obtain means and standard deviations.

3.3.3 The thiol peroxidase systems

Steady-state kinetics of *Mt*TPx activity with *t*-butyl hydroperoxide and *Mt*TrxB as substrates (Fig. 3.9) display a classical ping-pong pattern, which can be depicted as a sequence of consecutive reactions,

$$Trx_{red} + TPx_{ox} \leftrightarrow Trx_{ox} + TPx_{red} \quad (5)$$

$$TPx_{red} + ROOH \rightarrow TPx_{ox} + ROH + H_2O \quad (6)$$

where ROH is the corresponding alcohol. These redox reactions are typically observed with peroxidases.

With *Mt*TrxC as substrate, however, the slopes in reciprocal primary plots (Fig. 3.10) appear not to be strictly parallel and show marked deviations from linearity at high peroxide concentrations, particularly pronounced at low cosubstrate levels. To some extent, that could also be observed with the TrxC-dependent AhpC system. As is evident at least from the upper curves in Fig. 3.10 A, the slope is clearly steeper at high hydroperoxide concentrations. Qualitatively, the same phenomenon is seen in the curves obtained at higher TrxC concentrations. Unfortunately, for technical reasons the two phases of the curves could not be assessed with the same accuracy. Only the flatter slopes observed over a wide range of lower hydroperoxide concentrations, could be used for further data processing. Accordingly, the Dalziel coefficients and kinetic constants, obtained from the secondary plot (Fig. 3.10 B) and compiled in Table 3.1, ignore the deviations from the classical ping-pong pattern at extreme substrate concentrations and thus, serve to characterize the enzyme in its predominantly reduced conformation.

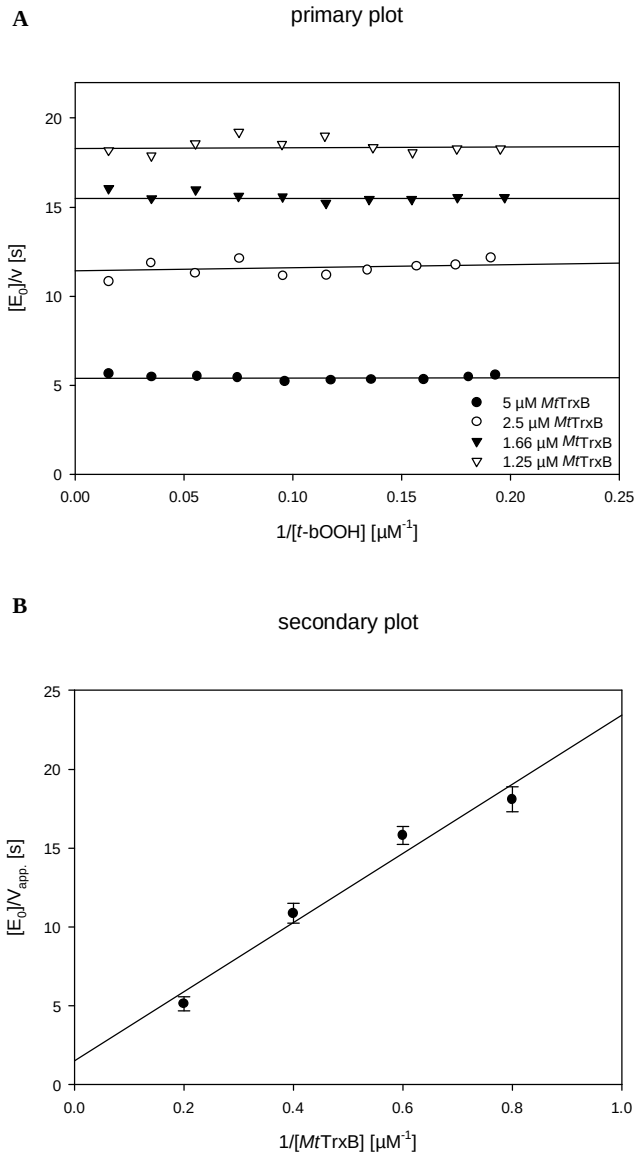

Fig. 3.9: Steady-state-kinetic analysis of *Mt*TPx with *Mt*TrxB as cosubstrate. Substrate turnover by *Mt*TPx was monitored continuously by NADPH consumption in a coupled test system at 25 °C and pH 7.4 with *t*-bOOH as substrate and *Mt*TrxB as cosubstrate. Three sets of data were analyzed according to Dalziel (1957). Results are presented in terms of the general Dalziel-equation for two-substrate reaction ($[E_o]/v = \phi_0 + \phi_1/[ROOH] + \phi_2/[reductant]$; see Table 3.1). **(A)** Example of primary Dalziel plot showing enzyme-normalized inverse initial velocities ($[E_0]/v$) dependent on the reciprocal hydroperoxide concentration at different *Mt*TrxB concentrations, kept constant by continuous regeneration. The slopes correspond to ϕ_1. **(B)** Secondary Dalziel plot: The ordinate intercepts of (A), i. e. the apparent maximum velocities at [A] = ∞, are plotted against 1/[*Mt*TrxB] for evaluation of Dalziel coefficient ϕ_2 (slope), limiting $K_{M\ MtTrxB}$ (abscissa intercept is $1/K_{M\ MtTrxB}$) and real maximum velocities (ordinate intercept is $\phi_0 = [E_0]/V_{max}$). Primary data of three independent analyses, as shown in (A), were used to obtain means and standard deviations.

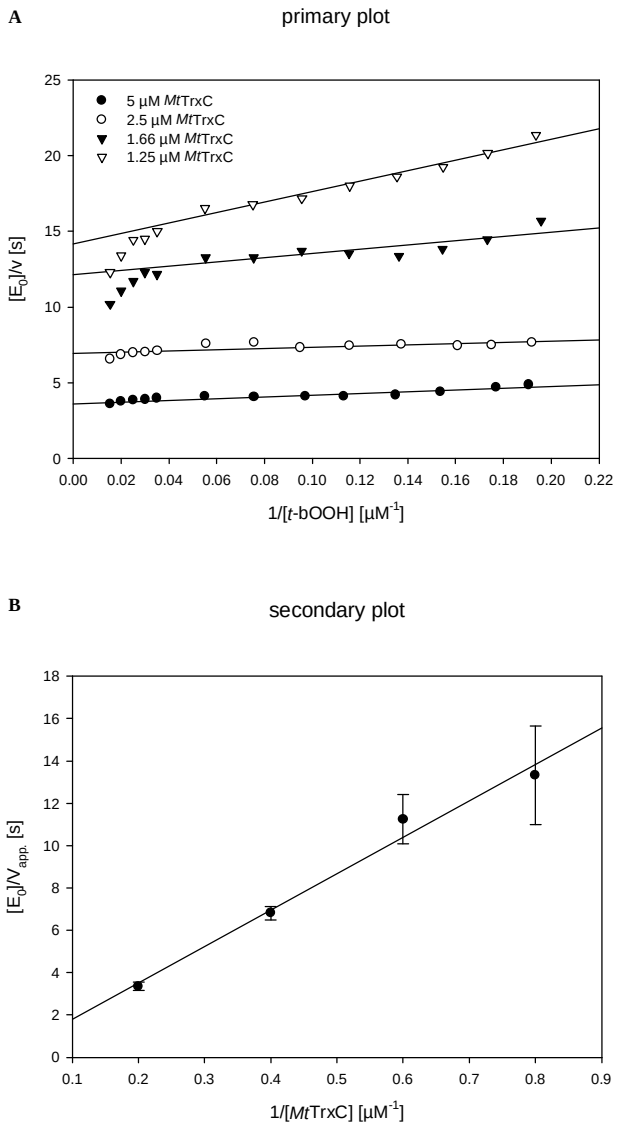

Fig. 3.10: Steady-state-kinetic analysis of *Mt*TPx with *Mt*TrxC as cosubstrate. Substrate turnover by *Mt*TPx was monitored continuously by NADPH consumption in a coupled test system at 25 ° C and pH 7.4 with *t*-bOOH as substrate and *Mt*TrxC as cosubstrate. Three sets of data were analyzed according to Dalziel (1957). Results are presented in terms of the general Dalziel-equation for two-substrate reaction ($[E_o]/v = \phi_0 + \phi_1/[ROOH] + \phi_2/[reductant]$; see Table 3.1). **(A)** Example of primary Dalziel plot showing enzyme-normalized inverse initial velocities ($[E_0]/v$) in dependent on the reciprocal hydroperoxide concentration at different *Mt*TrxC concentrations, kept constant by continuous regeneration. The slopes correspond to ϕ_1. Note the biphasic slopes; only the flatter parts were used for data processing. **(B)** Secondary Dalziel plot: The ordinate intercepts of (A), i. e. the apparent maximum velocities at [A] = ∞, are plotted against 1/[*Mt*TrxC] for evaluation of Dalziel coefficient ϕ_2 (slope) , limiting $K_{M\ MtTrxC}$ (abscissa intercept is $1/K_{M\ MtTrxC}$) and real maximum velocities (ordinate intercept is $\phi_0 = [E_0]/V_{max}$). Primary data of three independent analyses, as shown in (A), were used to obtain means and standard deviations.

As mentioned previously this kinetic anomaly has also been reported for other oligomeric peroxiredoxins, and for *Mt*AhpC in this study. The phenomenon is interpreted as being indicative of negative cooperativity between subunits. Gel permeation analyses of native *Mt*TPx yielded an average size of ~ 36 kDa for the oxidized and reduced enzymes, respectively, indicating that two TPx monomers self-associate in solution independent of their redox state (data not shown). The kinetic anomalies of *Mt*TPx could thus be due to allosteric phenomena as inferred for other oligomeric peroxiredoxins, and for *Mt*AhpC in this study.

The peroxidation efficiency of *Mt*TPx is about one order of magnitude higher than that of *Mt*AhpC. With *Mt*TrxB as cosubstrate a k'_1 value 3.3 x 10^5 $M^{-1}s^{-1}$ was measured and that appears to be more reliable than the corresponding value of 0.9 x 10^5 $M^{-1}s^{-1}$ obtained with *Mt*TrxC. In a ping-pong mechanism, the values should be identical but the latter is likely an underestimate due to the deviations from linearity in the reciprocal plots (Fig. 3.10 A). The k'_2 values of *Mt*TPx for both thioredoxins are similar and slightly higher than *Mt*AhpC for *Mt*TrxC but lower than the *Mt*AhpC/*Mt*AhpD combination. The highest V_{max} was obtained for the *Mt*TPx/*Mt*TrxC system.

Table 3.1: Kinetic constants of *Mt*AhpC and *Mt*TPx. Rate constants were derived from steady-state analysis; the empirical Dalziel coefficients ϕ_0, ϕ_1 and ϕ_2 correspond to the reciprocal values of k_{cat}, k'_1 and k'_2, the latter being net rate constants for the forward reaction of the enzymes with *t*-bOOH and the reductants, respectively.

Enzyme	Reductant	k_{cat} [s^{-1}]	k'_1 [$M^{-1}s^{-1}$]	k'_2 [$M^{-1}s^{-1}$]	$K_{M\ ROOH}$ [µM]	$K_{M\ reductant}$ [µM]
*Mt*AhpC	*Mt*AhpD	0.63 ± 0.10	0.95 x 10^4 ± 0.08	2.7 x 10^6 ± 1.43	65.65	0.23
*Mt*AhpC	*Mt*TrxC	0.13 ± 0.00	2.3 x 10^4 ± 0.07	2.5 x 10^4 ± 0.12	5.64	5.10
*Mt*TPx	*Mt*TrxB	0.66 ± 0.11	3.4 x 10^5 ± 0.48	4.6 x 10^4 ± 0.35	1.95	14.46
*Mt*TPx	*Mt*TrxC	11.11 ± 0.10	0.9 x 10^5 ± 0.22	5.8 x 10^4 ± 0.22	120.68	184.48

3.4 Specificity of *Mt*AhpC and *Mt*TPx for reactive oxygen and nitrogen intermediates

Organic hydroperoxides, peroxynitrite ($ONOO^-$), and other reactive nitrogen and oxygen intermediates produced by macrophages play a role in host defense against invading bacteria (Yu *et al.*, 1999; Nathan and Shiloh, 2000; Akaki *et al.*, 2000; Darrah *et al.*, 2000; Paziak-Domanska *et al.*, 2000; Shiloh and Nathan, 2000). Consequently, many bacterial pathogens have evolved with protection mechanisms against reactive oxygen and nitrogen intermediates (Zahrt and Deretic, 2002).

Like other peroxiredoxins (Hofmann *et al*., 2002), also *Mt*AhpC and *Mt*TPx reduced a variety of hydroperoxides including H_2O_2, yet *Mt*AhpC was inactive with phosphatidylcholin hydroperoxide (PCOOH) and *Mt*TPx did not reduce linoleic acid hydroperoxide (LOOH). The percentage activities listed in Table 3.2 may be considered to correspond to relative changes in k'_1 values, since they were obtained at identical concentrations of reductants.

Table 3.2: Specificity of *Mt*AhpC and *Mt*TPx for hydroperoxide substrates. The enzyme activities with *t*-butyl hydroperoxide (*t*-bOOH) were set to 100 %. LOOH, PCOOH and COOH mean linoleic acid hydroperoxide, phosphatidylcholin hydroperoxide and cumene hydroperoxide, respectively. *The activities with H_2O_2 were difficult to estimate due to the basal activity of the TR/Trx system (see 2.7.4).

Enzyme	Reductant	*t*-bOOH	LOOH	PCOOH	H_2O_2	COOH
***Mt*AhpC**	*Mt*TrxC	(100)	30	0	140*	60
***Mt*TPx**	*Mt*TrxB	(100)	0	6	150*	54

*Mt*AhpC also reduces peroxynitrite (Bryk *et al*., 2000), which is formed by activated macrophages from $\cdot O_2^-$ and ·NO (Alvarez *et al*., 2002) and participates in the oxide-dependent killing of *M. tuberculosis* (St John *et al.*, 2001). The k'_1 value of *Mt*AhpC for peroxynitrite was reported to be 1.33 x 10^6 $M^{-1}s^{-1}$. The reactivity of peroxynitrite with *Mt*TPx, that can not be investigated by steady-state kinetics due to its short half-life (< 1 s at pH 7.4; Radi *et al.*, 2000), was evaluated by stopped-flow techniques: Direct monitoring of peroxynitrite decay at 302 nm yielded the expected first order rate constant of 0.3 s^{-1}. In the presence of 15 µM of reduced *Mt*TPx at 25 ° C, the initial rate of peroxynitrite reduction was too fast to be reliably measured but entire decay curves reasonably complied with that calculated with second order rate constant k'_1 of 1.2 x 10^7 $M^{-1}s^{-1}$ (Fig. 3.11). This fast peroxynitrite reduction was completely inhibited by NEM that is known to inhibit the peroxidatively active thiol of peroxiredoxins (Nogoceke *et al.*, 1997). An independent measurement of k'_1 for the reaction of MtTPx with peroxynitrite by stopped-flow was obtained by measuring the competition with Mn^{3+} porphyrin, that reduces peroxynitrite with a k'_1 of 1.2 x 10^9 $M^{-1}s^{-1}$. The rate constant for *Mt*TPx/peroxynitrite interaction calculated therefrom was 1.5 x 10^7 $M^{-1}s^{-1}$ and thus is the highest so far observed for any of the enzymes working with sulfur catalysis (Fig. 3.12).

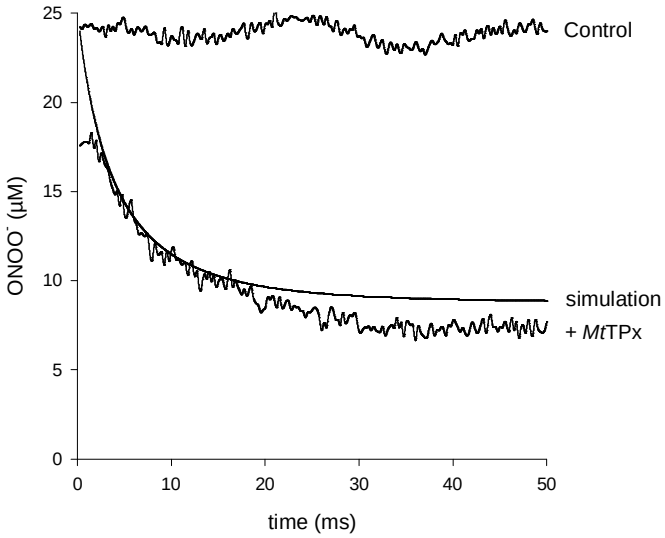

Fig. 3.11: Peroxynitrite reduction by *Mt*TPx. Peroxynitrite (24 µM) decomposition in 100 mM sodium phosphate buffer, 0.1 mM DPTA, pH 7.4, either in the absence (control) or in the presence of reduced *Mt*TPx (15 µM) was followed at 302 nm. The continuous line shows the computer-assisted simulated decay of peroxynitrite (24 µM) in the presence of 15 µM *Mt*TPx assuming a value of 1.2 x 10^7 $M^{-1}s^{-1}$ for the apparent (pH-dependent) second order rate constant between peroxynitrite and the enzyme. Deviations at times longer than 20 ms reflect the reaction of peroxynitrite with targets in the enzyme other than its reactive thiol (Ferrer-Sueta *et al*., 1999).

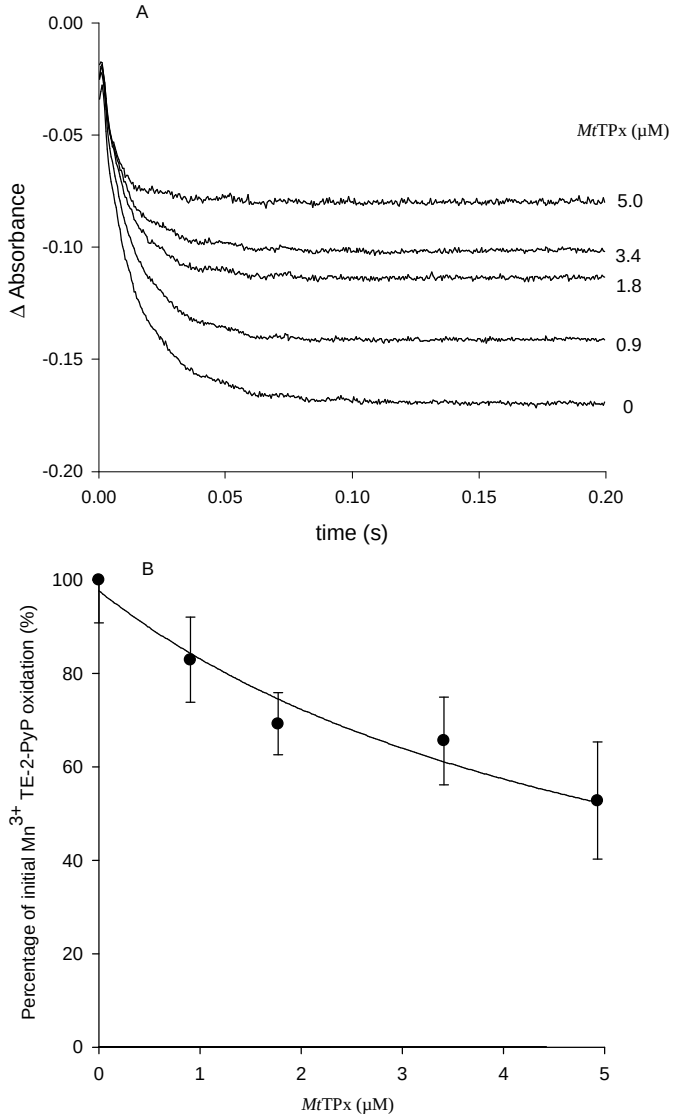

Fig. 3.12: Competition of peroxynitrite-dependent Mn^{3+}-TE-2-PyP oxidation by *Mt*TPx. (A) Mn^{3+}-TE-2-PyP (7µM) was oxidized by peroxynitrite (2µM) in 50 mM sodium phosphate buffer, 0.1 mM DPTA, pH 7.4 at 25 ° C in the absence or presence of different *Mt*TPx concentrations. **(B)** Plotting the initial rate of Mn^{3+}-TE-2-Pyp oxidation against *Mt*TPx concentrations yields a hyperbolic function indicating 50 % inhibition by 5.7 µM *Mt*TPx. With the known rate constant for Mn^{3+}-TE-2-PyP a k'_1 value of the competing *Mt*TPx is therefrom calculated to be 1.5×10^7 $M^{-1}s^{-1}$.

4 Discussion

M. tuberculosis does not exhibit the classical oxidative stress responses, with the *oxyR* regulator being absent from its genome (Deretic *et al*., 1995; Deretic *et al*., 1997; Cole *et al*., 1998). In the absence of OxyR-regulated defense, the catalase/peroxidase enzyme encoded by the *katG* gene has been reported to be the only peroxide-inducible gene in *M. tuberculosis*. The isoniazid-resistant strains of *M. tuberculosis* are especially susceptible to oxidative damage due to a non-functional catalase/peroxidase. Therefore, in the absence of a functional *oxyR* response and the malfunctional *katG*, the tuberculosis bacilli are faced with an unusual situation of survival within the host's macrophages without an effective oxidative stress response. In these strains of *M. tuberculosis*, the *ahpC* gene has been shown to be frequently overexpressed (Wilson and Collins, 1996). AhpC has also been shown to be vital for mycobacterial survival within macrophages (Wilson *et al*., 1998), and is therefore an attractive drug target.

The second peroxidase system discovered and characterized in this study, the TPx system, seems to play another leading role in peroxide detoxification in *M. tuberculosis*, independent of isoniazid susceptibility, and therefore it too represents an attractive drug target. Recent findings provide support for the importance of an AhpC-independent peroxide detoxifying system like the TPx system. It is likely that KatG, AhpC, and TPx participate in partially overlapping defense activities, and that they undergo stage-specific and/or tissue-specific expression with compensatory activities, as previously noted (Musser, 1995; Sherman *et al*., 1996; Dhandayuthapani *et al*., 1996; Heym *et al*., 1997; Wallis *et al.*, 1999; Wallis *et al.*, 2000; Master *et al.*, 2001). The absence of *oxyR*, the silencing of *ahpC*, and its differential expression and infection-stage-specific induction (Springer *et al*., 2001) most likely reflect adaptations of various aspects to the infectious cycle of *M. tuberculosis*. For

example, upon transmission to a new host or possibly during initial stages of reactivation from latent infection, the stationary-phase *M. tuberculosis* probably infects naïve, resting monocytes where AhpC may play a role in resistance to the very early, innate cidal mechanisms of macrophages (Master *et al*., 2002). Once IFN-γ and other protective cytokines become available, AhpC may play a minor role, as indicated by the loss of differential survival between *ahpC*$^+$ and *ahpC*$^-$ cells in macrophages (Springer *et al*., 2001; Master *et al*., 2002). Thus, at that stage TPx systems may play the lead role in peroxide detoxification.

4.1 AhpC and TPx: Members of the peroxiredoxin family

AhpC and TPx are members of the ubiquitous peroxiredoxin (Prx) family within the thioredoxin superfamily of protein folds. Prxs form a family of peroxidases that act on a variety of hydroperoxides using thiols as co-substrates. Until now they were reported to be comprised of glutathione, thioredoxin, tryparedoxin, or the CXXC motifs of bacterial AhpF and AhpD. With most bacterial Prxs, disulfide reduction is achieved by the specialized electron donor AhpF (Poole *et al.*, 2000). In comparison many other Prx systems (both bacterial and eukaryotic), including the AhpC and TPx systems described in this study, receive electrons from a reducing system composed of thioredoxin and thioredoxin reductase (Hofmann *et al*., 2002; Wood *et al*., 2003a). To detoxify peroxides, the reduced N-terminal Cys (peroxidatic cysteine), which is conserved in all Prxs, attacks the peroxide -O–O- bond, with concomitant formation of a cysteine sulfenic acid (Cys–SOH) intermediate,

$$Cys{-}S^- + H^+ + ROOH \rightarrow Cys{-}SOH + ROH. \qquad (7)$$

It then condenses with a conserved C-terminal Cys (resolving cysteine) to regenerate the stable disulfide bond at the active site (Poole and Ellis, 2002; Baker and Poole, 2003)

$$Cys{-}SOH + RSH \rightarrow Cys{-}S{-}SR + H_2O. \quad (8)$$

Prxs are divided into three classes: typical 2-Cys Prxs; atypical 2-Cys Prxs; and 1-Cys Prxs. All Prxs share the same basic catalytic mechanism, in which an active-site cysteine (the peroxidatic cysteine) is oxidized to a sulfenic acid by the peroxide substrate. The recycling of the sulfenic acid back to a thiol is what distinguishes the three enzyme classes.

The typical 2-Cys Prxs are the largest class of Prxs and are identified by the conservation of their two redox-active cysteines, the peroxidatic cysteine (generally near residue 50) and the resolving cysteine (near residue 170) (Hofmann *et al*., 2002). Typical 2-Cys Prxs are obligate homodimers containing two identical active sites (Hirotsu *et al*., 1999; Alphey *et al.*, 2000; Schroeder *et al*., 2000; Wood *et al*., 2002). In the second step of the peroxidase reaction, the peroxidatic cysteine sulfenic acid from one subunit is attacked by the resolving cysteine located in the C-terminus of the other subunit. This condensation reaction results in the formation of a stable intersubunit disulfide bond, which is then reduced by one of several cell-specific disulfide oxidoreductases (e.g. thioredoxin, AhpF, tryparedoxin or AhpD (Nogoceke *et al*., 1997; Poole *et al*., 2000; Bryk *et al*., 2002)), completing the catalytic cycle.

The second class of Prxs are the atypical 2-Cys Prxs, which have the same mechanism as typical 2-Cys Prxs but are functionally monomeric (Seo *et al.*, 2000; Declercq *et al.*, 2001; Baker and Poole, 2003). In these Prxs, both the peroxidatic cysteine and its corresponding resolving cysteine are contained within the same polypeptide, with the condensation reaction resulting in the formation of an intramolecular disulfide bond. Although the resolving cys-

teines of typical and atypical 2-Cys Prxs are not conserved in sequence, they are functionally equivalent.

The last class of Prxs, the 1-Cys Prxs, conserve only the peroxidatic cysteine and do not contain a resolving cysteine (Choi *et al.*, 1998). Their cysteine sulfenic acid generated through reaction with peroxides is presumably reduced by a thiol-containing electron donor. In few examples, the donor has been shown to be glutathione (GSH) (Hofmann *et al*., 2002), but the identity of the redox partner is not yet clear in most cases.

4.2 AhpC and TPx homologues

AhpC has sequence homology to the two cysteine containing AhpC proteins from other organisms and seems to belong to the typical 2-Cys Prxs. It has a higher similarity to the Gram-positive (*M. bovis, M. smegmatis*, *Corynebacterium diphtheriae*, and *Streptomyces viridosporus*) than to the Gram-negative (*E. coli*, *S. typhimurium*, *Bacillus subtilis*, and *Staphylococcus aureus*) AhpC proteins. Interestingly the *M. tuberculosis* AhpC possesses three Cys residues, two located in close vicinity in the C-terminal region, at positions 174 and 176. The conserved N-terminal Cys residue is located at position 61. Both the Cys-174 and Cys-176 residues can form a disulfide bond with the conserved N-terminal Cys residue (Chauhan and Mande, 2001) and all the three Cys residues are important for activity. Cys-61 and Cys-174 play a critical role but Cys-176 is also involved in the catalytic cycle (Hillas *et al*., 2000; Chauhan and Mande, 2002).

Homologues of TPx are distributed throughout most or all Gram-positive and Gram-negative bacteria, but biochemical analyses have been limited primarily to *E. coli* TPx. *Ec*TPx is part of an oxidative stress defense system that uses equivalents from thioredoxin and thioredoxin reductase to reduce alkyl hydroperoxides. TPx homologues typically contain three Cys residues,

Cys-93, Cys-80, and Cys-60 in *Mt*TPx, and the latter residue aligns with the N-terminal active site Cys of other peroxidases in the Prx family.

4.3 Structural and conformational properties of *Mt*AhpC and *Mt*TPx

AhpC and TPx are both members of the Prx family; however, the two *M. tuberculosis* Prx members are highly divergent from one another and are representatives of two distinct Prx subfamilies: typical 2-Cys Prxs (*Mt*AhpC), and atypical 2-Cys Prxs (*Mt*TPx) (Hofmann *et al*., 2002; Wood *et al*., 2003a). Generally, the active site of typical 2-Cys Prxs contains a disulfide bond composed of a conserved N-terminal Cys (Cys-46 from *S. typhimurium* AhpC) and the C-terminal Cys (Cys-165 from *S. typhimurium* AhpC) from the other subunit of the parallel, but directionally opposite, dimer (Ellis and Poole, 1997). Crystal structures of reduced (tryparedoxin peroxidase from *Crithidia fasciculata*), oxidized (HBP23 from rat) and overoxidized (TPxB from human) typical 2-Cys Prx homologues showed that reduction of the disulfide bridge induces a conformational change in the quarternary structure from a dimeric to a decameric form or *vice versa* (Hirotsu *et al*., 1999; Alphey *et al*., 2000; Schroeder *et al*., 2000). Although oligomerization seems to be a general property of 2-Cys Prxs, the *in vivo* parameters inducing oligomerization and its function are unknown. Low or high ionic strength, acidic pH, and reducing or oxidizing conditions are reported to promote oligomerization but differ in their effects upon various 2-Cys Prxs (Chauhan and Mande, 2001; Wood *et al*., 2002; Budde *et al*., 2003; König *et al.*, 2003). Gel permeation analyses and electron microscopy studies provide evidence for a redox-dependent process in *M. tuberculosis* AhpC whereby reduced decamers disassociate very rapidly into dimers upon oxidation. That was also reported for *S. typhimurium* AhpC (Wood *et al*., 2002). A facilitated interaction of *Mt*AhpC with its reductant *Mt*AhpD due to redox-dependent conforma-

tional changes and ‘activation’ could explain the unsual lag phase in time progression curves (see Fig. 3.4).

Atypical 2-Cys Prxs like *Mt*TPx are proposed to be functionally monomeric (Declercq *et al*., 2001). For the *E. coli* homologue of TPx it was reported that it does not form the hallmark intersubunit disulfide linkage of typical 2-Cys Prxs, and instead Cys-61 (Cys-60 from *Mt*TPx) links with Cys-95 (Cys-93 from *Mt*TPx) through an intra-molecular disulfide bond. Cys-95 participates as a disulfide partner and is functionally equivalent to the resolving cysteine that resides in another subunit of the more common typical 2-Cys Prxs. Based on the structural data of *C. fasciculata* TXNPx (Hofmann *et al*., 2001) and other peroxiredoxins (Hirotsu *et al*., 1999; Schroeder *et al*., 2000) a model of TPx from *M. tuberculosis* was created, which provides evidence for a similar mechanism for *Mt*TPx (Fig. 4.1). Gel permeation analyses revealed a homodimeric nature of *Mt*TPx, as was also shown for *Ec*TPx by ultracentrifugation analyses (Baker and Poole, 2003). 1-Cys Prxs are also functionally monomeric, but form homodimers at protein concentrations > 1 mg/ml (Choi *et al*., 1998) and therefore, the formation of *Mt*TPx dimers could occur due to high protein concentration. In conclusion, unlike the more common typical 2-Cys Prxs, which operate by an intersubunit disulfide mechanism, *Mt*TPx contains a redox-active intrasubunit disulfide bond yet is homodimeric in solution.

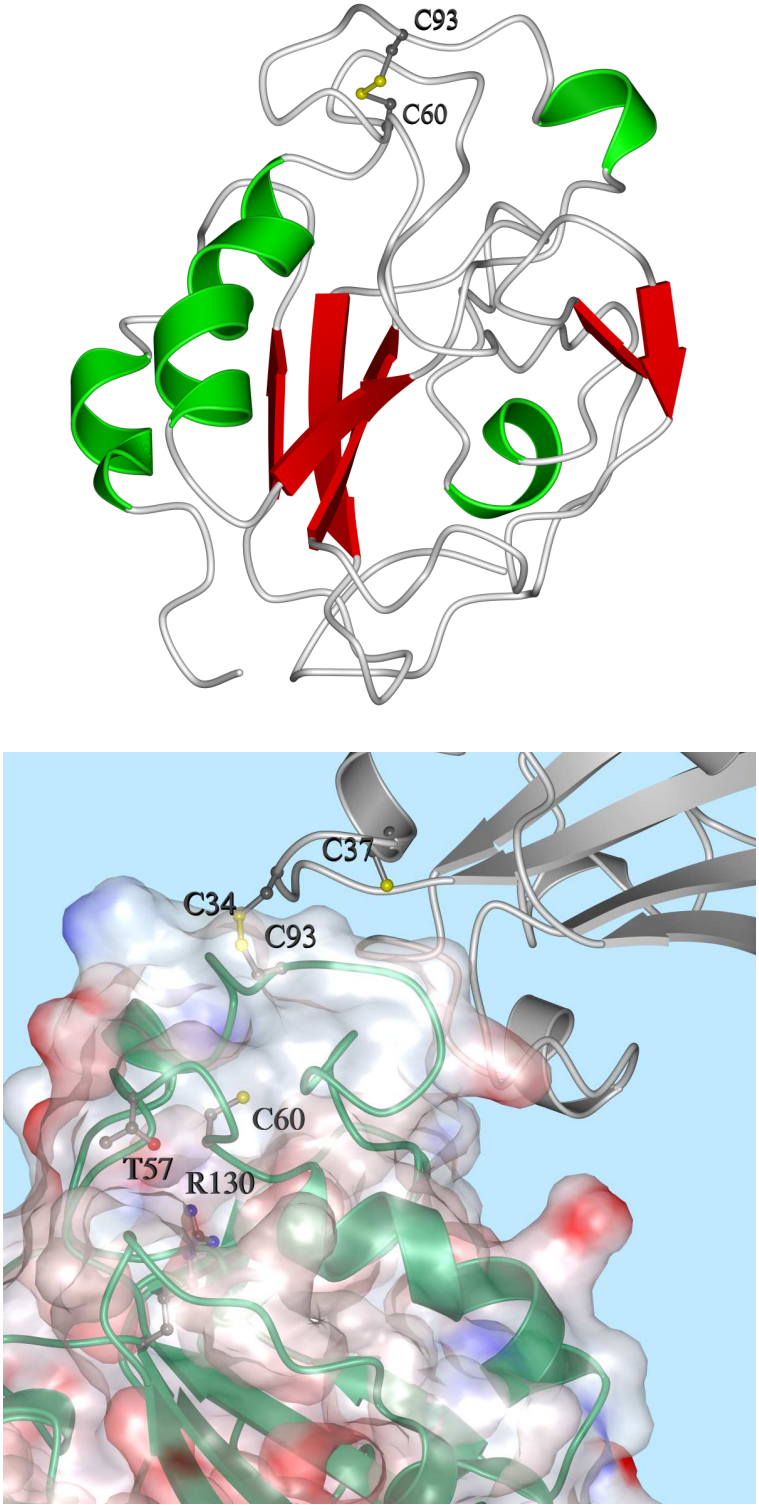

Fig. 4.1: Model of *Mt*TPx (upper panel) and a TPx/Trx catalytic intermediate (lower panel). Upper panel: Conformation of oxidized MtTPx, as modeled into the structure of *C. fasciculata* TXNPx. The intramolecular disulfide bond is shown as balls and sticks. Lower panel: Model of a catalytic intermediate demonstrating potential TPx/Trx interactions. The solvent exposed C34 of the *Mt*TrxC (ribbon diagram) has reacted with the accessible C93 (resolving cysteine) of the *Mt*TPx. Surface charges are shown in red (negative) and blue (positive), residue designations in red.

The kinetic analyses of the TrxC/AhpC and TrxC/TPx system did not comply with a simple ping-pong mechanism, as is common for peroxidases. In other words, oxidation of the enzyme by the hydroperoxide substrate followed by an independent reaction with the reductant (Dalziel, 1957; Ursini *et al.*, 1995; Flohé and Brigelius-Flohé, 2001; Hofmann *et al*., 2002). Particularly intriguing were deviations from linearity in the double-reciprocal plots (Fig. 3.8 A; Fig. 3.10 A). Such irregularities had already been reported for the kinetic behaviour of the mitochondrial TXNPx of *Leishmania infantum* (Castro *et al*., 2002) and the TXNPx of *Trypanosoma brucei brucei* (Budde *et al*., 2003). In those cases, the phenomenon was interpreted as negative cooperativity between subunits. Our kinetic and morphological data support the concept of negative cooperativity to be valid also for *Mt*AhpC and *Mt*TPx. Taking into account the growing number of Prxs with an irregular kinetic behaviour, not following strictly linear Lineweaver-Burk or Dalziel plots might rather be the rule than the exception for Prxs.

It remains an intriguing question as to what extent the cooperativity concept may be extended to other 2-Cys Prxs. Certainly there are qualitative differences: with TXNPxs of *L. infantum* and *T. brucei brucei*, for instance, a dimer to decamer transition was reported to be induced by oxidation (Castro *et al*., 2002; Budde *et al*., 2003). In contrast, with AhpC of *M. tuberculosis* and *S. typhimurium* (Wood *et al*., 2002) the decamer is stabilized by reduction. In general, however, the 2-Cys Prxs qualify as potentially cooperative proteins. Since the early conceptual thoughts as to why proteins form oligomers that communicate with each other, cooperativity has been considered as a tool for metabolic regulation (Monod *et al*., 1965; Koshland, 1970; Stadtman, 1970). The Prxs appear to support that view. If not in control of peroxide detoxification Prxs are evidently involved in regulating signaling cascades or metabolic processes (Hofmann *et al*., 2002; Wood *et al*., 2003b). The evident cooperative potential of the Prxs deserves particular attention when the biological function of this novel family of proteins is to be explored.

4.4 Physiological relevance of the *Mt*AhpC and *Mt*TPx systems

The kinetic constants compiled in Table 3.1 and derived from Fig. 3.11 and Fig. 3.12 allow the estimation of turnover rates for the different mycobacterial peroxidase systems (Fig. 4.2), by means of the general rate equation for two-substrate ping-pong mechanisms,

$$[E_0]/v = \phi_0 + \phi_1/[ROOH] + \phi_2/[reductant] \quad (9)$$

if, as a first approximation, the peculiarities of peroxiredoxin kinetics at extreme substrate concentrations are ignored. Unfortunately, however, the concentrations of the enzymes appear to vary between strains and substrate concentrations can only be roughly estimated. At low peroxide level and high supply of reductants, as is commonly assumed for unstressed situations, the turnover depends on the level of reduced peroxidase that should approximately equal $[E_0]$, on k'_1 and on the peroxide concentration

$$v = k'_1 [E_{red}] [ROOH]. \quad (10)$$

AhpC is hardly detected in most of the *katG*$^+$ strains of *M. tuberculosis* and *M. marinum*, but is easily found in *M. smegmatis* and *M. bovis* BCG. In contrast, *Mt*TPx is consistently seen in proteomes of *M. tuberculosis*. Its concentration may be estimated to be much higher than AhpC (Pagan-Ramos *et al*., 1998; Jungblut *et al.*, 1999; Mollenkopf *et al.*, 1999; Springer *et al*., 2001). Being the dominant peroxiredoxin and having a higher k'_1 than AhpC, *Mt*TPx may definitely be rated as the more relevant enzyme.

Under H_2O_2 stress the reductant capacity may become limiting according to

$$v = k'_2 [E_{ox}] [reductant]. \quad (11)$$

The concentration of the reductants is linked in a complex manner to the NADH and NADPH pools and depends on the speed of regenerating en-

zymes and the pool size of the reductant, only the latter being easily estimated. AhpD is identifiable in *M. tuberculosis* proteomes as a minor spot corresponding to a low molarity level. In comparison, *Mt*TrxB, although known by its sequence and characterized here as a specific substrate of *Mt*TPx, so far could not be identified in proteomes. To the contrary, *Mt*TrxC is always seen as a major protein in all *M. tuberculosis* strains investigated. *Mt*TR is a medium spot in all mycobacterial proteomes analyzed (Nagai *et al.*, 1991; Sonnenberg and Belisle, 1997; Weldingh *et al.*, 1998; Jungblut *et al*., 1999; Mollenkopf *et al*., 1999; Rosenkrands *et al.*, 2000a; Rosenkrands *et al.*, 2000b). Thus, because of their high reduction capacities, the *Mt*TR/TrxC-mediated detoxification systems should become particularly relevant under conditions of oxidative stress.

Considering both rate constants and capacities, NADPH-driven H_2O_2 reduction by the *Mt*TR/*Mt*TrxC/*Mt*AhpC and the *Mt*TR/*Mt*TrxC/*Mt*TPx systems should be at least as efficient as the NADH-driven, AhpD/AhpC-mediated system in coping with H_2O_2 challenge in *katG*$^-$ strains. Both peroxiredoxin-type peroxidases, however, may also satisfy special antioxidant requirements in *katG*$^+$ strains by acting on a broad spectrum of hydroperoxides. *Mt*AhpC reduces complex lipid hydroperoxides with complementary efficiencies and *Mt*TPx can even compete with catalase in peroxynitrite reduction (Table 3.2; Fig. 3.11 and Fig. 3.12). Therefore, both *Mt*AhpC and *Mt*TPx complement catalase in antioxidant defense of *M. tuberculosis* as do broad spectrum selenoperoxidases, such as GPx-1, in the host (Flohé and Brigelius-Flohé, 2001; Fig. 4.2 A), where the peroxiredoxins fall short in catalytic efficiencies and are more likely involved in specific redox regulation of metabolic processes (Hofmann *et al*., 2002; Wood *et al*., 2003b). In mycobacteria, being devoid of the GSH-dependent detoxification system, the peroxiredoxins should significantly contribute to the pathogen's resistance to the oxidative and nitrosative stress exerted by the innate immune response.

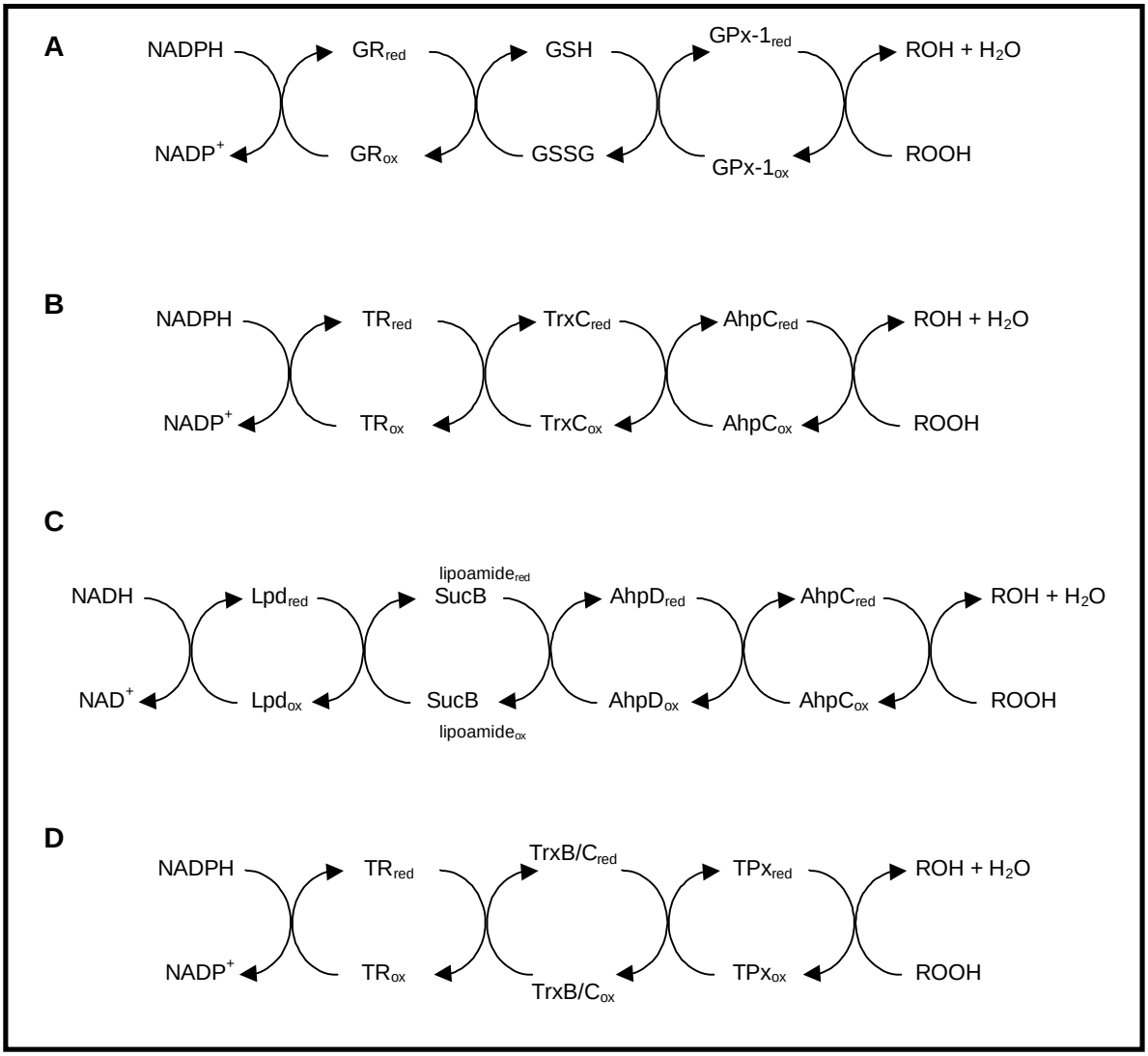

Fig. 4.2: Hydroperoxide detoxifying systems in *M. tuberculosis*. (A) The main route of mammalian hydroperoxide reduction is shown for comparison. **(B)** NADPH-driven hydroperoxide reduction by AhpC, mediated by TR and TrxC. **(C)** NADH-driven and AhpD-mediated hydroperoxide reduction by AhpC according to Bryk *et al*. (2002). **(D)** NADPH-driven hydroperoxide reduction by TPx, mediated by TR and TrxB or TrxC, respectively. AhpC, alkyl hydroperoxide reductase subunit C; AhpD, alkyl hydroperoxide reductase subunit D; GPx-1, type-1 glutathione peroxidase; GR, glutathione reductase; GSH, glutathione; GSSG, oxidized glutathione; Lpd, dihydrolipoamide dehydrogenase; SucB, dihydrolipoamide succinyltransferase; TPx, thiol peroxidase; TR, thioredoxin reductase; Trx, thioredoxin.

4.5 AhpC and TPx are potential drug targets

Tuberculosis has re-emanated as a growing global health problem not only because of the lack of proper therapeutic agents for its treatment but also due to the development of drug-resistant strains. The disease still continues its ravenous journey across the world killing young and middle-aged adults faster than any disease other than AIDS. Despite the widespread use of the bacillus Calmette-Guérin vaccine and the availability of antibiotics against *M. tuberculosis*, it is estimated that in 1997 there were approximately eight million new cases of tuberculosis and nearly two million deaths due to the disease (Dye *et al*., 1999). The emergence of MDR strains of the deadly pathogen render the current mode of treatment very difficult and in many cases completely ineffective. Thus, newer and more efficient anti-TB drugs are desperately needed. The unravelling of the *M. tuberculosis* genome sequence (Cole *et al*., 1998), gives new dimensions to anti-TB drug research. It has initiated a hunt for genes of interest either for vaccine development, as candidates for protective antigens or as molecular targets to screen for inhibitors that might prove useful as antituberculous drugs. New methods for identifying the enzymes/proteins involved in essential biochemical pathways of *M. tuberculosis* are now available. The discovery of novel hydroperoxide detoxifying pathways in the present study is a promising example of how to make use of genome information. A better understanding of the underlying molecular mechanisms of *M. tuberculosis* virulence and pathogenicity will hopefully lead to the development of new therapies against tuberculosis.

In my view, there are two main ways to approach the identification of potential new drug targets from the TB genome:

- To select for targets that are conserved amongst different species of bacteria but poorly conserved or alternatively unconserved in humans.

Targeting such molecules may lead to broad-spectrum antimicrobial agents.

- To identify potential targets that are unique to *M. tuberculosis* for developing specific anti-TB drugs.

In the present study the second approach was pursued. The different peroxidase systems described here were discovered by systematic screening of the *M. tuberculosis* genome sequence for homologues of AhpF, thioredoxin-related proteins and peroxiredoxins. The isolated gene products were functionally analyzed and tested with regard to the relevance for mycobacterial peroxide detoxification. The *in vitro* recombination of the gene products resulted in two novel redox cascades. Due consideration of the *in vivo* concentrations of the participating enzymes and their kinetic efficiency, qualify the thioredoxin-dependent AhpC and TPx systems as relevant ones. Thereby, *Mt*AhpC and *Mt*TPx, and their supportive enzymes *Mt*TR and *Mt*TrxC, deserve interest as potential targets for the design of anti-TB agents. Specific inhibitors of those enzymes should have tuberculostatic or even tuberculocidal effects and could serve as a powerful tool in fighting against INH-resistant and/or MDR strains.

5 Summary

Drug resistance and virulence of *M. tuberculosis* are in part related to the pathogen's antioxidant defense systems. *KatG*$^{-}$ strains are resistant to the first line tuberculostatic isoniazid but they need to compensate their catalase deficiency by alternative peroxidase systems to remain virulent. So far only NADH-driven and AhpD-mediated hydroperoxide reduction by AhpC has been implicated as such a virulence-determining mechanism. In search of more likely metabolic links of AhpC, the genome of *M. tuberculosis* was screened for homologues of AhpF, thioredoxin-related proteins and peroxiredoxins. The genes were expressed heterologously in *E. coli* or *M. smegmatis* and purified to homogeneity. By means of those tools, two novel pathways were discovered that underscore the importance of the thioredoxin system for antioxidant defense in *M. tuberculosis.* They are: (1) NADPH-driven hydroperoxide reduction by AhpC that is mediated by thioredoxin reductase and thioredoxin C and (2) hydroperoxide reduction by the atypical peroxiredoxin TPx that equally depends on thioredoxin reductase but can use both thioredoxin B and C. According to kinetic analyses of hydroperoxide and peroxynitrite reduction and estimated enzyme levels, the redox cascade comprising thioredoxin reductase, thioredoxin C and TPx should be the most efficient system *in situ* to protect *M. tuberculosis* against oxidative and nitrosative stress.

6 References

Akaki,T., Tomioka,H., Shimizu,T., Dekio,S., and Sato,K. (2000). Comparative roles of free fatty acids with reactive nitrogen intermediates and reactive oxygen intermediates in expression of the anti-microbial activity of macrophages against *Mycobacterium tuberculosis*. *Clin.Exp.Immunol.* **121**: 302-310.

Alphey,M.S., Bond,C.S., Tetaud,E., Fairlamb,A.H., and Hunter,W.N. (2000). The structure of reduced tryparedoxin peroxidase reveals a decamer and insight into reactivity of 2-Cys-peroxiredoxins. *J Mol.Biol.* **300**: 903-916.

Alvarez,M.N., Trujillo,M., and Radi,R. (2002). Peroxynitrite formation from biochemical and cellular fluxes of nitric oxide and superoxide. *Methods Enzymol.* **359**: 353-366.

Am.Thorac.Soc. (2003). Diagnostic standards and classification of tuberculosis in adults and children. *Am.J.Respir.Crit.Care Med.* **161**: 1376-1395.

Armstrong,J.A., and Hart,P.D. (1975). Phagosome-lysosome interactions in cultured macrophages infected with virulent tubercle bacilli. Reversal of the usual nonfusion pattern and observations on bacterial survival. *J.Exp.Med.* **142**: 1-16.

Aslund,F., Zheng,M., Beckwith,J., and Storz,G. (1999). Regulation of the OxyR transcription factor by hydrogen peroxide and the cellular thiol-disulfide status. *Proc.Natl.Acad.Sci.U.S.A.* **96**: 6161-6165.

Baker,L.M., and Poole,L.B. (2003). Catalytic mechanism of thiol peroxidase from *Escherichia coli*. Sulfenic acid formation and overoxidation of essential Cys61. *J.Biol.Chem.* **278**: 9203-9211.

Baker,L.M., Raudonikiene,A., Hoffman,P.S., and Poole,L.B. (2001). Essential thioredoxin-dependent peroxiredoxin system from *Helicobacter pylori*: genetic and kinetic characterization. *J.Bacteriol.* **183**: 1961-1973.

Banerjee,A., Dubnau,E., Quemard,A., Balasubramanian,V., Um,K.S., Wilson,T., Collins,D., de Lisle,G., and Jacobs,W.R., Jr. (1994). *InhA*, a gene encoding a target for isoniazid and ethionamide in *Mycobacterium tuberculosis*. *Science* **263**: 227-230.

Beckman,J.S., Chen,J., Ischiropoulos,H., and Crow,J.P. (1994). Oxidative chemistry of peroxynitrite. *Methods Enzymol.* **233**:229-240.

Bradford,M.M. (1976). A rapid and sensitive method for the quantitation of microgram quantities of protein utilizing the principle of protein-dye binding. *Anal.Biochem.* **72**: 248-254.

Brightbill,H.D., Libraty,D.H., Krutzik,S.R., Yang,R.B., Belisle,J.T., Bleharski,J.R., Maitland,M., Norgard,M.V., Plevy,S.E., Smale,S.T., Brennan,P.J., Bloom,B.R., Godowski,P.J., and Modlin,R.L. (1999). Host defense mechanisms triggered by microbial lipoproteins through toll-like receptors. *Science* **285**: 732-736.

Bryk,R., Griffin,P., and Nathan,C. (2000). Peroxynitrite reductase activity of bacterial peroxiredoxins. *Nature* **407**: 211-215.

Bryk,R., Lima,C.D., Erdjument-Bromage,H., Tempst,P., and Nathan,C. (2002). Metabolic enzymes of mycobacteria linked to antioxidant defense by a thioredoxin-like protein. *Science* **295**: 1073-1077.

Budde,H., and Flohé,L. (2002). Enzymes of the thiol-dependent hydroperoxide metabolism in pathogens as potential drug targets. In *Thiol metabolism and redox regulation of cellular functions*. Pompella,A., Bánhegyi,G., and Wellman-Rousseau,M. (eds). Amsterdam: IOS Press, pp. 85-95.

Budde,H., Flohé,L., Hecht,H.J., Hofmann,B., Stehr,M., Wissing,J., and Lünsdorf,H. (2003). Kinetics and redox-sensitive oligomerisation reveal negative subunit cooperativity in tryparedoxin peroxidase of *Trypanosoma brucei brucei*. *Biol.Chem.* **384**: 619-633.

Castro,H., Budde,H., Flohé,L., Hofmann,B., Lünsdorf,H., Wissing,J., and Tomas,A.M. (2002). Specificity and kinetics of a mitochondrial peroxiredoxin of *Leishmania infantum*. *Free Radic.Biol.Med.* **33**: 1563-1574.

Cha,M.K., Kim,H.K., and Kim,I.H. (1995). Thioredoxin-linked "thiol peroxidase" from periplasmic space of *Escherichia coli*. *J.Biol.Chem.* **270**: 28635-28641.

Cha,M.K., Kim,H.K., and Kim,I.H. (1996). Mutation and mutagenesis of thiol peroxidase of *Escherichia coli* and a new type of thiol peroxidase family. *J.Bacteriol.* **178**: 5610-5614.

Chae,H.Z., Robison,K., Poole,L.B., Church,G., Storz,G., and Rhee,S.G. (1994a). Cloning and sequencing of thiol-specific antioxidant from mammalian brain: alkyl hydroperoxide reductase and thiol-specific antioxidant define a large family of antioxidant enzymes. *Proc.Natl.Acad.Sci.U.S.A.* **91**: 7017-7021.

Chae,H.Z., Chung,S.J., and Rhee,S.G. (1994b). Thioredoxin-dependent peroxide reductase from yeast. *J.Biol.Chem.* **269**: 27670-8.

Chae,H.Z., Kim,H.J., Kang,S.W., and Rhee,S.G. (1999). Characterization of three isoforms of mammalian peroxiredoxin that reduce peroxides in the presence of thioredoxin. *Diabetes Res.Clin.Pract.* **45**: 101-112.

Chauhan,R., and Mande,S.C. (2001). Characterization of the *Mycobacterium tuberculosis* H37Rv alkyl hydroperoxidase AhpC points to the importance of ionic interactions in oligomerization and activity. *Biochem.J.* **354**: 209-215.

Chauhan,R., and Mande,S.C. (2002). Site-directed mutagenesis reveals a novel catalytic mechanism of *Mycobacterium tuberculosis* alkylhydroperoxidase C. *Biochem.J.* **367**: 255-261.

Chen,L., Xie,Q.W., and Nathan,C. (1998). Alkyl hydroperoxide reductase subunit C (AhpC) protects bacterial and human cells against reactive nitrogen intermediates. *Mol.Cell* **1**: 795-805.

Choi,H.J., Kang,S.W., Yang,C.H., Rhee,S.G., and Ryu,S.E. (1998). Crystal structure of a novel human peroxidase enzyme at 2.0 Å resolution. *Nat.Struct.Biol.* **5**: 400-406.

Christman,M.F., Morgan,R.W., Jacobson,F.S., and Ames,B.N. (1985). Positive control of a regulon for defenses against oxidative stress and some heat-shock proteins in *Salmonella typhimurium*. *Cell* **41**: 753-762.

Cole,S.T., Brosch,R., Parkhill,J., Garnier,T., Churcher,C., Harris,D., Gordon,S.V., Eiglmeier,K., Gas,S., Barry,C.E., III, Tekaia,F., Badcock,K., Basham,D., Brown,D., Chillingworth,T., Connor,R., Davies,R., Devlin,K., Feltwell,T., Gentles,S., Hamlin,N., Holroyd,S., Hornsby,T., Jagels,K., Krogh,A., McLean,J., Moule,S., Murphy,L., Oliver,K., Osborne,J., Quail,M.A., Rajandream,M.-A., Rogers, J., Rutter,S., Seeger,K., Skelton,J., Squares,R., Squares,S., Sulston,J.E., Taylor,K., Whitehead,S., and Barrell,B.G. (1998). Deciphering the biology of *Mycobacterium tuberculosis* from the complete genome sequence. *Nature* **393**: 537-544.

Comtois,S.L., Gidley,M.D., and Kelly,D.J. (2003). Role of the thioredoxin system and the thiol-peroxidases Tpx and Bcp in mediating resistance to oxidative and nitrosative stress in *Helicobacter pylori*. *Microbiology* **149**: 121-129.

Cooper,A.M., Segal,B.H., Frank,A.A., Holland,S.M., and Orme,I.M. (2000). Transient loss of resistance to pulmonary tuberculosis in p47(*phox-/-*) mice. *Infect.Immun.* **68**: 1231-1234.

Crofton,J., Chaulet,P., Maher,D., Grosset,J., Harris,W., Norman,H., Iseman,M., and Watt,B. (1997). WHO/TB/96.210. World Health Organization.

Dalziel,K. (1957). Initial steady state velocities in the evaluation of enzyme-coenzyme-substrate reaction mechanisms. *Acta Chem.Scand.* **11**: 1706-1723.

Darrah,P.A., Hondalus,M.K., Chen,Q., Ischiropoulos,H., and Mosser,D.M. (2000). Cooperation between reactive oxygen and nitrogen intermediates in killing of *Rhodococcus equi* by activated macrophages. *Infect.Immun.* **68**: 3587-3593.

Declercq,J.P., Evrard,C., Clippe,A., Stricht,D.V., Bernard,A., and Knoops,B. (2001). Crystal structure of human peroxiredoxin 5, a novel type of mammalian peroxiredoxin at 1.5 Å resolution. *J.Mol.Biol.* **311**: 751-759.

Deretic,V., Philipp,W., Dhandayuthapani,S., Mudd,M.H., Curcic,R., Garbe,T., Heym,B., Via,L.E., and Cole,S.T. (1995). *Mycobacterium tuberculosis* is a natural mutant with an inactivated oxidative-stress regulatory gene: implications for sensitivity to isoniazid. *Mol.Microbiol.* **17**: 889-900.

Deretic,V., Song,J., and Pagan-Ramos,E. (1997). Loss of *oxyR* in *Mycobacterium tuberculosis*. *Trends Microbiol.* **5**: 367-372.

Dhandayuthapani,S., Zhang,Y., Mudd,M.H., and Deretic,V. (1996). Oxidative stress response and its role in sensitivity to isoniazid in mycobacteria: characterization and inducibility of *ahpC* by peroxides in *Mycobacterium smegmatis* and lack of expression in *M. aurum* and *M. tuberculosis*. *J.Bacteriol.* **178**: 3641-3649.

Dower,W.J., Miller,J.F., and Ragsdale,C.W. (1988). High efficiency transformation of *E. coli* by high voltage electroporation. *Nucl.Acids Res.* **16**: 6127-6145.

Dye,C., Scheele,S., Dolin,P., Pathania,V., and Raviglione,M.C. (1999). Consensus statement. Global burden of tuberculosis: estimated incidence, prevalence,

and mortality by country. WHO Global Surveillance and Monitoring Project. *JAMA* **282**: 677-686.

Ehlers,M.R., and Daffe,M. (1998). Interactions between *Mycobacterium tuberculosis* and host cells: are mycobacterial sugars the key? *Trends Microbiol.* **6**: 328-335.

Ellis,H.R., and Poole,L.B. (1997). Roles for the two cysteine residues of AhpC in catalysis of peroxide reduction by alkyl hydroperoxide reductase from *Salmonella typhimurium*. *Biochemistry* **36**: 13349-13356.

Ernst,J.D. (1998). Macrophage receptors for *Mycobacterium tuberculosis*. *Infect.Immun.* **66**: 1277-1281.

Farr,S.B., and Kogoma,T. (1991). Oxidative stress responses in *Escherichia coli* and *Salmonella typhimurium*. *Microbiol.Rev.* **55**: 561-585.

Ferrari,G., Langen,H., Naito,M., and Pieters,J. (1999). A coat protein on phagosomes involved in the intracellular survival of mycobacteria. *Cell* **97**: 435-447.

Ferrer-Sueta,G., Batinic-Haberle,I., Spasojevic,I., Fridovich,I., and Radi,R. (1999). Catalytic scavenging of peroxynitrite by isomeric Mn(III) N- methylpyridylporphyrins in the presence of reductants. *Chem.Res.Toxicol.* **12**: 442-449.

Ferrer-Sueta, G., Vitturi, D., Batinic-Haberle, I., Fridovich, I., Goldstein, S., Czapski, G., and Radi, R. (2003). Reactions of manganese porphyrins with peroxynitrite and carbonate radical anion. *J.Biol.Chem.* **16**: In press.

Flohé,L., and Brigelius-Flohé,R. (2001). Selenoproteins of the glutathione system. In *Selenium. Its Molecular Biology and Role in Human Health*. Hatfield,D.L. (ed). Boston/Dordrecht/London: Kluwer Academic Publishers, pp. 157-178.

Gatfield,J., and Pieters,J. (2000). Essential role for cholesterol in entry of mycobacteria into macrophages. *Science* **288**: 1647-1650.

Grossman,T.H., Kawasaki,E.S., Punreddy,S.R., and Osburne,M.S. (1998). Spontaneous cAMP-dependent derepression of gene expression in stationary phase plays a role in recombinant expression instability. *Gene* **209**: 95-103.

Hanahan,D. (1983). Studies on transformation of *Escherichia coli* with plasmids. *J.Mol.Biol.* **166**: 557-580.

Harth,G., and Horwitz,M.A. (1999). An inhibitor of exported *Mycobacterium tuberculosis* glutamine synthetase selectively blocks the growth of pathogenic mycobacteria in axenic culture and in human monocytes: extracellular proteins as potential novel drug targets. *J.Exp.Med.* **189**: 1425-1436.

Heym,B., Alzari,P.M., Honore,N., and Cole,S.T. (1995). Missense mutations in the catalase-peroxidase gene, *katG*, are associated with isoniazid resistance in *Mycobacterium tuberculosis*. *Mol.Microbiol.* **15**: 235-245.

Heym,B., and Cole,S.T. (1997). Multidrug resistance in *Mycobacterium tuberculosis*. *Int.J.Antimicrob.Agents* **8**: 61-70.

Heym,B., Honore,N., Truffot-Pernot,C., Banerjee,A., Schurra,C., Jacobs,W.R., Jr., van Embden,J.D., Grosset,J.H., and Cole,S.T. (1994). Implications of multidrug resistance for the future of short-course chemotherapy of tuberculosis: a molecular study. *Lancet* **344**: 293-298.

Heym,B., Stavropoulos,E., Honore,N., Domenech,P., Saint-Joanis,B., Wilson,T.M., Collins,D.M., Colston,M.J., and Cole,S.T. (1997). Effects of overexpression of the alkyl hydroperoxide reductase AhpC on the virulence and isoniazid resistance of *Mycobacterium tuberculosis*. *Infect.Immun.* **65**: 1395-1401.

Hillas,P.J., del Alba,F.S., Oyarzabal,J., Wilks,A., and Ortiz de Montellano,P.R. (2000). The AhpC and AhpD antioxidant defense system of *Mycobacterium tuberculosis*. *J.Biol.Chem.* **275**: 18801-18809.

Hirotsu,S., Abe,Y., Okada,K., Nagahara,N., Hori,H., Nishino,T., and Hakoshima,T. (1999). Crystal structure of a multifunctional 2-Cys peroxiredoxin heme-binding protein 23 kDa/proliferation-associated gene product. *Proc.Natl.Acad.Sci.U.S.A.* **96**: 12333-12338.

Hofmann,B., Budde,H., Bruns,K., Guerrero,S.A., Kalisz,H.M., Menge,U., Montemartini,M., Nogoceke,E., Steinert,P., Wissing,J.B., Flohé,L., and Hecht,H.J. (2001). Structures of tryparedoxins revealing interaction with trypanothione. *Biol.Chem.* **382**: 459-471.

Hofmann,B., Hecht,H.J., and Flohé,L. (2002). Peroxiredoxins. *Biol.Chem.* **383**: 347-364.

Jacobson,F.S., Morgan,R.W., Christman,M.F., and Ames,B.N. (1989). An alkyl hydroperoxide reductase from *Salmonella typhimurium* involved in the defense of DNA against oxidative damage. Purification and properties. *J.Biol.Chem.* **264**: 1488-1496.

Johnsson,K., King,D.S., and Schultz,P.G. (1995). Studies on the mechanism of action of isoniazid and ethionamide in the chemotherapy of tuberculosis. *J.Am.Chem.Soc.* **117**: 5009-5010.

Johnsson,K., and Schultz,P.G. (1994). Mechanistic studies of the oxidation of isoniazid by the catalase peroxidase from *Mycobacterium tuberculosis*. *J.Am.Chem.Soc.* **116**: 7425-7426.

Jones,T.A., Zou,J.Y., Cowan,S.W., and Kjeldgaard,M.M. (1991). Improved methods for building protein models in electron density maps and the location of errors in these models. *Acta Crystallogr.A.* **47**: 110-119.

Jungblut,P.R., Schaible,U.E., Mollenkopf,H.J., Zimny-Arndt,U., Raupach,B., Mattow,J., Halada,P., Lamer,S., Hagens,K., and Kaufmann,S.H. (1999). Comparative proteome analysis of *Mycobacterium tuberculosis* and *Mycobacterium bovis* BCG

strains: towards functional genomics of microbial pathogens. *Mol.Microbiol.* **33**: 1103-1117.

Kaufmann,S.H. (1999). In *Fundamental Immunology*. Paul,W. (ed). New York: Lippincott-Raven, pp. 1335-1371.

Kaufmann,S.H. (2001). How can immunology contribute to the control of tuberculosis? *Nat.Rev.Immunol.* **1**: 20-30.

Keshavjee,S., and Becerra,M.C. (2000). Disintegrating health services and resurgent tuberculosis in post- Soviet Tajikistan: an example of structural violence. *JAMA* **283**: 1201.

Kim,H.K., Kim,S.J., Lee,J.W., Lee,J.W., Cha,M.K., and Kim,I.H. (1996). Identification of promoter in the 5'-flanking region of the *E. coli* thioredoxin-linked thiol peroxidase gene: evidence for the existence of oxygen-related transcriptional regulatory protein. *Biochem.Biophys.Res.Commun.* **221**: 641-646.

Kim,S.J., Han,Y.H., Kim,I.H., and Kim,H.K. (1999). Involvement of ArcA and Fnr in expression of *Escherichia coli* thiol peroxidase gene. *IUBMB.Life* **48**: 215-218.

Koppenol,W.H., Moreno,J.J., Pryor,W.A., Ischiropoulos,H., and Beckman,J.S. (1992). Peroxynitrite, a cloaked oxidant formed by nitric oxide and superoxide. *Chem.Res.Toxicol.* **5**: 834-842.

Koshland Jr.,D.E. (1970). The molecular basis for enzyme regulation. In *The Enzymes, Structures and Control*. Boyer,P.D. (ed). New York/London: Academic Press, pp. 341-396.

König, J., Lotte, K., Plessow, R., Brockhinke, A., Baier, M., and Dietz, K. J. (2003). Reaction mechanism of plant 2-Cys peroxiredoxin: Role of the C-terminus and the quarternary structure. *J.Biol.Chem.*: In press.

Laemmli,U.K. (1970). Cleavage of structural proteins during the assembly of the head of bacteriophage T4. *Nature* **227**: 680-685.

Lee,A.S., Teo,A.S., and Wong,S.Y. (2001). Novel mutations in *ndh* in isoniazid-resistant *Mycobacterium tuberculosis* isolates. *Antimicrob.Agents Chemother.* **45**: 2157-2159.

Link,A.J., Robison,K., and Church,G.M. (1997). Comparing the predicted and observed properties of proteins encoded in the genome of *Escherichia coli* K-12. *Electrophoresis* **18**: 1259-1313.

Luthman,M., and Holmgren,A. (1982). Rat liver thioredoxin and thioredoxin reductase: purification and characterization. *Biochemistry* **21**: 6628-6633.

Lünsdorf,H., and Spiess,E. (1986). A rapid method for preparing perforated supporting foils for the thin carbon films used in high resolution transmission electron microscopy. *J.Microsc.* **144**: 213.

Master,S., Zahrt,T.C., Song,J., and Deretic,V. (2001). Mapping of *Mycobacterium tuberculosis katG* promoters and their differential expression in infected macrophages. *J.Bacteriol.* **183**: 4033-4039.

Master,S.S., Springer,B., Sander,P., Boettger,E.C., Deretic,V., and Timmins,G.S. (2002). Oxidative stress response genes in *Mycobacterium tuberculosis*: role of *ahpC* in resistance to peroxynitrite and stage-specific survival in macrophages. *Microbiology* **148**: 3139-3144.

McKinney,J.D., Honer zu,B.K., Munoz-Elias,E.J., Miczak,A., Chen,B., Chan,W.T., Swenson,D., Sacchettini,J.C., Jacobs,W.R., Jr., and Russell,D.G. (2000). Persistence of *Mycobacterium tuberculosis* in macrophages and mice requires the glyoxylate shunt enzyme isocitrate lyase. *Nature* **406**: 735-738.

Mdluli,K., Slayden,R.A., Zhu,Y., Ramaswamy,S., Pan,X., Mead,D., Crane,D.D., Musser,J.M., and Barry,C.E., III (1998). Inhibition of a *Mycobacterium tuberculosis* beta-ketoacyl ACP synthase by isoniazid. *Science* **280**: 1607-1610.

Mendes,P. (1997). Biochemistry by numbers: simulation of biochemical pathways with Gepasi 3. *Trends Biochem.Sci.* **22**: 361-363.

Middlebrook,G. (1952). Sterilization of tubercle bacilli by isonicotinic acid hydrazide and the incidence of variants resistant to the drug *in vitro*. *Am.Rev.Tuberc.* **65**: 765-767.

Middlebrook,G., and Cohn,M.L. (1953). Some observations on the pathogenicity of isoniazid-resistant variants of tubercle bacilli. *Science* **118**: 297-299.

Mollenkopf,H.J., Jungblut,P.R., Raupach,B., Mattow,J., Lamer,S., Zimny-Arndt,U., Schaible,U.E., and Kaufmann,S.H. (1999). A dynamic two-dimensional polyacrylamide gel electrophoresis database: the mycobacterial proteome via Internet. *Electrophoresis* **20**: 2172-2180.

Monod,J., Wyman,J., and Changeux,J.P. (1965). On the nature of allosteric transitions: a plausible model. *J.Mol.Biol.* **12**: 88-118.

Moore,R.B., Mankad,M.V., Shriver,S.K., Mankad,V.N., and Plishker,G.A. (1991). Reconstitution of Ca(2+)-dependent K+ transport in erythrocyte membrane vesicles requires a cytoplasmic protein. *J.Biol.Chem.* **266**: 18964-18968.

Musser,J.M. (1995). Antimicrobial agent resistance in mycobacteria: molecular genetic insights. *Clin.Microbiol.Rev.* **8**: 496-514.

Musser,J.M., Kapur,V., Williams,D.L., Kreiswirth,B.N., van Soolingen,D., and van Embden,J.D. (1996). Characterization of the catalase-peroxidase gene (*katG*) and *inhA* locus in isoniazid-resistant and -susceptible strains of *Mycobacterium tuber-*

culosis by automated DNA sequencing: restricted array of mutations associated with drug resistance. *J.Infect.Dis.* **173**: 196-202.

Nagai,S., Wiker,H.G., Harboe,M., and Kinomoto,M. (1991). Isolation and partial characterization of major protein antigens in the culture fluid of *Mycobacterium tuberculosis*. *Infect.Immun.* **59**: 372-382.

Nathan,C., and Shiloh,M.U. (2000). Reactive oxygen and nitrogen intermediates in the relationship between mammalian hosts and microbial pathogens. *Proc.Natl.Acad.Sci.U.S.A.* **97**: 8841-8848.

Nogoceke,E., Gommel,D.U., Kiess,M., Kalisz,H.M., and Flohé,L. (1997). A unique cascade of oxidoreductases catalyses trypanothione-mediated peroxide metabolism in *Crithidia fasciculata*. *Biol.Chem.* **378**: 827-836.

Nunn,C.M., Djordjevic,S., Hillas,P.J., Nishida,C.R., and Ortiz de Montellano,P.R. (2002). The crystal structure of *Mycobacterium tuberculosis* alkylhydroperoxidase AhpD, a potential target for antitubercular drug design. *J.Biol.Chem.* **277**: 20033-20040.

Pablos-Mendez,A., Raviglione,M.C., Laszlo,A., Binkin,N., Rieder,H.L., Bustreo,F., Cohn,D.L., Lambregts-van Weezenbeek,C.S., Kim,S.J., Chaulet,P., and Nunn,P. (1998). Global surveillance for antituberculosis-drug resistance, 1994-1997. World Health Organization-International Union against Tuberculosis and Lung Disease Working Group on Anti-Tuberculosis Drug Resistance Surveillance. *N.Engl.J.Med.* **338**: 1641-1649.

Pagan-Ramos,E., Song,J., McFalone,M., Mudd,M.H., and Deretic,V. (1998). Oxidative stress response and characterization of the *oxyR-ahpC* and *furA-katG* loci in *Mycobacterium marinum*. *J.Bacteriol.* **180**: 4856-4864.

Paziak-Domanska,B., Klink,M., Jurkiewicz,M., and Rudnicka,W. (2000). Production of reactive nitrogen and oxygen intermediates in human granulocytes and

monocytes during internalization of live BCG bacilli. *Med.Dosw.Mikrobiol.* **52**: 353-360.

Peshenko,I.V., and Shichi,H. (2001). Oxidation of active center cysteine of bovine 1-Cys peroxiredoxin to the cysteine sulfenic acid form by peroxide and peroxynitrite. *Free Radic.Biol.Med.* **31**: 292-303.

Pfyffer,G.E., Auckenthaler,R., van Embden,J.D., and van Soolingen,D. (1998). *Mycobacterium canettii*, the smooth variant of *M. tuberculosis*, isolated from a Swiss patient exposed in Africa. *Emerg.Infect.Dis.* **4**: 631-634.

Poole,L.B., and Ellis,H.R. (1996). Flavin-dependent alkyl hydroperoxide reductase from *Salmonella typhimurium*. 1. Purification and enzymatic activities of overexpressed AhpF and AhpC proteins. *Biochemistry* **35**: 56-64.

Poole,L.B., and Ellis,H.R. (2002). Identification of cysteine sulfenic acid in AhpC of alkyl hydroperoxide reductase. *Methods Enzymol.* **348**: 122-136.

Poole,L.B., Reynolds,C.M., Wood,Z.A., Karplus,P.A., Ellis,H.R., and Li,C.M. (2000). AhpF and other NADH:peroxiredoxin oxidoreductases, homologues of low Mr thioredoxin reductase. *Eur.J.Biochem.* **267**: 6126-6133.

Radi,R., Beckman,J.S., Bush,K.M., and Freeman,B.A. (1991). Peroxynitrite oxidation of sulfhydryls. The cytotoxic potential of superoxide and nitric oxide. *J.Biol.Chem.* **266**: 4244-4250.

Radi,R., Denicola,A., Alvarez,B., Ferrer-Sueta,G., and Rubbo,H. (2000). The biological chemistry of peroxynitrite. In *Nitric Oxide*. Ignarro,L. (ed). New York: Academic Press, pp. 57-89.

Rosenkrands,I., King,A., Weldingh,K., Moniatte,M., Moertz,E., and Andersen,P. (2000a). Towards the proteome of *Mycobacterium tuberculosis*. *Electrophoresis* **21**: 3740-3756.

Rosenkrands,I., Weldingh,K., Jacobsen,S., Hansen,C.V., Florio,W., Gianetri,I., and Andersen,P. (2000b). Mapping and identification of *Mycobacterium tuberculosis* proteins by two-dimensional gel electrophoresis, microsequencing and immunodetection. *Electrophoresis* **21**: 935-948.

Rouse,D.A., DeVito,J.A., Li,Z., Byer,H., and Morris,S.L. (1996). Site-directed mutagenesis of the *katG* gene of *Mycobacterium tuberculosis*: effects on catalase-peroxidase activities and isoniazid resistance. *Mol.Microbiol.* **22**: 583-592.

Rouse,D.A., and Morris,S.L. (1995). Molecular mechanisms of isoniazid resistance in *Mycobacterium tuberculosis* and *Mycobacterium bovis*. *Infect.Immun.* **63**: 1427-1433.

Rubin,E., and Farber,J.L. (1999). *Pathology* Rubin,E., Farber,J.L. (eds). New York: Lippincoot Williams & Wilkins Publishers.

Russell,D.G., Dant,J., and Sturgill-Koszycki,S. (1996). *Mycobacterium avium* - and *Mycobacterium tuberculosis* - containing vacuoles are dynamic, fusion-compentent vesicles that are accessible to glycosphingolipids from the host cell plasmalemma. *J.Immunol.* **156**: 4764-4773.

Sambrook,J., Russell,D.W., and Sambrook,J. (2001). *Molecular Cloning: A Laboratory Manual*. Rockville: Cold Spring Harbor Laboratory Press.

Sanger,F., Nicklen,S., and Coulson,A.R. (1977). DNA sequencing with chain-terminating inhibitors. *Proc.Natl.Acad.Sci.U.S.A.* **74**: 5463-5467.

Schaible,U.E., Collins,H.L., and Kaufmann,S.H. (1999). Confrontation between intracellular bacteria and the immune system. *Adv.Immunol.* **71**: 267-377.

Schaible,U.E., Sturgill-Koszycki,S., Schlesinger,P.H., and Russell,D.G. (1998). Cytokine activation leads to acidification and increases maturation of *Mycobacterium avium*-containing phagosomes in murine macrophages. *J.Immunol.* **160**: 1290-1296.

Schomburg,D., and Reichelt,J. (1988). BRAGI: A comprehensive protein modelling program system. *J.Molec.Graphics* **6**: 161-165.

Schorey,J.S., Carroll,M.C., and Brown,E.J. (1997). A macrophage invasion mechanism of pathogenic mycobacteria. *Science* **277**: 1091-1093.

Schroeder,E., Littlechild,J.A., Lebedev,A.A., Errington,N., Vagin,A.A., and Isupov,M.N. (2000). Crystal structure of decameric 2-Cys peroxiredoxin from human erythrocytes at 1.7 Å resolution. *Structure.Fold.Des.* **8**: 605-615.

Schroeder,E., and Ponting,C.P. (1998). Evidence that peroxiredoxins are novel members of the thioredoxin fold superfamily. *Protein Sci.* **7**: 2465-2468.

Seaver,L.C., and Imlay,J.A. (2001). Alkyl hydroperoxide reductase is the primary scavenger of endogenous hydrogen peroxide in *Escherichia coli*. *J.Bacteriol.* **183**: 7173-7181.

Seo,M.S., Kang,S.W., Kim,K., Baines,I.C., Lee,T.H., and Rhee,S.G. (2000). Identification of a new type of mammalian peroxiredoxin that forms an intramolecular disulfide as a reaction intermediate. *J.Biol.Chem.* **275**: 20346-20354.

Sherman,D.R., Mdluli,K., Hickey,M.J., Arain,T.M., Morris,S.L., Barry III,C.E., and Stover,C.K. (1996). Compensatory *ahpC* gene expression in isoniazid-resistant *Mycobacterium tuberculosis*. *Science* **272**: 1641-1643.

Sherman,D.R., Mdluli,K., Hickey,M.J., Barry III,C.E., and Stover,C.K. (1999). AhpC, oxidative stress and drug resistance in *Mycobacterium tuberculosis*. *Biofactors* **10**: 211-217.

Sherman,D.R., Sabo,P.J., Hickey,M.J., Arain,T.M., Mahairas,G.G., Yuan,Y., Barry III,C.E., and Stover,C.K. (1995). Disparate responses to oxidative stress in saprophytic and pathogenic mycobacteria. *Proc.Natl.Acad.Sci.U.S.A.* **92**: 6625-6629.

Shiloh,M.U., and Nathan,C.F. (2000). Reactive nitrogen intermediates and the pathogenesis of *Salmonella* and mycobacteria. *Curr.Opin.Microbiol.* **3**: 35-42.

Sonnenberg,M.G., and Belisle,J.T. (1997). Definition of *Mycobacterium tuberculosis* culture filtrate proteins by two-dimensional polyacrylamide gel electrophoresis, N-terminal amino acid sequencing, and electrospray mass spectrometry. *Infect.Immun.* **65**: 4515-4524.

Springer,B., Master,S., Sander,P., Zahrt,T., McFalone,M., Song,J., Papavinasasundaram,K.G., Colston,M.J., Boettger,E., and Deretic,V. (2001). Silencing of oxidative stress response in *Mycobacterium tuberculosis*: expression patterns of *ahpC* in virulent and avirulent strains and effect of *ahpC* inactivation. *Infect.Immun.* **69**: 5967-5973.

Sreevatsan,S., Pan,X., Zhang,Y., Deretic,V., and Musser,J.M. (1997). Analysis of the *oxyR-ahpC* region in isoniazid-resistant and -susceptible *Mycobacterium tuberculosis complex* organisms recovered from diseased humans and animals in diverse localities. *Antimicrob.Agents Chemother.* **41**: 600-606.

St John,G., Brot,N., Ruan,J., Erdjument-Bromage,H., Tempst,P., Weissbach,H., and Nathan,C. (2001). Peptide methionine sulfoxide reductase from *Escherichia coli* and *Mycobacterium tuberculosis* protects bacteria against oxidative damage from reactive nitrogen intermediates. *Proc.Natl.Acad.Sci.U.S.A.* **98**: 9901-9906.

Stadtman,E.R. (1970). Mechanism of enzyme regulation in metabolism. In *The Enzymes, Structure and Control*. Boyer,P.D. (ed). New York/London: Academic Press, pp. 397-459.

Storz,G., Jacobson,F.S., Tartaglia,L.A., Morgan,R.W., Silveira,L.A., and Ames,B.N. (1989). An alkyl hydroperoxide reductase induced by oxidative stress in *Salmonella typhimurium* and *Escherichia coli*: genetic characterization and cloning of *ahp*. *J.Bacteriol.* **171**: 2049-55.

Storz,G., Tartaglia,L.A., and Ames,B.N. (1990). Transcriptional regulator of oxidative stress-inducible genes: direct activation by oxidation. *Science* **248**: 189-194.

Stover,C.K., de la Cruz, V, Fuerst,T.R., Burlein,J.E., Benson,L.A., Bennett,L.T., Bansal,G.P., Young,J.F., Lee,M.H., and Hatfull,G.F. (1991). New use of BCG for recombinant vaccines. *Nature* **351**: 456-460.

Thoma-Uszynski,S., Stenger,S., Takeuchi,O., Ochoa,M.T., Engele,M., Sieling,P.A., Barnes,P.F., Rollinghoff,M., Bolcskei,P.L., Wagner,M., Akira,S., Norgard,M.V., Belisle,J.T., Godowski,P.J., Bloom,B.R., and Modlin,R.L. (2001). Induction of direct antimicrobial activity through mammalian toll-like receptors. *Science* **291**: 1544-1547.

Thompson,J.D., Gibson,T.J., Plewniak,F., Jeanmougin,F., and Higgins,D.G. (1997). The CLUSTAL_X windows interface: flexible strategies for multiple sequence alignment aided by quality analysis tools. *Nucleic Acids Res.* **25**: 4876-82.

Unson,M.D., Newton,G.L., Davis,C., and Fahey,R.C. (1998). An immunoassay for the detection and quantitative determination of mycothiol. *J.Immunol.Methods* **214**: 29-39.

Ursini,F., Maiorino,M., Brigelius-Flohé,R., Aumann,K.D., Roveri,A., Schomburg,D., and Flohé,L. (1995). Diversity of glutathione peroxidases. *Methods Enzymol.* **252**: 38-53.

Valentine,R.C., Shapiro,B.M., and Stadtman,E.R. (1968). Regulation of glutamine synthetase. XII. Electron microscopy of the enzyme from *Escherichia coli*. *Biochemistry* **7**: 2143-2152.

Vergauwen,B., Pauwels,F., Vaneechoutte,M., and van Beeumen,J.J. (2001). Probing mycothiol for completing the *Mycobacterium tuberculosis* AhpC peroxidatic cycle. *Arch.Physiol.Biochem.* **113**: B22.

Wallis,R.S., Patil,S., Cheon,S.H., Edmonds,K., Phillips,M., Perkins,M.D., Joloba,M., Namale,A., Johnson,J.L., Teixeira,L., Dietze,R., Siddiqi,S., Mugerwa,R.D., Eisenach,K., and Ellner,J.J. (1999). Drug tolerance in *Mycobacterium tuberculosis*. *Antimicrob.Agents Chemother.* **43**: 2600-2606.

Wallis,R.S., Perkins,M.D., Phillips,M., Joloba,M., Namale,A., Johnson,J.L., Whalen,C.C., Teixeira,L., Demchuk,B., Dietze,R., Mugerwa,R.D., Eisenach,K., and Ellner,J.J. (2000). Predicting the outcome of therapy for pulmonary tuberculosis. *Am.J.Respir.Crit.Care Med.* **161**: 1076-1080.

Wan,X.Y., Zhou,Y., Yan,Z.Y., Wang,H.L., Hou,Y.D., and Jin,D.Y. (1997). Scavengase p20: a novel family of bacterial antioxidant enzymes. *FEBS Lett.* **407**: 32-36.

Weber,I., Fritz,C., Ruttkowski,S., Kreft,A., and Bange,F.C. (2000). Anaerobic nitrate reductase (*narGHJI*) activity of *Mycobacterium bovis* BCG *in vitro* and its contribution to virulence in immunodeficient mice. *Mol.Microbiol.* **35**: 1017-1025.

Weldingh,K., Rosenkrands,I., Jacobsen,S., Rasmussen,P.B., Elhay,M.J., and Andersen,P. (1998). Two-dimensional electrophoresis for analysis of *Mycobacterium tuberculosis* culture filtrate and purification and characterization of six novel proteins. *Infect.Immun.* **66**: 3492-3500.

Wilson,T., de Lisle,G.W., Marcinkeviciene,J.A., Blanchard,J.S., and Collins,D.M. (1998). Antisense RNA to *ahpC*, an oxidative stress defence gene involved in isoniazid resistance, indicates that AhpC of Mycobacterium bovis has virulence properties. *Microbiology* **144**: 2687-2695.

Wilson,T.M., and Collins,D.M. (1996). *AhpC*, a gene involved in isoniazid resistance of the *Mycobacterium tuberculosis* complex. *Mol.Microbiol.* **19**: 1025-1034.

Winder,F.G. (1982). In *The biology of the mycobacteria*. Ratledge,C., Stanford,J. (eds). New York: Academic Press, pp. 354-438.

Winder,F.G., and Collins,P.B. (1970). Inhibition by isoniazid of synthesis of mycolic acids in *Mycobacterium tuberculosis*. *J.Gen.Microbiol.* **63**: 41-48.

Wood,Z.A., Poole,L.B., Hantgan,R.R., and Karplus,P.A. (2002). Dimers to doughnuts: redox-sensitive oligomerization of 2-cysteine peroxiredoxins. *Biochemistry* **41**: 5493-5504.

Wood,Z.A., Schroeder,E., Robin,H.J., and Poole,L.B. (2003a). Structure, mechanism and regulation of peroxiredoxins. *Trends Biochem.Sci.* **28**: 32-40.

Wood,Z.A., Poole,L.B., and Karplus,P.A. (2003b). Peroxiredoxin evolution and the regulation of hydrogen peroxide signaling. *Science* **300**: 650-653.

WHO (1998). Global Tuberculosis Control. *WHO Report 1998*. WHO/TB/98.253.

WHO (1999). Global Tuberculosis Control. *WHO Report 1999*. WHO/TB/99.260.

WHO (2001). Global Tuberculosis Control. *WHO Report 2001.* WHO/CDS/TB/2001.287.

WHO (2002). Global Tuberculosis Control. *WHO Report 2002*. WHO/CDS/TB/2002.295.

Yu,K., Mitchell,C., Xing,Y., Magliozzo,R.S., Bloom,B.R., and Chan,J. (1999). Toxicity of nitrogen oxides and related oxidants on mycobacteria: *M. tuberculosis* is resistant to peroxynitrite anion. *Tuber.Lung Dis.* **79**: 191-198.

Zahrt,T.C., and Deretic,V. (2002). Reactive nitrogen and oxygen intermediates and bacterial defenses: unusual adaptations in *Mycobacterium tuberculosis*. *Antioxid.Redox.Signal.* **4**: 141-159.

Zhang,Y., Garbe,T., and Young,D. (1993). Transformation with *katG* restores isoniazid-sensitivity in *Mycobacterium tuberculosis* isolates resistant to a range of drug concentrations *Mol.Microbiol.* **8**: 521-524.

Zhang,Y., Heym,B., Allen,B., Young,D., and Cole,S. (1992). The catalase-peroxidase gene and isoniazid resistance of *Mycobacterium tuberculosis*. *Nature* **358**: 591-593.

Zhang,Y., and Young,D.B. (1993). Molecular mechanisms of isoniazid: a drug at the front line of tuberculosis control. *Trends Microbiol.* **1**: 109-113.

7 Appendix

7.1 Abbreviations

Å	Ångström
A_x	absorption at x nm
AhpC	alkyl hydroperoxide reductase subunit C
AhpD	alkyl hydroperoxide reductase subunit D
AhpF	alkyl hydroperoxide reductase subunit F
AIDS	aquired immune deficiency syndrome
AFB	acid-fast bacilli
APS	ammoniumperoxodisulfate
ATCC	American Type Culture Collection
bp	base pair
BCG	Bacille Calmette Guérin
BD	Becton Dickinson
BSA	bovine serum albumine
COOH	cumene hydroperoxide

Da	Dalton
deion	deionized
dest	destilled
DNA	deoxyribonucleic acid
dNTP	deoxyribonucleoside triphosphate
DOTS	directly observed treatment short-course
DPTA	diethylene-triamine-pentaacetic acid
DSMZ	German Culture Collection of Microorganisms and Cell Cultures
DTT	dithiothreitol
E_x	extinction at x nm
Ec	*Escherichia coli*
EDTA	ethylenediaminetetraacetic acid
EFTEM	energy-filtered transmission electron microscope
Fig	figure
GBF	German Research Centre for Biotechnology
GPx-1	type-1 glutathione peroxidase

GR	glutathione reductase
GSH	glutathione
HBP23	heme binding protein 23 kDa
HEPES	4-(2-hydroxyethyl)-1-piperazineethanesulfonic acid
HIV	human immunodeficiency virus
HSP	heat shock protein
i.e.	in example
IFN-γ	interferon-γ
INH	isoniazid
InhA/*inhA*	acyl carrier protein-enoyl reductase
IPTG	isopropyl-β-D-thiogalactopyranoside
KatG/*katG*	catalase peroxidase
kDa	Kilodalton
LB	Luria Bertani medium
LOOH	13-hydroperoxy octodecadienoic acid hydroperoxide
Lpd	dihydrolipoamide dehydrogenase

LT-α3	lymphotoxin-α3
MALDI-TOF	matrix-assisted laser desorption and ionization time-of-flight
MDR	multi-drug-resistant
MIC	minimum inhibiting concentration
Mn^{3+}-TE-2-PyP	Mn^{3+}-meso-tetrakis[(N-ethyl)pyridinium-2-yl]porphyrin
MSB	master seed bank
Mt	*Mycobacterium tuberculosis*
MycR	mycothiol reductase
MSH	mycothiol
NADH	nicotinamide adenine dinucleotide
NADPH	nicotinamide adenine dinucleotide phosphate
Ndh/*ndh*	NADH dehydrogenase
NEM	N-ethylmaleimid
NTA	nitrilotriacetic acid
OD_x	optical density at x nm
ORF	open reading frame

OxyR/*oxyR*	oxidative stress regulator
PAGE	polyacrylamide gel electrophoresis
PCOOH	phosphatidylcholin hydroperoxide
PCR	polymerase chain reaction
Prx	peroxiredoxin
PVDF	polyvinylidendifluoride
RMP	rifampin/rifampicin
RNI	reactive nitrogen intermediates
ROI	reactive oxygen intermediates
rpm	rounds per minute
RT	room temperature
SDS	sodium dodecyl sulfate
SucB	dihydroliponamide succinyl-transferase
TB	tuberculosis
TBE	tris-borate EDTA
t-bOOH	*tert*-butyl hydroperoxide

TEMED	N,N,N',N'-tetramethylethylenediamine
TNF-α	tumour-necrosis factor-α
TPx	thiol peroxidase
TR	thioredoxin reductase
Trx	thioredoxin
TXNPx	tryparedoxin peroxidase
UNAM	Universidad Nacional Autónoma de México
vol	volume
WHO	World Health Organization

7.2 Abbreviations of nucleotides and amino acids

Table 7.1: Abbreviations of nucleotides

nucleotide	abbreviations
adenine	A
cytosine	C
guanine	G
uracile	U
thymine	T

Table 7.2: Abbreviations of amino acids

amino acid	1 letter code	3 letter code
alanine	Ala	A
arginine	Arg	R
asparagine	Asn	N
aspartic acid	Asp	D
cysteine	Cys	C
glutamine	Gln	Q
glutamic acid	Glu	E
glycine	Gly	G
histidine	His	H
isoleucine	Ile	I
leucine	Leu	L
lysine	Lys	K
methionine	Met	M
phenylalanine	Phe	F
proline	Pro	P
serine	Ser	S
threonine	Thr	T
tryptophan	Trp	W
tyrosine	Tyr	Y
valine	Val	V

Danksagung

Die vorliegende Arbeit wurde unter der wissenschaftlichen Anleitung von Prof. Dr. Dr. h.c. L. Flohé und Prof. Dr. M. Singh in der Abteilung für der Biochemie der Technischen Universität Braunschweig an der Gesellschaft für Biotechnologische Forschung mbH (GBF) angefertigt.

Herrn Prof. Dr. Leopold Flohé und Herrn Prof. Dr. Mahavir Singh danke ich für die Überlassung der interessanten Themenstellung, ihre ständige Hilfs- und Diskussionsbereitschaft und für das große Interesse, das sie meiner Abeit entgegen gebracht haben.

Bei Heike Budde und Marcelo Comini möchte ich mich für die ausgesprochene Hilfsbereitschaft bedanken. Das fröhliche und familiäre Laborklima hat maßgeblich zum guten Gelingen der Arbeit beigetragen.

An dieser Stelle sei auch allen Kollegen der “TU-AG” für die freundliche Unterstützung gedankt.

Besonderer Dank gilt Tanja Behn, Martina Bittner, Sergio Guerrero, Joop van den Heuvel, Carsten Hornig, Roland Schucht, Ralf Spallek und Ute Widow für die zahlreichen fachlichen und nicht-fachlichen Gespräche und ihre stete Hilfsbereitschaft, auch über Arbeitsgruppengrenzen hinweg.

Karin Plank-Schumacher und Claudia Wylegalla gilt mein Dank für die zahlreichen DNA-Sequenzierungen. Rita Getzlaff danke ich für die Proteinsequenzierungen und Ulrich Menge für die tatkräftige Unterstützung bei der Mycothiol-Isolation.

Birgit Hofmann und Hans-Jürgen Hecht danke ich für die Hilfestellung bei allen strukturbiologischen Fragestellungen. Heinrich Lünsdorf danke ich für die elektronenmikroskopischen Aufnahmen. Madia Trujillo und Rafael Radi gilt mein Dank für die unkomplizierte Zusammenarbeit und die Durchführung

der stopped-flow Analysen. Clara Espitia danke ich für die Überlassung der Mykobakterien und des pMV-Vektors. Tom Ottenhoff danke ich für das *Mt*TR-Expressionsplasmid. Regina Brigelius-Flohé gilt mein Dank für die Hydroperoxide. Helena Castro danke ich für die Kinetik-Starthilfe und Sagar Krupa für das kritische Lesen dieser Arbeit.

Besonders danke ich Ina für ihre tatkräftige Hilfe und moralische Unterstützung während der gesamten Zeit meiner Promotion, die oft das Arbeiten erleichtert haben.

Besonderer Dank gilt auch meinen Eltern, die mich in dieser Zeit nach allen Kräften unterstützt und mir in jeder Situation zur Seite standen.

Diese Arbeit wurde finanziell durch die Deutsche Forschungsgemeinschaft und die GBF unterstützt.

Lebenslauf

Name	Timo Jäger
Geburtsdatum und -ort	10.10.1974 in Gießen
Staatsangehörigkeit	deutsch
Familienstand	ledig
Schulausbildung	1981 - 1983: Grundschule Pohlheim-Holzheim 1983 - 1985: Grundschule Braunschweig-Völkenrode 1985 - 1987: Orientierungsstufe Wendeburg 1987 - 1990: Martino-Katharineum, Gymnasium, Braunschweig 1990 - 1994: Liebigschule, Gesamtschule, Gießen
Schulabschluß	Abitur am 10.06.1994
Studium	01.10.1994 - 31.03.2000: Technische Universität Braunschweig, Fachrichtung Biologie-Diplom, Hauptfach: Mikrobiologie, Nebenfächer: Zellbiologie, Biochemie/Biotechnologie

Studienabschluß	Diplom am 04.12.1999, Diplomarbeit „Die L-Alanin-Dehydrogenase und die Alkylhydroperoxid-Reduktase von pathogenen Mykobakterien: Untersuchungen zum Einsatz in der Diagnostik und Knockout-Versuche”
Promotionsarbeit	seit 01.01.2000: Abteilung für Biochemie der Technischen Universität Braunschweig an der Gesellschaft für Biotechnologische Forschung mbH (GBF), Braunschweig